TAGSEA PROGRAM
FINAL REPORT
VOLUME I
CLUTTER MODELS

BR-9254-1

27 AUGUST 1976

Prime Contract No. N00017-73-C-2244

RAYTHEON COMPANY
MISSILE SYSTEMS DIVISION

SUMMARY

A sidelooking radar mounted on a wing pod of an A-3 aircraft was used to gather X-band sea clutter data. Measurements were performed for grazing angles between 6 and 47 degrees on the East and West Coasts with a resolution of 70 by 100 feet. Analysis of the clutter data was accomplished by Raytheon. Monthly technical meetings with NAVSEA, the Johns Hopkins University, Applied Physics Laboratory and Technology Service Corporation were held throughout the planning, testing and analysis phases of the program to ensure the validity or the results.

The mean backscatter (σ_o) and statistical clutter models presented in this report are valid only within the constraints in which the data were collected: high resolution, medium grazing angle and moderate to high sea states.

TAGSEA PROGRAM

FINAL REPORT

VOLUME I.

CLUTTER MODELS

BR-9254-1

27 AUGUST 1976

Prepared for
GENERAL DYNAMICS
Pomona, California

Under
Prime Contract No. N00017-73-C-2244

Prepared by
RAYTHEON COMPANY
MISSILE SYSTEMS DIVISION
Bedford, Massachusetts

"The sea never changes and its works,
for all the talk of men, are wrapped
in mystery."

Joseph Conrad

ABSTRACT

Radar sea clutter modeling, with associated data gathering and analysis, is reported with specific emphasis on clutter returns with a probability of occurence of a minimum of 1 in 10^6 referenced to the mean. Data was gathered and reduced as a function of sea state, wind direction, grazing angle and polarization off the East and West Coasts with a basic radar resolution of 100 by 100 feet at X-band. Analyses reported characterize sea clutter in terms of mean clutter backscatter coefficient (σ_o), probability density, statistical variability, temporal and spatial power spectral density and autocorrelation function, and conditionsl probability. Models of sea clutter are formulated (and validated by simulation) with several levels of refinement for use primarily in specification, design and evaluation of missile systems. The material is presented in a form to be useful in other applications as well.

Although this report is presented in four volumes, attention should be directed primarily to Volume 1 which, on a stand-alone basis, contains an overview and presents summarized results and the full clutter models. The work was performed by the Raytheon Company Missile System Division, Bedford, Massachusetts, under subcontract to General Dynamics/Pomona Division as a part of NAVSEA prime contract N00017-73-C-2244.

FOREWORD

This final report summarizes the work done by Raytheon Missile Systems Division for the TAGSEA Program under General Dynamics PO #304490-PB, prime contract no. N00017-73-C-2244. It is submitted in compliance with Data Item A015 and is organized into four volumes to ease handling and for the convenience of the readers.

Volume I, Clutter Models, reports the essence of the work and contains the models themselves which were the prime objective of the clutter portion of the TAGSEA program; it can be read on a stand-alone basis. Enough peripheral material is also included to provide a framework for a good understanding of the models. Volume II, Procedures and Output Forms, provides details and explanations on methodology including the form of the outputs and the structures of the clutter simulation effort. Volume III, Supportive Analyses and Outputs, provides analytical back-up and a more complete detailed view of the simulation software. Volume IV, Standard Clutter Analysis Outputs, is a compilation in various forms of the mass of data analyzed during the program. Each volume has its own table of contents which serves to outline the specific material presented therein.

Raytheon wishes to acknowledge the valuable aid and support given by members of the team composed of personnel from NAVSEA, APL/JHU, Technology Service Corporation and General Dynamics. Many helpful suggestions were made during a series of critiques and reviews which most assuredly contributed to a better resultant output. The assistance received ranged all the way from general support and overall guidance to specific supportive analyses, detailed unpublished comparative data, and suggestions of exact forms of clutter models and plots which would be most informative to the community at large.

TABLE OF CONTENTS

LIST OF ILLUSTRATIONS

1. INTRODUCTION

This final report presents the results of the Raytheon clutter modeling contribution to the Terminal Active Guidance System Effectiveness Analysis (TAGSEA) work performed under sub-contract to General Dynamics, Pomona Division as part of NAVSEA prime contract N00017-73-C-2244. It is the purpose of this report to present the results of this work in a form that may be of use to the widest range of potential users.

Toward this end, every effort was made to remove hardware biases and idiosyncrasies as far as possible, to reduce the data carefully so as to prevent any false information from being included, and to analyze and present the pertinent data in the most useful form. Sea clutter data was gathered using a modified form of the active radar CMDR seeker developed for use in the Standard/Active Missile. This fixed some system parameters, such as operation at X-band, but other parameters were selected as being most responsive to the dictates of the problem. In summary the resultant data gathering parameters were:

X-band,

Side looking antenna,

Vertical or horizontal polarization,

A prf of approximately 19 KHz,

100 by 100 ft. resolution in-range and cross-range, (doppler, in this case), and

Five minutes for each run.

Modifications were made to hardware and data was collected during flight tests off both the East and West coasts. Data reduction and analyses were conducted following the flights in non-real time.

Emphasis was placed during data reduction on the elimination of as many hardware offset influences on the data as possible. The aim was to identify and characterize sea clutter in a way that would be independent of the observation means. Data reduction, however, served primarily as an intermediate analysis step where the mass of data was reduced to a more manageable size. The reduction was done by taking the fourier transform to obtain resolution in the doppler, or cross-range, direction resulting in approximately a 1600 foot (range) by 3200 foot (doppler) grid with 100 by 100 foot resolution. A new grid was obtained every 9 milliseconds, thereby providing about 17×10^6 separate data points for each run. This number was not chosen capriciously, but rather it was desired to quantize the random (or quasi-random) behavior of the sea to 1 part in 10^6. That is, it was desired to measure the probability of occurance of large amplitude clutter returns which occur on the average only once in every 10^6 samples. The problem is statistical in nature and about 17 samples of the rare large returns obtained during each run provide a good measure of the probability of occurance.

Further analyses of the reduced data served basically to examine the structure of the clutter returns so as to be able to describe the phenomena in quantitative terms and present the results in various ways. By virtue of the data gathering plus the reduction and analysis process, it has been possible to generalize the characteristics of sea clutter in terms of clutter models. Generation of these clutter models was the primary objective of the effort, and this Final Report (in four volumes) presents the results of detailed work performed between June 1975 and August 1976.

This volume, Clutter Models, presents a distillation of the effort with conclusive quantitative outputs of the TAGSEA clutter effort. The size of this volume was purposely kept to a minimum so as to provide maximum usefulness and accessibility

to the technical community. Section 2 first sets forth the objectives of the work as defined early in the program. Next, Section 3 presents an Executive Synopsis of the results aimed at providing the essential information within the smallest compass. Output Data, in Section 4, gives an overview and consolidated summary of results from the analyses. Clutter Models, the subject of the fifth section of this volume, is the heart of the matter; it is here that the reason for all the effort which has gone before is best expressed. What radar models of sea clutter most aptly express the true characteristics of the sea? The Clutter Model section provides answers in graphic, tabular and analytic form for models with three levels of sophistication which extend and supplement those currently available.

Section 6 contains a brief recapitulation of the program history, dealing principally with the interplay between uses and modifications of existing hardware, and data gathering/analysis requirements dictated by the nature of the clutter and the clutter modeling task. It also summarizes the contents of the remaining three volumes.

2. OBJECTIVES

Objectives for the TAGSEA clutter model task were consolidated and formally established in December 1975 as: "Quantitative data supported by test conditions, and an interpretation of reduced data including the following characterizations have been specified as The Deliverables for the TAGSEA Clutter Model tasks:

1.1 Complete histograms and distribution functions
1.2 Tail histograms and distribution functions
1.3 Mean, median, mode and moments 2,3,4 tabulation
1.4 Parent distribution
1.5 Temporal Autocorrelation Function (ACF)
1.6 Spatial ACF
1.7 Stationary analysis and conclusion
1.8 Conditional probability maps."

More fully, the objectives included reducing data obtained during flight testing and analyzing the data so as to provide the deliverables listed above. The purpose of this report is to make available all of the items listed above and to interpret them in ways which will be most useful to the technical community.

Foremost in this interpretation, and indeed the single output which brings all of the deliverables into focus, was the formulation of the clutter models. The goal of this work was to first make a detailed examination of the data, then further reduce, study and analyze the reduced data. From this study it was desired to draw conclusions aimed at consolidating the whole effort into precisely and compactly stated clutter models in graphic, analytic and tabular form based on the quantitative outputs. This model

would be useful in specifying, designing and evaluating the performance of missile seekers operating against targets with a sea clutter background.

All of the specific and general objectives and goals of the clutter modeling task have been achieved.

3. EXECUTIVE SYNOPSIS

Raytheon's contribution to the TAGSEA (Terminal Active Guidance System Effectiveness Analysis) program consisted in essence of defining and modeling sea clutter to a level not previously achieved. The work followed the classic pattern for an experiment rigidly founded on data; i.e., design the experiment, gather data, analyze the results, draw conclusions, publish the results. In order to extend the available data on sea clutter to a level which would be meaningful for the specification, design and performance evaluation of radar missile seekers, it was necessary to gather and analyze a very large data base under a variety of conditions. The objective was to characterize the surface of the sea as it would be seen by a class of radars not by a single specific radar. To do this required that all biases in the data gathering radar be removed to the maximum practical extent and to further delete anomalies by careful reduction, editing and weighting of the data, based only on theoretical considerations or verifiable tests. Only by doing so could the data then be used to develop the required outputs.

Computational alteration of the selected data then resulted in obtaining looks at several different aspects of sea clutter. This process produced the outputs of the analysis from which conclusions were drawn. First among these outputs was the mean backscatter coefficient, σ_o. This single output was characterized as a function of grazing angle, vertical and horizontal polarization, sea state, aspect with respect to the surface winds and possible differences between normally choppy seas off the East Coast versus swells off the West Coast. In essence, consistent results were obtained over the range of variables which were explored. Comparison with averages from

previous published[1] and unpublished[2] work showed the TAGSEA levels for σ_o to be from 5 to 10dB higher. This is not surprizing when it is realized that the determination of sea state alone can introduce this much variation. Also, data on which the averages of the references were based have a similar scatter. This does not invalidate either the TAGSEA values or those of the references; it only says that large variations are to be expected and account must be taken of this factor in design.

Another aspect, and a vitally important one, which characterizes sea clutter is the distribution function. This defines for stated conditions the probability that the clutter return at any instant will exceed a given amplitude. It was a goal of this effort to define the distribution over the range of conditions listed under σ_o above to better than a probability of 10^{-6}. This was the main requirement for gathering and reducing a very large amount of data. Most comparable studies have gone only to a probability of 10^{-4} but the lower probability should be known for more exact design and performance evaluation of radar seekers. The point that is affected in the design is the false alarm rate which in many systems must be kept at 10^{-6} or lower. Given the large data base, it was possible to define the region of the distribution functions from the 10^{-4} through the 10^{-6} points or "tails" and, in some cases, beyond. It has often been stated that these tails extend the distribution function past those obtained from a pure noise process (often called a Rayleigh process) such as receiver noise. The TAGSEA work confirmed this statement and the shape of the distribution functions were more precisely defined.

---

(1) Nathanson, F.E., "Radar Design Principles", McGraw-Hill, 1969

(2) Nathanson, F.E., and Brooks, P.R., "Data Points for X-Band Sea Reflectivity", Technology Service Corporation memo TSC-WO-251/br B 50711, dated 29 June 1976.

Two distinct groups of distribution functions were generated. The first called A-type, normalized the function with respect to the long term mean; here the variations in amplitude of the returns were averaged over a full run of up to five minutes. The result was that the tails of the distributions were extended due principally to the contributions from returns when the mean was temporarily high. The second type of distribution function, called N-type, used normalization on a much shorter time basis, about five seconds. The result was that the tails were reduced. Comparison of the distributions with previous work[3][4], to the 10^{-4} point which was available shows fair agreement which gives credence to the tails in which we are mainly interested.

The third major aspect of sea clutter studies as a part of the work to characterize radar returns were the spatial and temporal correlation functions. Simply put, how dependent are radar returns from the sea on their near neighbors in space and time? Here again two types of correlation were considered. First, the instant-to-instant and resolution cell-to-resolution cell showed almost no correlation. Each look at the sea can be said to be independent. However for the second type of correlation, longer term looks or averages were employed. This resulted in the characterization of a varying mean. The average value of the returns changes relatively slowly. This effect had also been reported previously in the literature and was verified and quantified.

---

(3) Trunk, G.V., "Modification of Radar Properties of Non-Rayleigh Sea Clutter", IEEE Trans. on Aerospace and Electronic Systems, p. 110, January 1973.

(4) Sodergren, P.R., "A Revised Ku-Band Sea Clutter Model", JHU/APL memo MPD-72-C-033, dated July 19, 1972.

Conditional probability in the vicinity of large hits was the final major aspect considered as part of the analysis work. The question to be answered was stated as, "Are large clutter returns grouped and if so how can the grouping be described? The answer to the first part is that large returns are grouped in time but not quite in the way first postulated. The conditional probability to be explored was the probability of getting a return at the 10^{-3} level within a small space ($\pm$700 feet) and time ($\pm$0.06 second) frame around a return at the 10^{-5} level. This is important in some radar systems where the higher return triggers a verify mode which then sets a threshold at a lower level in an attempt to verify the presence of a valid target. In essence the conclusions drawn were that for horizontal polarization the large returns seem to persist for a long time but for vertical polarization they appear to be spread over a greater surface of the sea.

Output plots and tables were prepared in many different forms for each of the aspects noted above. However the major conclusions drawn from the entire effort were consolidated into the formulation of clutter models. These models are meant to be used for the specifications, design and performance evaluation of missile systems which must operate with a sea clutter background. Three orders of model sophistication were developed each with a family of four selectable input parameters. The selectable inputs are horizontal or vertical polarization and typical or worse-case conditions. The first-order model considers only σ_o. This is in keeping with the usual practice of specifying σ_o as a function of grazing angle. This simple model is useful as such but it also forms the basis for the other two. The second-order model adds to σ_o the A-type distribution function; thus statistical properties are added to the model. The third-order model substitutes the K-type distribution and adds a model of the time varying mean. This ultimate model comes as close as possible to the TAGSEA perception of sea clutter.

Any of the models can be used for analysis but the third-order model is really only practical for computer simulation. This was in effect done as part of the validation process. A computer program was written, models inserted, simulated clutter generated and results obtained which were then compared with the results from real clutter. For each of the major aspects noted above and for the associated outputs the comparisons were excellent and the model work was verified.

Thus all of the objectives and goals set for the TAGSEA clutter work were met and the models generated are available for use in future missile system programs.

4. OUTPUT DATA

The overall goal of generating clutter models substantiated by quantitative outputs has been achieved, and these outputs are presented here. They are organized so as to be most compatible with the form of the clutter models to be presented in Section 5, and in the manner discussed below.

Subsection 4.1 discusses the data gathering flights. It includes commentaries on the runs, and acquired data and the sea conditions so as to provide background information against which to assess the summarized outputs. In Subsection 4.2, as an indication of the scenario dependence of the data and outputs, the effect of environmental and radar variables are reviewed with conclusions drawn as to which outputs are functions of which variables.

In keeping with the clutter model organization, Subsection 4.3 presents the mean backscatter coefficient outputs, (σ_o), in consolidated form. In addition, comparisons are made with data from other sources as a partial check of the validity of the TAGSEA work and because the more familiar prior σ_o values may be used as part of the clutter model.

Distribution functions are then discussed in some detail in Subsection 4.4 and summarized as an important input to the model. Comparisons are also made with other work for validation purposes.

Finally, in Subsection 4.5, the distribution of the mean of the observed clutter model is covered as the last element of the series which contributes to, and in fact defines, the clutter model.

It must be understood that the outputs presented here are in summary form and that the mass of the individual outputs are to be found in great detail in the appendices of Volumes III and IV. The reason for summarizing them here is to consolidate the quantitative material in a form which is suitable for use in the clutter model which itself is the final refinement of the entire TAGSEA clutter task.

4.1 Flight and Data Summary

Data gathering flights made both on the East and West coasts were fully reported in the General Dynamics Flight Test Report[5] and the equipments, procedures and flights are presented in Volume II of this report. This subsection summarizes pertinent flight parameters and presents a data matrix to provide a background for understanding the outputs.

In general, runs were made at one of four altitudes, 500, 1100, 2200 or 3300 ft. to provide grazing angle average of 6.4° to 4.7°, 14.3° to 10.4°, 29.3° to 21.1° and 47.2° to 32.8° respectively. Each run was a nominal 5 minutes in length with the antenna looking either upwind, downwind or crosswind. Tables 4-1 and 4-2 identify the run numbers used. Run 5 of Flight 6, for example, is identified as run 605.

In addition to the East Coast-West Coast, grazing angle and aspect with respect to the wind, two other parameters were covered by the flight testing; these were polarization and sea state.

(5) General Dynamics, Flight Test Operations Final Report, 1 May 1976, Data Item A001 CDRL Contract N00017-73-C-2244, Document Confidential

TABLE 4-1
FLIGHT RUN MATRIX FULL FLIGHT

Run 0	Camera Run		300'	1 min.
Run 1	Radar Looking	Upwind	1.1Kft	5 min.
2	Radar Looking	Downwind	1.1Kft	5 min.
3	Radar Looking	Crosswind	1.1Kft	5 min.
4	Radar Looking	Upwind	2.2Kft	5 min.
5	Radar Looking	Downwind	2.2Kft	5 min.
6	Radar Looking	Crosswind	2.2Kft	5 min.
7	Radar Looking	Upwind	3.3Kft	5 min.
8	Radar Looking	Downwind	3.3Kft	5 min.
9	Radar Looking	Crosswind	3.3Kft	5 min.

TABLE 4-2
FLIGHT RUN MATRIX LOW ALTITUDE FLIGHT

Run 0	Camera Run		300'	1 min.
Run 1	Radar Looking	Upwind	500'	5 min.
Run 2	Radar Looking	Downwind	500'	5 min.
Run 3	Radar Looking	Crosswind	500'	5 min.

Table 4-3 is a matrix of the flights with sea state commentary and was taken from the aforementioned flight report. Data collected during the flights was evaluated for its usefulness as a base to determine the clutter outputs. Data was rejected if it did not meet the clutter-to-noise criterion, if extraneous signals were present or if for any other reason the record was unusable. The requirement was to use as a data base only information truly representative of clutter and free from contamination. Tables 4-4A and 4-4B presents the data commentaries for the East and West coast flights respectively; Table 4-5 lists the runs for which valid clutter data was obtained and also identifies the range gates which were not used. As indicated by the 12 in Run 812, this run is the exception to the rule; it was a run to observe the Nantucket Shoals Lightship and as such contains data on the ship, not on clutter.

TABLE 4-3
SEA CONDITIONS FOR TAGSEA CLUTTER FLIGHTS

Flight No. E = East Coast W = West Coast	Date of Flight (1976)	General Description of Sea	Wave Direction (Deg True - From)	Wave Length (Ft)	Wave Period (Sec)	Wave Height Crest to Trough (Ft)	Wind Velocity (KTS) / Wind Direction (Deg True-From)	Sea State (Hydrographic) and Description
3E	2/5	Many white caps. Moderate waves with wind shearing.	300	177	5	6	20 / 340	4 Rough
4E	2/9	Small amount of white caps. Small waves with some uniformity.	280	93	4	4	14 / 320	3 Moderate
5E	2/11	Confused sea with moderate amount of white caps. Haze and rain in test vicinity.	210	131	4	6	23 / 240	4 Rough
6E	2/12	Large amount of white caps, foam streaking, and spraying. Large waves with breaking crests.	300	220	6	8	24 / 300	5 Very Rough
7E	2/12	Same as 6 except more confusion of sea surface.	278	241	6	10	30 / 310	5 Very Rough
8E	2/13	Same as 3.	220	164	7	6	17 / 210	4 Rough
9E	2/14	Same as 3 except more wind shearing and confusion of sea surface.	355	155	6	7	18 / 350	4 Rough
10W	3/9	No white caps or foam. Ripples with little or no wind.	360	16	3	1/2	3 / 45	1 Smooth
11W	3/10	Same as 10.	290	19	2	1	3 / 285	1 Smooth
12W	3/12	No white caps or foam. Small waves with some capillary motion.	310	31	2	3	10 / 290	2 Slight
13W	3/17	Same as 12.	280	42	3	2	9 / 285	2 Slight
15W	3/22	Same as 12.	285	35	3	3	10 / 295	2 Slight
16W	3/23	Same as 3 except less wind shearing.	300	143	6	6	15 / 285	4 Rough
17W	3/23	Same as 16.	325	132	6	6	15 / 285	4 Rough

*OP = Operability Flight

TABLE 4-4A
EAST COAST DATA FLIGHT COMMENTARY

FLT NO.	DATE 1976	AIM	FLT. TIME (HRS)	EST. SEA STATE	DATA COLLECTION	DATA REDUCTION	OUTPUTS
1	1/28	O(V)	3.00				None
2	2/3	O(V)	1.75				None
3	2/5	D(V)	3.33	4-5	Full Data Set	No reduction-Calibration circuit problem, Trig. time set incorrectly.	None
4	2/9	D(V)	1.75	3	Partial Data Set Mincom Recorder Failure	1.1KFT only for Runs 1 and 3. Run 2 had bad tape.	2 Runs
5	2/11	D(V)	1.75	4	Partial Data Set Coolant Pump Failure	No reduction. Data set too limited.	None
6	2/12	D(V)	3.50	5-6	Full Data Set	Full reduction except Run 1, problem with tape.	8 Runs
7	2/12	D(H)	3.50	5	Full Data Set	Full reduction except Run 5, problem with tape.	8 Runs
8	2/13	D-LG (V)	2.67	4	Full Data Set	Partial reduction. Some data contains point target.	3 Runs
9	2/14	D(V)	1.75	4	No Data; DCU Failure	No reductions.	None

Notes: O = Operability; D = Data Collection; LG = Low Grazing Angle Only; (V) = Vertical Polarization; (H) = Horizontal Polarization

UNCLASSIFIED

TABLE 4-4B
WEST COAST DATA FLIGHT COMMENTARY

FLT NO.	DATE 1976	AIM	FLT. TIME (HRS)	EST. SEA STATE	DATA COLLECTION	DATA REDUCTION	OUTPUTS
10	3/9	O(V)	2.50	1			None
11	3/10	D(V)	2.67	1	Full Data Set	Partial reduction, low alt. flights (Runs 1, 2,3) C/N ratio too low, also Run 6 bad tape.	5 Runs
12	3/12	D(V)	2.50	2	Full Data Set	Partial reduction Run 4 only. Data set eliminated, numerous surface contacts due to war games.	1 Run
13	3/17 AM	D(V)	2.16	2	No Data; Aborted due to war games, weather	No reduction.	None
14	3/17 PM	D(V)	1.50	2	No Data; Aborted due to system failure	No reduction.	None
15	3/22	D(V)	1.50	2	No Data; Aborted due to system failure	No reduction.	None
16	3/23 AM	D(V)	2.50	4	Full Data Set	Full reduction except Run 8, bad tape.	8 Runs
17	3/23 PM	D(H)	2.50	4	Full Data Set	Partial reduction, low alt. flights (Run 1, 2,3) C/N ratio too low, Run 5,9 bad tape.	4 Runs
18	3/24	D-LG (V)	1.80		No Data; Aborted due to system failure	No reduction.	None

Notes: O = Operability; D = Data Collection; LG = Low Grazing Angle Only; (V) = Vertical Polarization; (H) = Horizontal Polarization

UNCLASSIFIED

TABLE 4-5

RANGE GATES MISSING AND/OR ELIMINATED FROM DATA REDUCTION

FLT/RUN	RANGE GATE ELIMINATED	COMMENTS
401	No gates eliminated	
402	All	No data, bad tape
403	1, 13, 14, 15	RG #1 dropped out in mid-flight
601	All	No data, bad tape
602	No gates eliminated	
603	No gates eliminated	
604	No gates eliminated	
605	No gates eliminated	
606	No gates eliminated	
607	No gates eliminated	
608	No gates eliminated	
609	No gates eliminated	
701	6, 13, 14, 15	
702	3, 5, 8 thru 15	
703	3 thru 15	
704	No gates eliminated	
705	All	No data, bad tape
706	9 thru 15	
707	1, 15	
708	1, 5, 9	
709	1, 5, 15	
801	1, 13, 14, 15	
802	1, 5, 13, 14, 15	
803	1, 5 thru 15	
812	----------	Special run with ship target
1104	8 thru 15	Low C/N ratio
1105	8 thru 15	Low C/N ratio
1106	All	No data, bad tape
1107	No gates eliminated	
1108	15	
1109	No gates eliminated	
1204	No gates eliminated	
1601	11, 13, 14, 15	
1602	11	
1603	8 thru 15	
1604	No gates eliminated	
1605	15	
1606	11	
1607	11	
1608	All	No data, bad tape
1609	11	
1704	15	
1705	All	No data, bad tape
1706	10 thru 15	
1707	No gates eliminated	
1708	No gates eliminated	
1709	All	No data, bad tape

Even with the heavy editing of data to eliminate all extraneous material and with the normal failures experienced in captive flight testing, the resultant data base was large and ample for our purposes. The number of samples was, in fact, so large that special data reduction methods had to be devised to enable the analysis to be performed in two steps. The valid data was also large enough to enable characterization of the clutter distribution function to one part in 1,000,000.

4.2 Scenario Comparisons

It is desirable at this point to make some statements regarding the general characteristics of sea clutter as it is (or is not) affected by commonly encountered conditions or as influenced by radar parameters. Such generalizations are of course based on the TAGSEA work but have also been influenced by previous work. Only conclusions based on a substantial amount of evidence are drawn; if insufficient data on a particular point was available or if the data was indeterminate, no generalizations were made.

Parameters which influence the clutter returns and which were covered by the TAGSEA scenarios are grazing angle, polarization, sea state, aspect with respect to the wind and the form of the sea, i.e., chop versus swells. This last factor was the basic reason for operating off both the East and West Coasts. For each of these parameters it is desirable to be able to make a statement about the mean backscatter coefficient, σ_o, and about the amplitude ratio of large returns to the mean value of the clutter. This has been done where the evidence could support a conclusion.

a) Grazing Angle

The average reflectivity (σ_o) increased with grazing angle as expected, however at high grazing angles the dependence was somewhat less for vertical polarization than previous work

would indicate. The variability of the mean, and the behavior of large echoes seemed to be independent of grazing angle. The tails, that is large returns, of the mean-normalized distribution were relatively constant with grazing angle for vertical polarization. However, for the horizontal polarization runs observed, the 10^{-5} and 10^{-6} point on the distribution curves decreased 3dB as grazing angle increased from 10° to 40°.

b) Polarization

The average reflectivity was higher for vertical than for horizontal polarization as was expected. The tail-to-mean ratio was greater for horizontal than for vertical polarization, but when absolute cross-section was considered, the 10^{-6} point was still several decibels greater for vertical than for horizontal polarization.

The variation of the mean appeared to be independent of polarization. However, two runs examined for mean correlation showed about four times slower decorrelation for horizontal than for vertical polarization. Also, the conditional probability maps show more temporal extent for horizontal polarization, which bears out this conclusion. Spatial extent patches of large echoes appeared to be smaller for horizontal than vertical polarization.

c) Sea State

Again, the reflectivity showed the expected trend, increasing with sea state. However, the reflection coefficients were somewhat larger than expected. It is unknown whether this was an error in estimation of the sea state, a tolerance build-up in the radar or a truly higher σ_o.

The tails of the distributions which were not normalized locally, i.e., on a relatively short term basis (A-type normalization), became extended at low sea states. This was undoubtly because of large variations in the mean caused by local effects, and these variations upset the tail-to-mean ratio. When local

normalization was used (N-type normalization) the mean variation effect was removed and the tails of the distributions reduced to the same size as high sea state runs. The conclusion is that tails measured with respect to a long term mean will be extended.

d) Aspect

Reflectivity (σ_o) was noticeably lower for the cross-wind aspect compared to upwind and downwind. The latter two aspects had very nearly the same reflectivity. No other dependencies on aspect were observed.

e) Location

Chop and swell may give dissimilar results, however no clearly discernible dependencies on East or West coast locations were observed.

In general, the data tends to be consistent in all the flights and with the previous data. One could therefore conclude that the data is representative and forms a good base for clutter model generation.

4.3 Mean Backscatter Coefficient

Values of sea reflectivity (σ_o) obtained from the data, together with the model in Nathanson [1] are summarized in Figure 4-1. The data shows biases with respect to the reference varying from -3dB for horizontal polarization and high grazing angle to +10dB for low sea state, vertical polarization, and high grazing angle. However, almost all the TAGSEA data is moderately higher than the referenced curves. These biases may be contrasted with an estimated radar calibration error of $\pm$3dB(2σ), and a sea state estimation error of approximately 4dB per sea state.

---

(1) Nathanson, F.E., "Radar Design Principles", McGraw-Hill, 1969

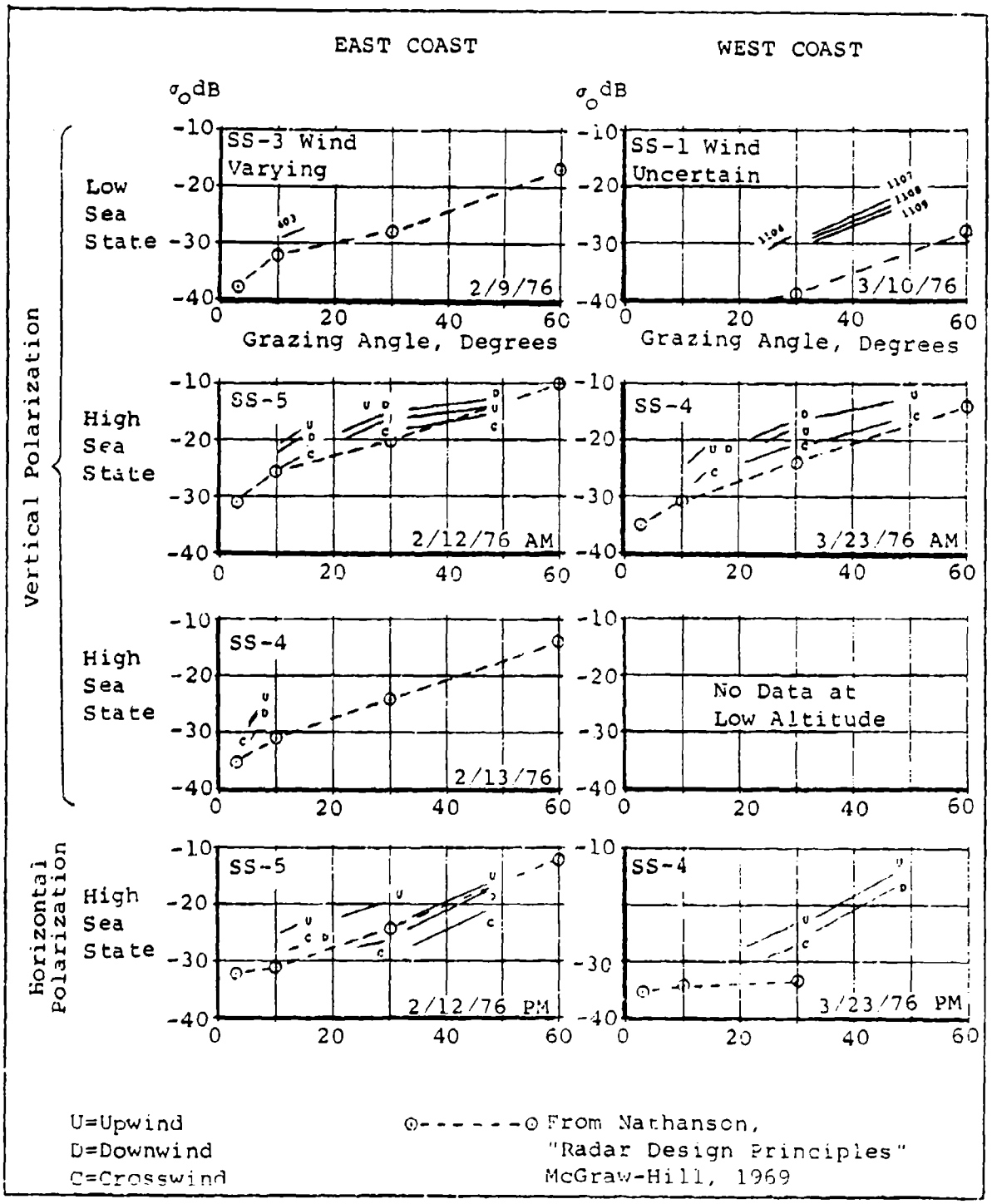

Figure 4-1 Comparison of σ_o With Previous Data

The data on each plot was taken within a period of about three hours, so reasonable consistency may be expected among different conditions on one chart. In addition, horizontal polarization flights were conducted within a few hours of companion vertical polarization flights. This provides a reasonable comparison of backscatter with different polarizations.

General trends in the measurements agree with the reference. The variation with grazing angle is somewhat less than the reference for high sea states within the 30° to 50° region.

Concerning effects of wind direction, the crosswind reflectivity was usually lower than for upwind and downwind conditions. On the other hand, upwind and downwind reflectivities were more nearly equal, and sometimes crossed over.

The higher reflectivity noted above was not unexpected considering the scatter of data which form the basis for the resultant composite curves. This scatter of data is shown in the plots of Figures 4-2 through 4-7 taken from Reference (2) on which the TAGSEA outputs are superimposed. The derived Technology Service Corporation models on the figures were fitted to all previous data noted (excluding TAGSEA) and weighted the Nathanson σ_o values more heavily than the other data. Figures associated with the TAGSEA data refer to the flight and run numbers and the last digits, i.e., 1,4 and 7 are upwind runs; 2,5 and 8 are downwind; and 3,6 and 9 crosswind.

Although the TAGSEA σ_o values follow the same general trend as the TSC derived model, it is evident that such a model for TAGSEA would be about 5dB higher.

---

(2) Nathanson, F.E., and Brooks, P.R., "Data Points for X-Band Sea Reflectivity", Technology Service Corporation memo TSC-WO-251/br B 50711, dated 29 June 1976.

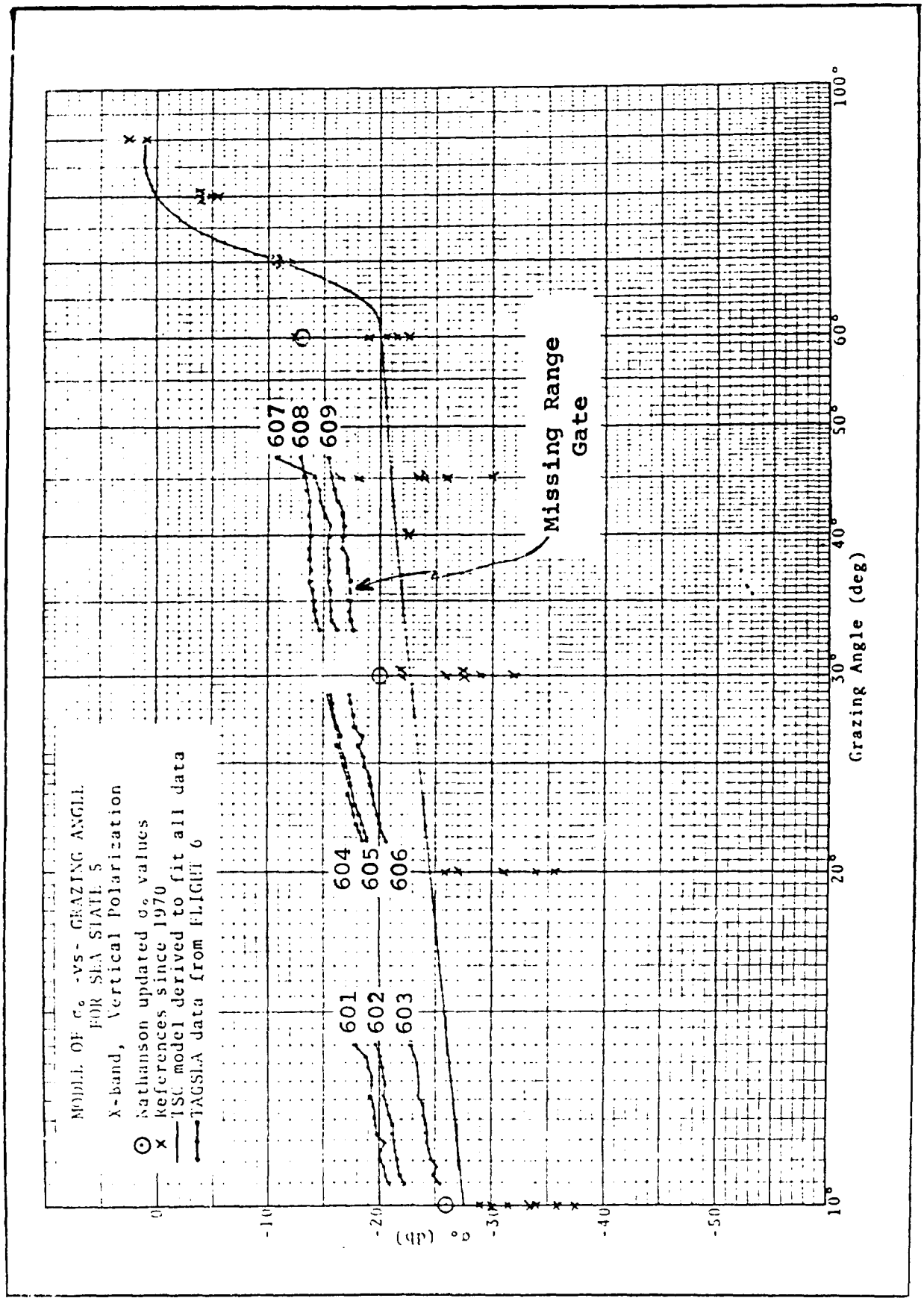

Figure 4-2 Clutter Comparison to Other Data-1

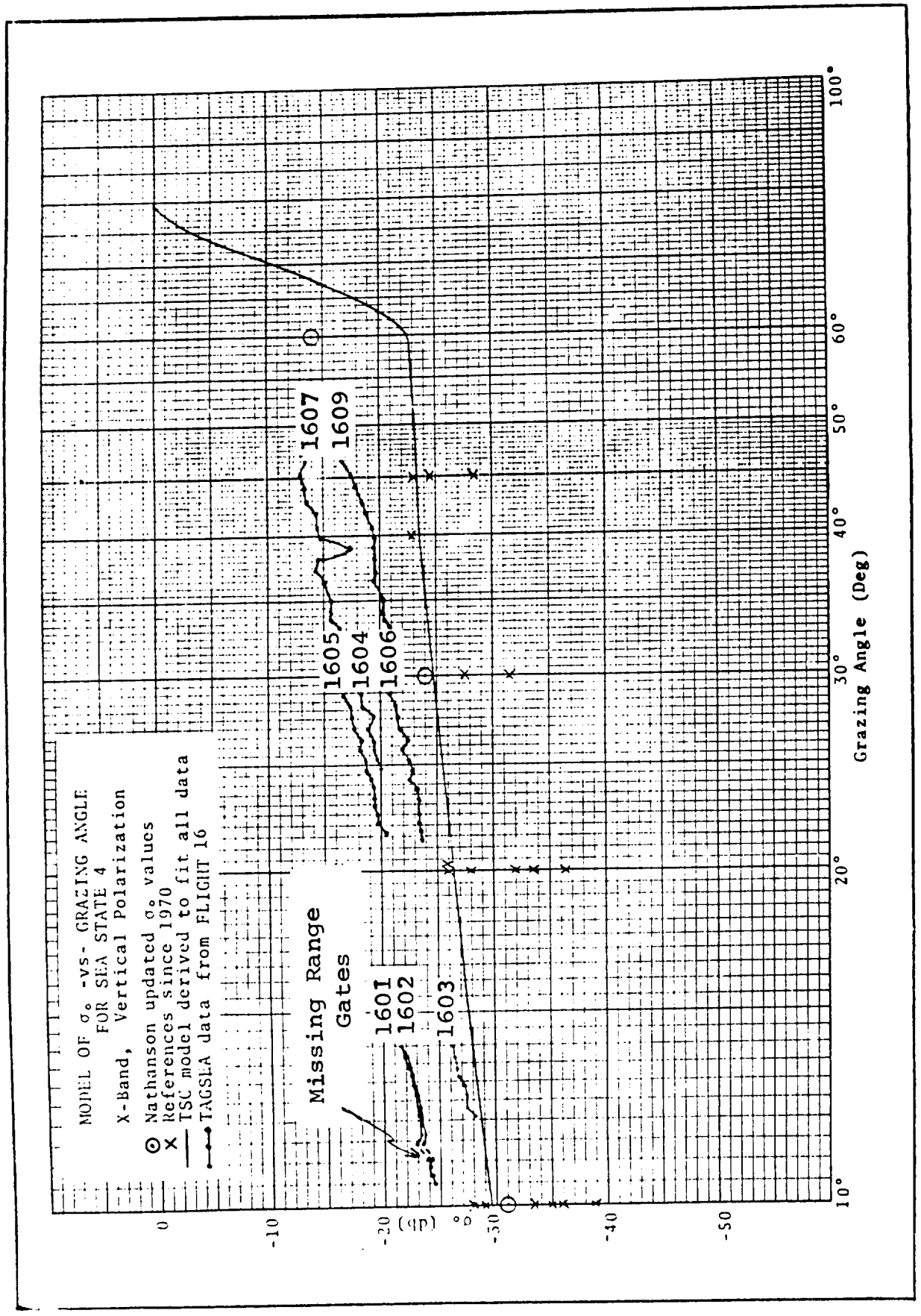

Figure 4-3 Clutter Comparison to Other Data-2

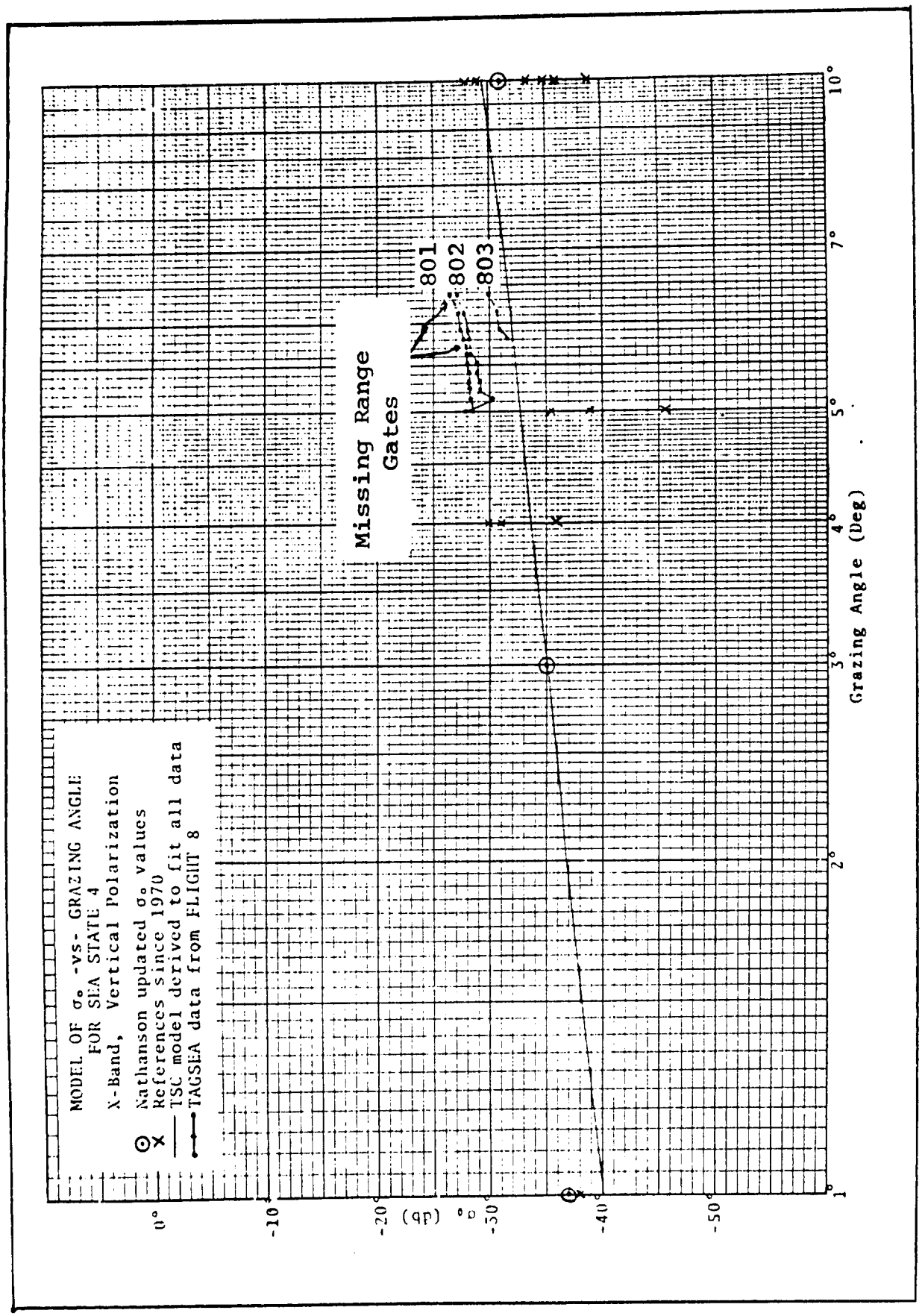

Figure 4-4 Clutter Comparison to Other Data-3

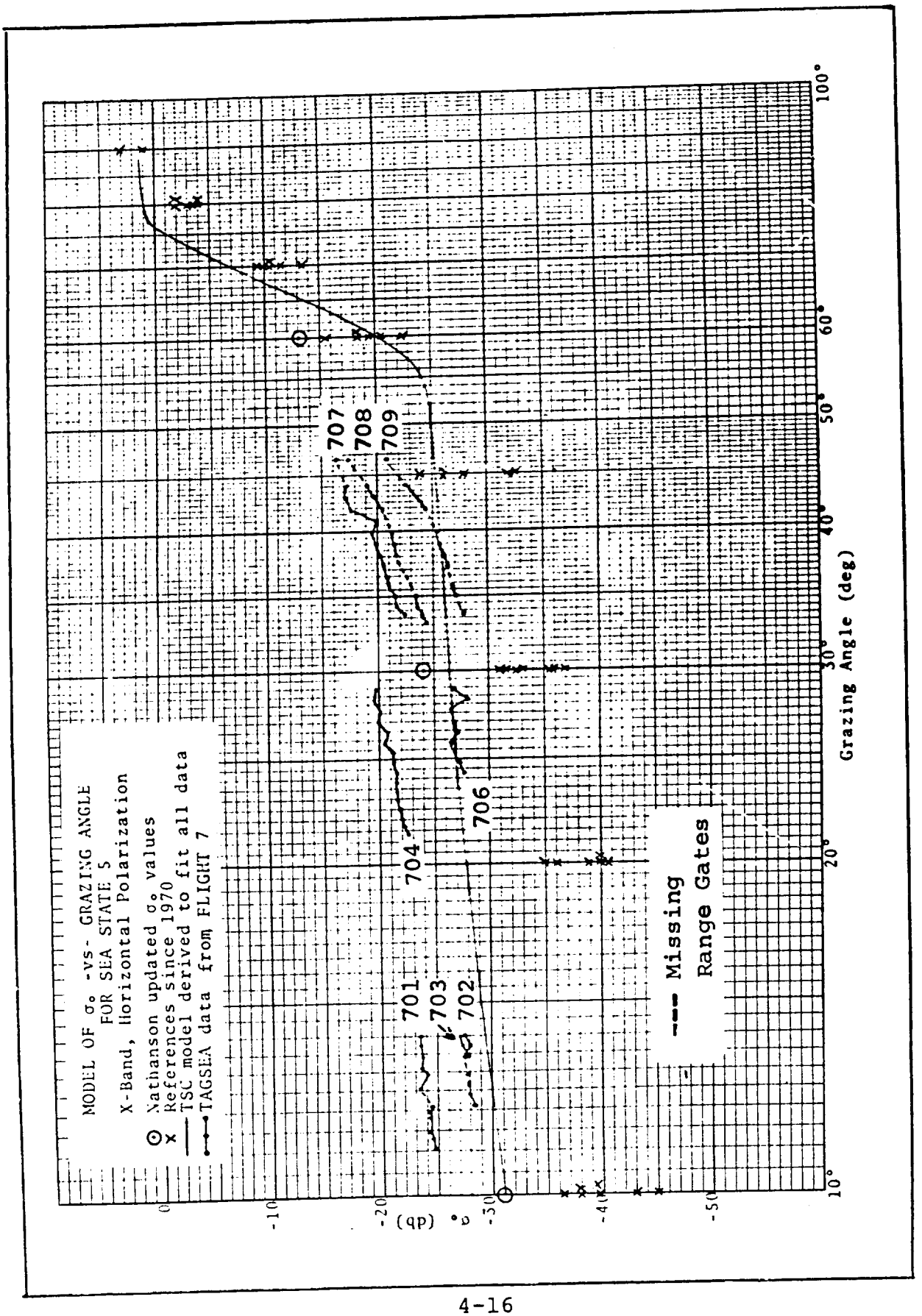

Figure 4-5 Clutter Comparison to Other Data-4

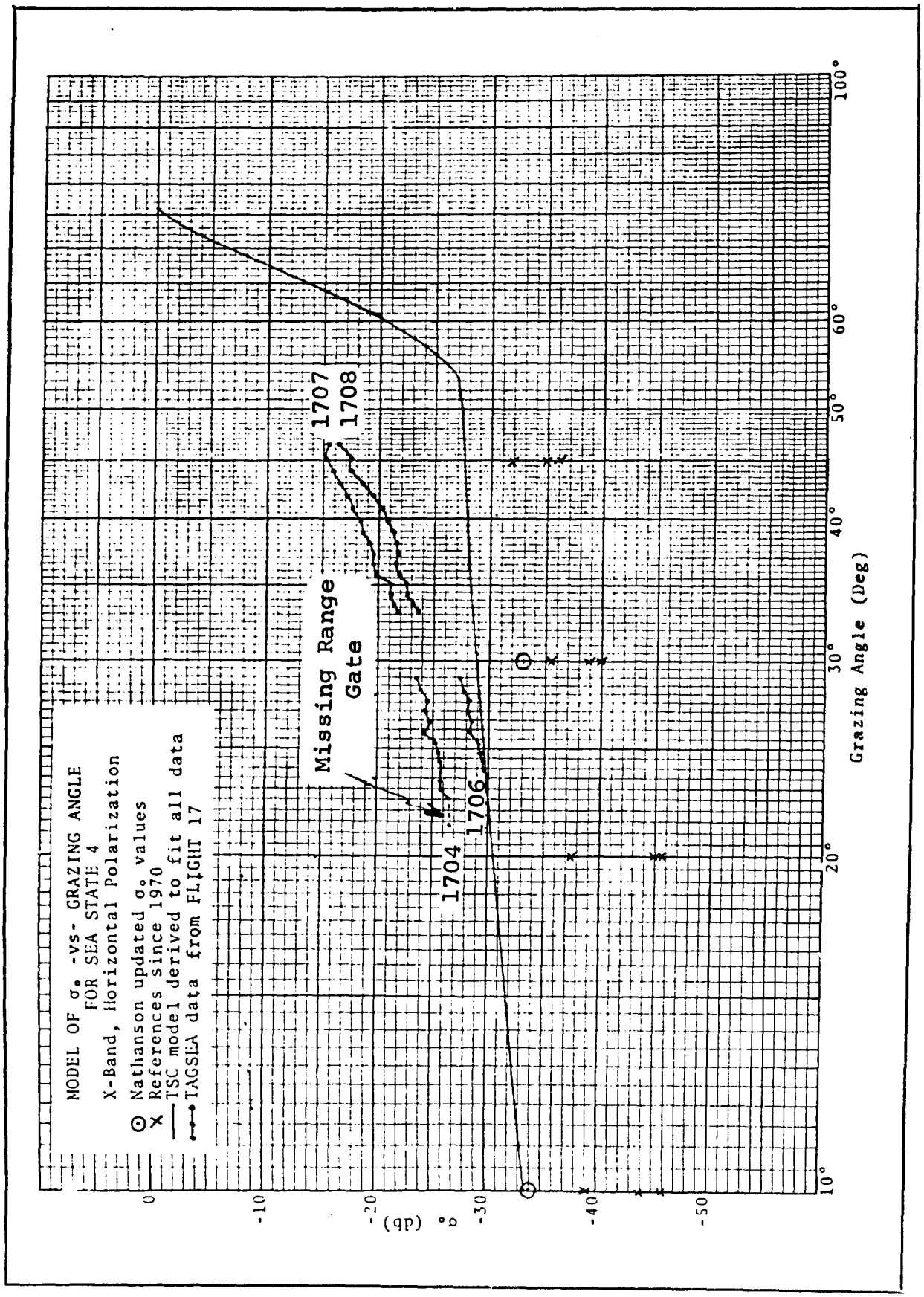

Figure 4-6 Clutter Comparison to Other Data-5

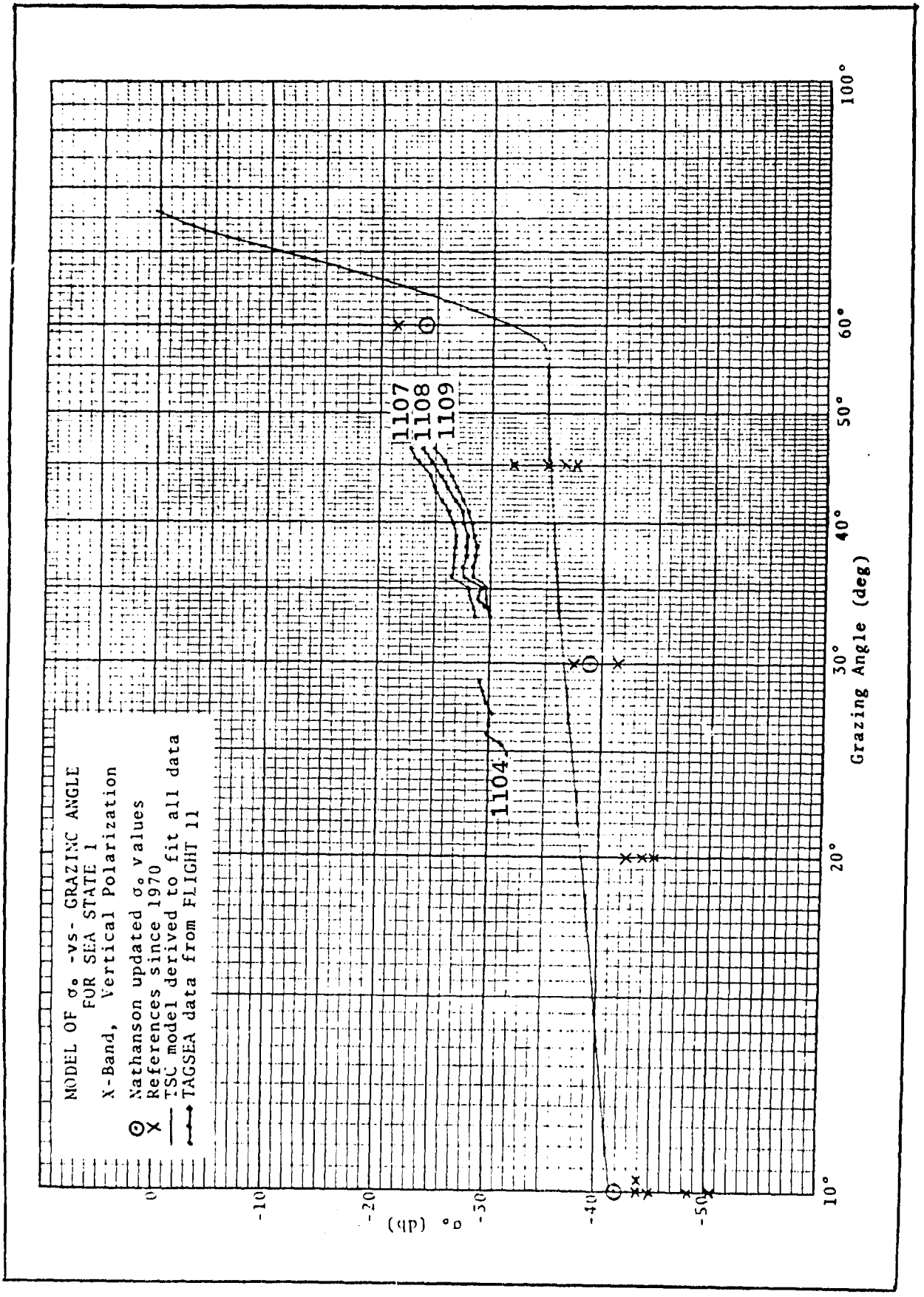

Figure 4-7 Clutter Comparison to Other Data-6

A total summary, with comparisons to the curves from Figures 4-2 through 4-7 is presented in Figure 4-8. The object is to consolidate the horizontal and vertical data for various sea states and present it in one figure for comparison purposes. The range of σ_o for each segment of TAGSEA data shown covers the same range as in the previous figures.

In keeping with the policy of only characterizing parameters for which a sound and extensive data base exists, only clutter models covering sea states 4 and 5 for vertical and horizontal polarization were generated. Data on sea state 1 is too sparse and the data on sea state 3 is too ambiguous as to wind direction and is also too sparse.

4.4 Distribution Functions

Much of the work towards clutter modeling was on determining the distribution functions of clutter returns. It was necessary to determine these functions for the conditions already mentioned and further to define them with some exactness out to the 10^{-6} point. This subsection thus goes to some length to summarize the results of this work and to explain the various methods and plots used.

4.4.1 Generation of Distribution Functions

One of the principal outputs generated during the course of the work was the distribution function of the clutter return. This subsection describes the various ways in which they were generated and are presented as well as some of the implications of the methods used. This will be done using one of the runs, number 403, as an example not because it is ideal but because it has variations and data anomalies which had to be considered in the analysis process.

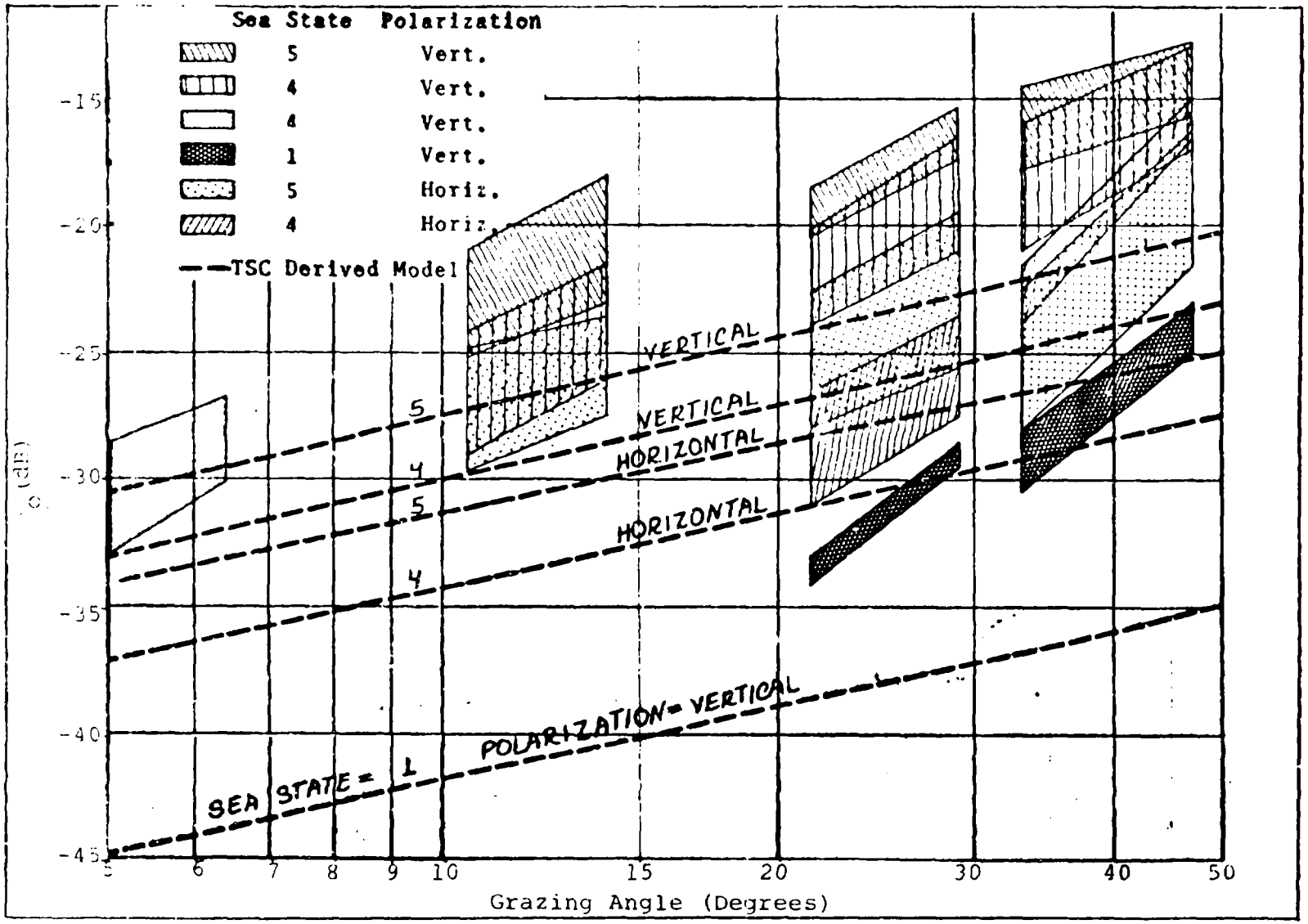

Figure 4-8 Summary Mean Backscatter Coefficient

When run 403 was reduced, the data from each range gate was divided into 54 time blocks, each corresponding to 600 FFT intervals, and a histogram was made from each block. These histograms each contained 600 X 32 = 19,200 samples sorted by amplitude into 1024 bins, and represent the data obtained from a radar window approximately 100 feet wide by 2200 feet long. The 2200 foot dimension is divided into 32 doppler resolution cells each about 67 feet wide. As the aircraft moved, the window moved lengthwise over the surface of the ocean. Each 600 FFT time block corresponded to 5.4 seconds, so the aircraft flew during this time 5.4 X 240 = 2268 feet, or approximately the length of the window. Therefore a new patch of sea was seen in each successive histogram, except for straddling. For run 403, twelve range gates, namely 0 and 2 through 12 were reduced. Range gate 1 was garbled, and range gates 13, 14 and 15 did not have an adequate clutter-to-noise ratio. The number of histograms produced in run 403 is given by multiplying the number of time blocks by the number of range gates, and is 54 X 12 = 648. The total number of samples is given by multiplying 648 X 19,200 = 12,441,600 for the whole run, providing about 12 samples at the 10^{-6} level.

Before the histograms from different range gates were combined, they were normalized to the same mean. This was done in two steps. First, a canned set of weighting factors was used to make the means approximately equal before sorting. Then the 54 histograms for each range gate were combined and a range gate mean determined for each. Figure 4-9 shows not only the mean, but also other points on the distribution function. The labels on the curves are the probability that the ordinate will be exceeded, except for the top one which is the maximum, and the bottom two which are the mean and median. The upward trend in the mean shows that the canned set of weights did not fully reflect the behavior of the actual data. This variation in

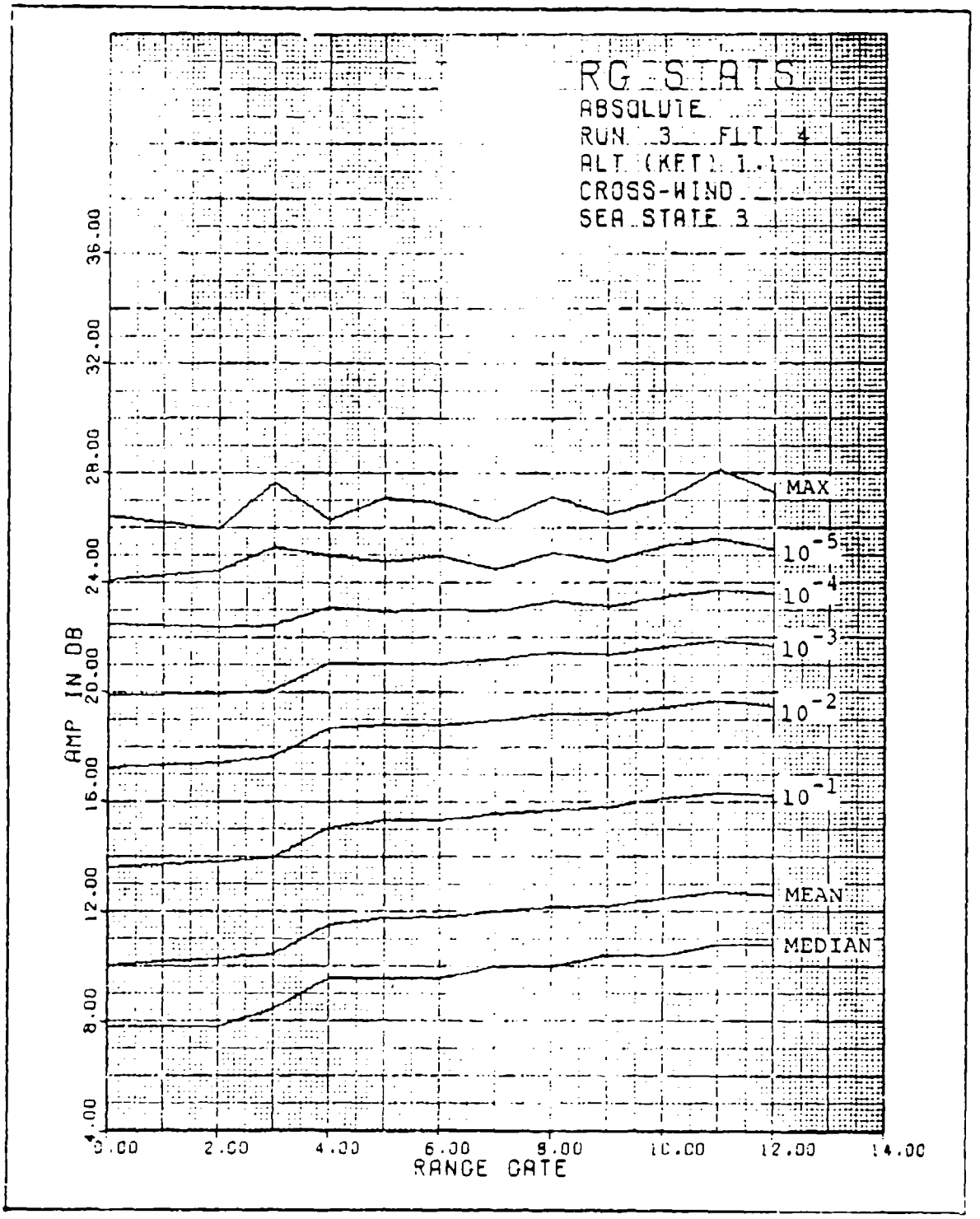

Figure 4-9 Distribution vs. Range Gate

mean was removed as shown in Figure 4-10. Now each distribution can be compared, showing agreement to one or two decibels for all curves through the 10^{-5} level. The combined distribution from these range-normalized distributions is plotted in Figure 4-11. The abscissa is Amplitude Relative to the Mean in dB and the ordinate is LOG Q(x) = LOG(1-P(x)).

Range gate normalization as explained above was important in development of the distribution functions. As can be seen from Figure 4-11 the determination of the location of points on the distribution (e.g. 10^{-3}, 10^{-4}, 10^{-5}, 10^{-6}) relative to the mean of the distribution defines the curve, and it is desirable to locate each point with as little scatter of the data as possible. If one point is now examined, the 10^{-3} probability point, the extent to which the scatter has been reduced by normalization can be appreciated.

Without normalization, the number of returns above a threshold which is set for a nominal 10^{-3} probability varies over a factor of 3 to 4 for the different range gates. The uppermost graph of Figure 4-12 shows, for run 4 of flight 6, the number of returns which exceeded the threshold as a function of range gate number. The second graph shows the relative mean power also by range gate. When the range gate returns are normalized by their respective means the number of returns exceeding the threshold is practically uniform over the range gates as shown in the thid graph. Thus, the number of returns above the 10^{-3} point which contribute to the formation of the distribution function is constant from range gate-to-range gate.

4.4.2 Variation of the Mean

It had been suggested that the clutter cross-section distribution could be modeled as a local distribution with a varying mean. In order to see variations in the behavior of the mean, the sum of the outputs from all doppler bins was

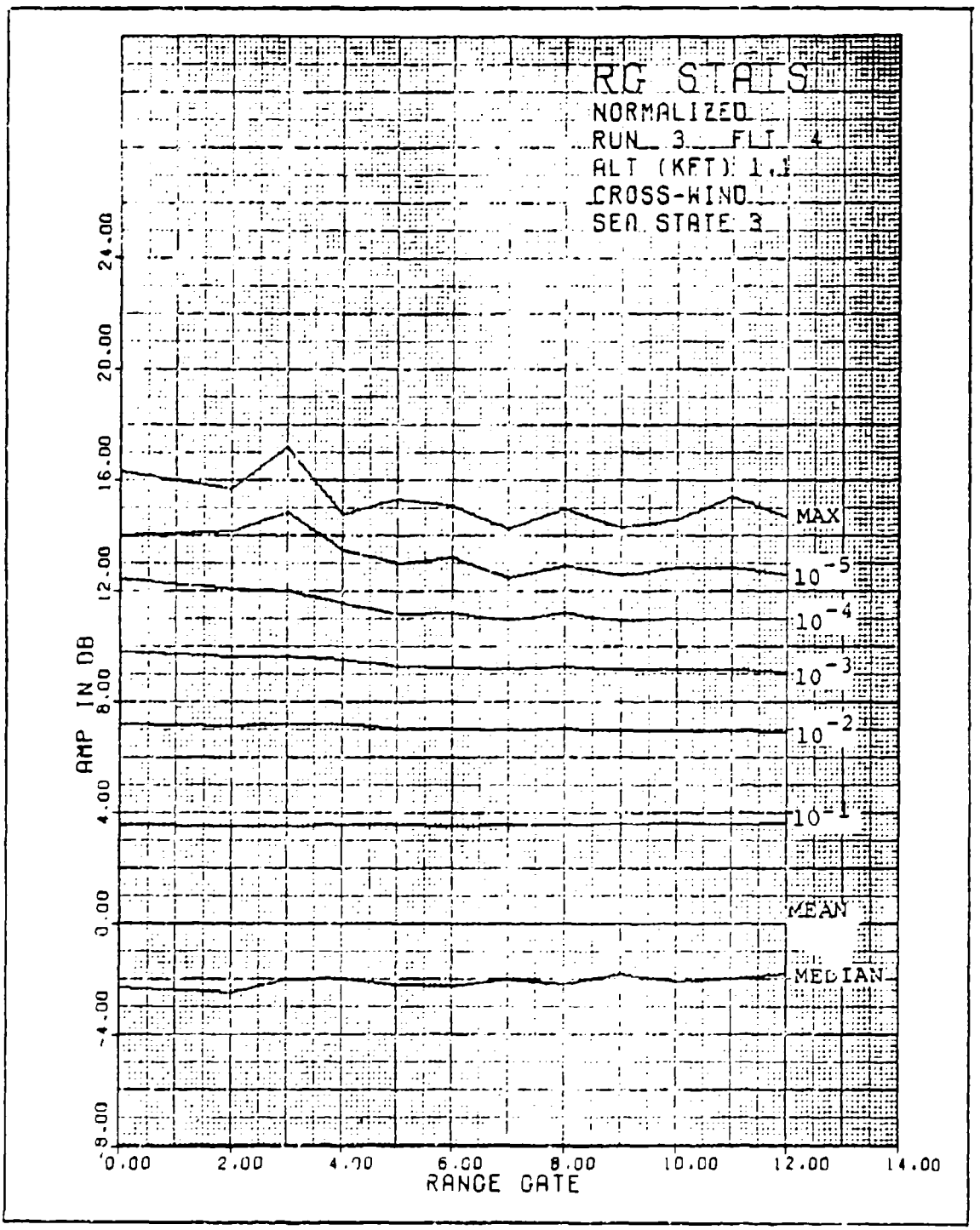

Figure 4-10 Distribution vs. Range Gate Mean Variation Removed

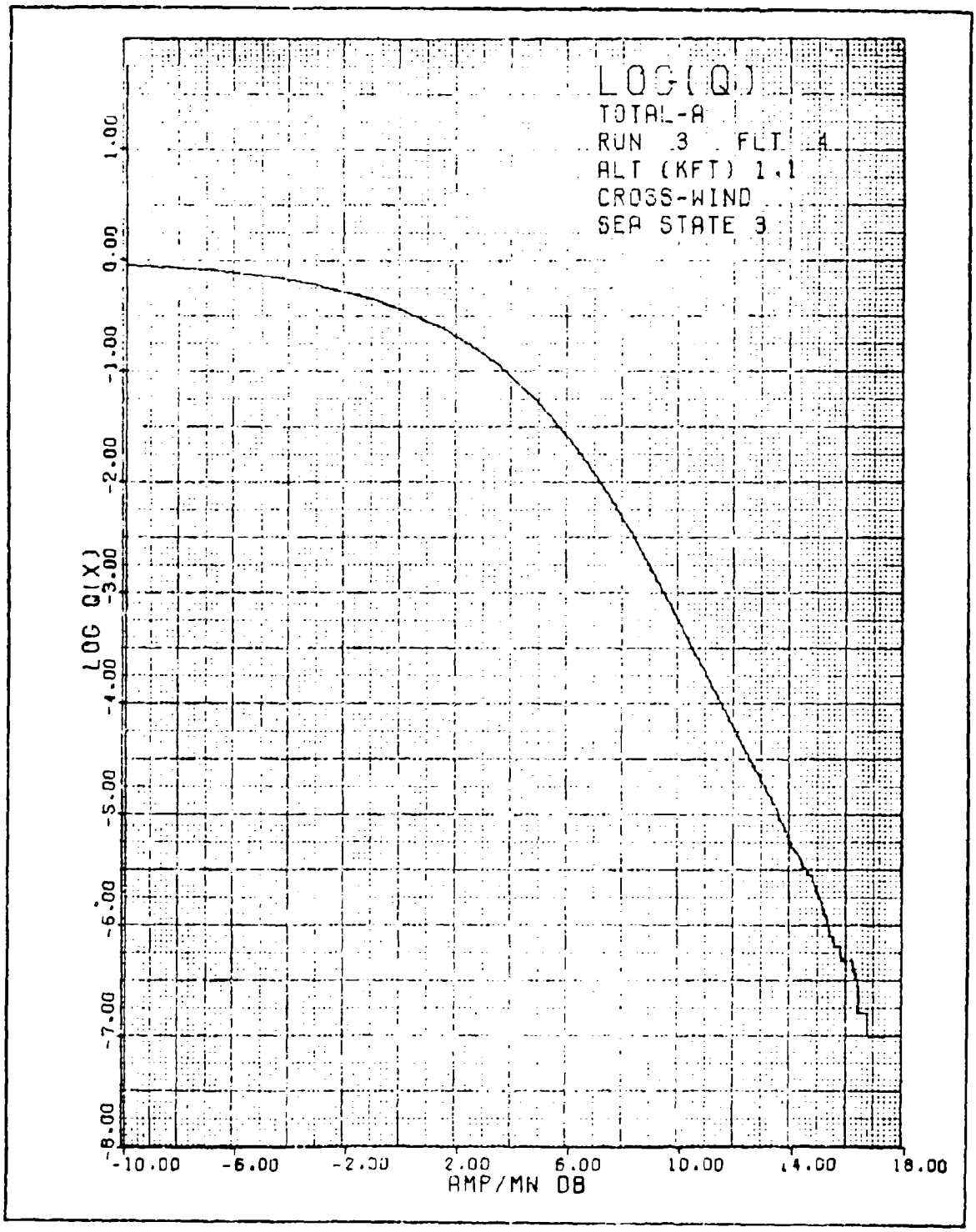

Figure 4-11 Distribution of the Range Normalized Histogram

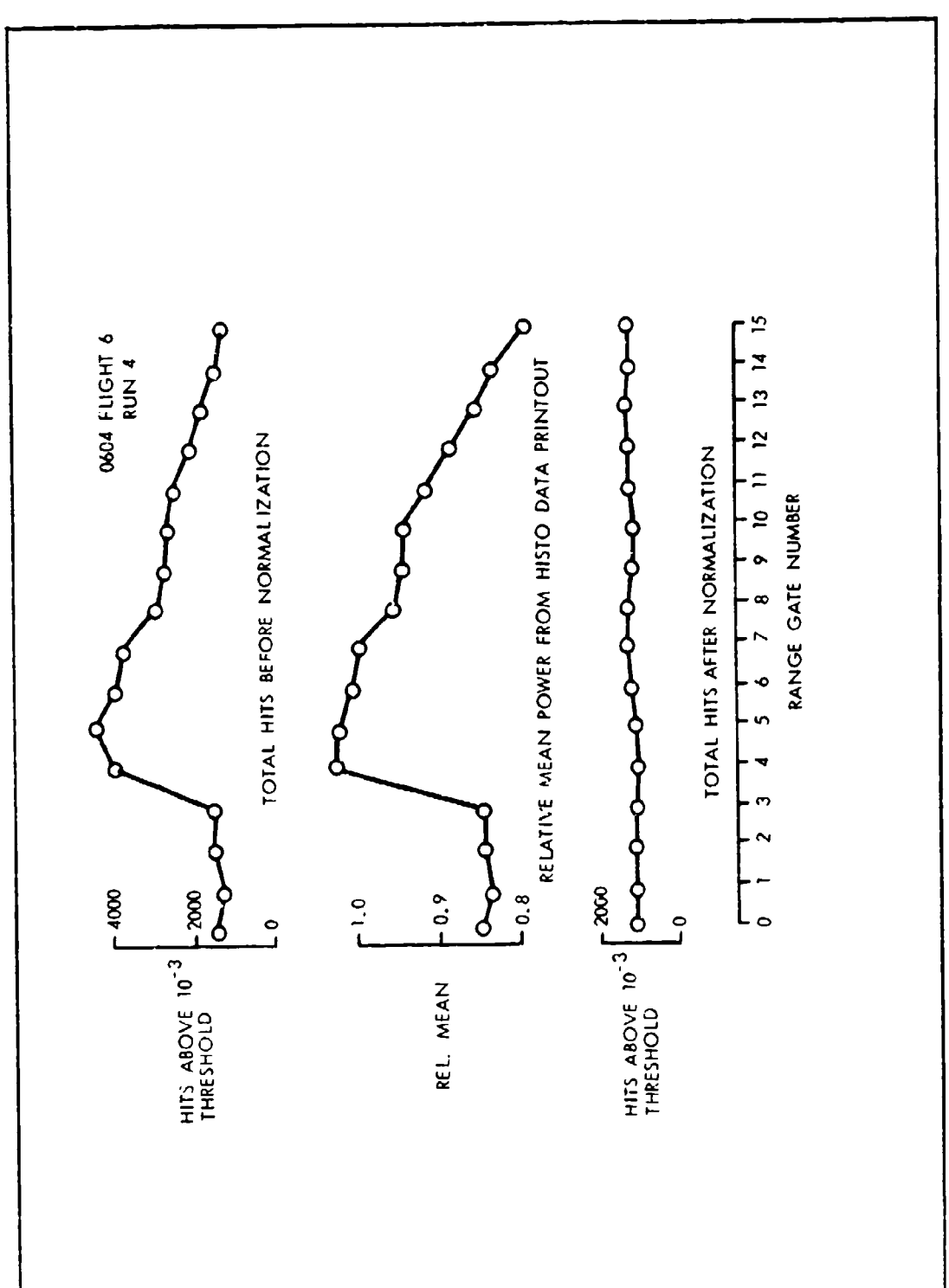

Figure 4-12 Range Gate Normalization

recorded for each FFT from each range gate. These were summed in groups of 100, and plotted in Figure 4-13. The uppermost plot is range gate 0. The gap below is left by the missing range gate 1, and the remaining plots are range gates 2 through 12. Each range gate outputs is offset by about 2dB from its neighbors for clarity. The low portion starting at time 330 is the receiver noise sample, and the raised portion which follows is the calibration signal. (The calibration signal is not to scale on this plot.) If the clutter portion of the plot is examined, dropouts can be seen in range gates 5,7 and 10. Also a drop-out can be seen in the noise portion of range gate 4. Neglecting these dropouts, it may be seen that except for some local phenomena between 100 and 140, the deviation is approximately 1/2dB rms during the clutter portion. On the other hand, the deviation during the noise portion is only about 1/10dB rms. This shows that the indicated clutter mean variations are due to actual change in the mean, and not due to sampling effects from the local distribution.

It is possible to estimate correlation by eye from this plot by seeing how rapidly the mean cross-section changes with time and from range gate to range gate. Keeping in mind that this plot represents an area about 1/4 nm wide by 20 nm long, it may be seen that the local phenomena cover spots of the order of hundreds of feet in diameter. The valleys indications are probably effects of receiver noise. However the peaks are an accurate indication, and they are more important, since they cause extended tails in the distribution.

The distribution is plotted as a function of frame number (5.4 sec/frame) in Figure 4-14. The correspondence with the mean plot may be checked by noting that 600 FFT's are equivalent to one frame. The valley at frame 17 is seen to correspond to 100 point on the mean plot. Also, the peak at frame 23 corresponds to the 137 point. It is apparent then that there is good correspondence between the plots.

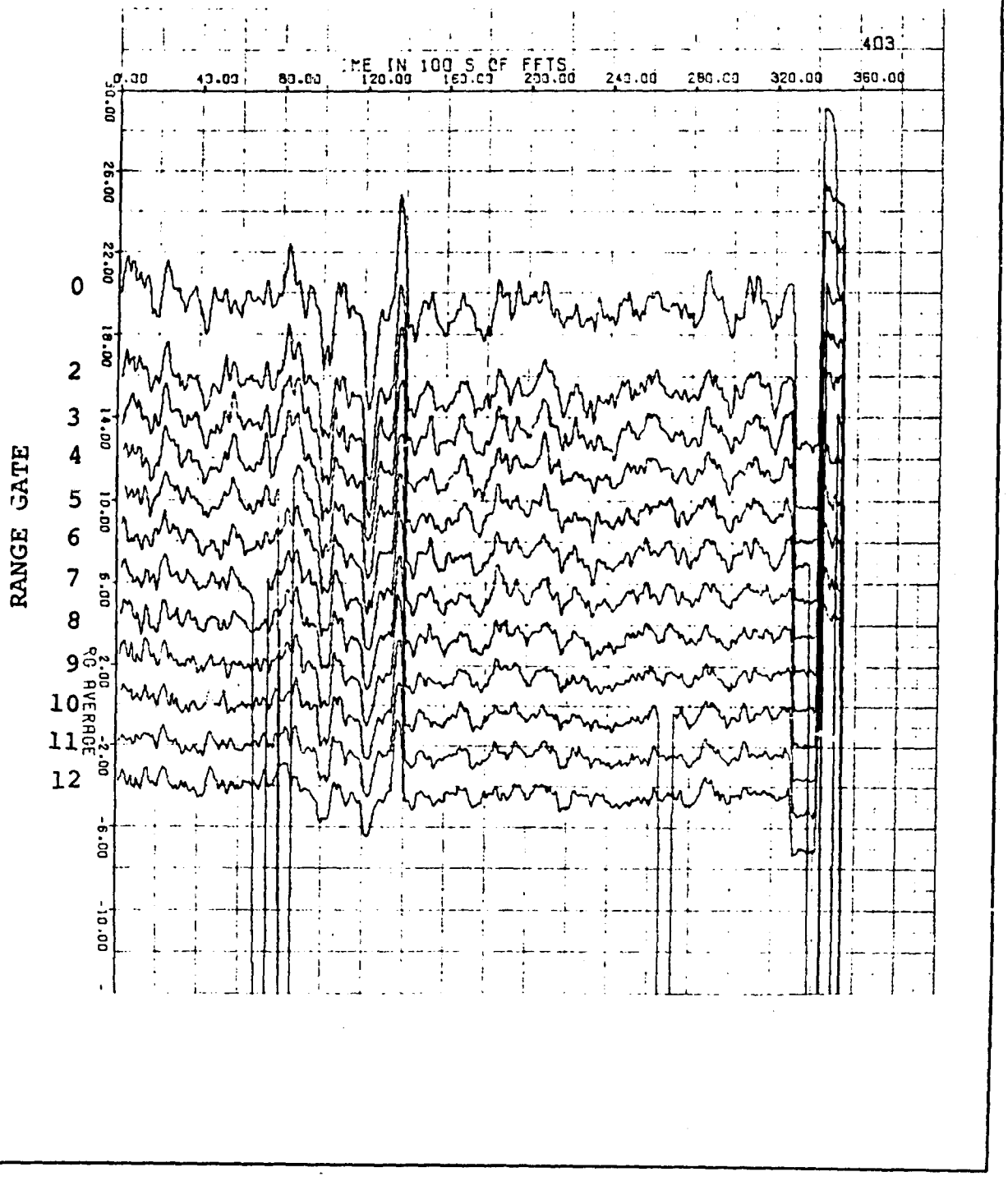

Figure 4-13 Clutter Means vs. Time

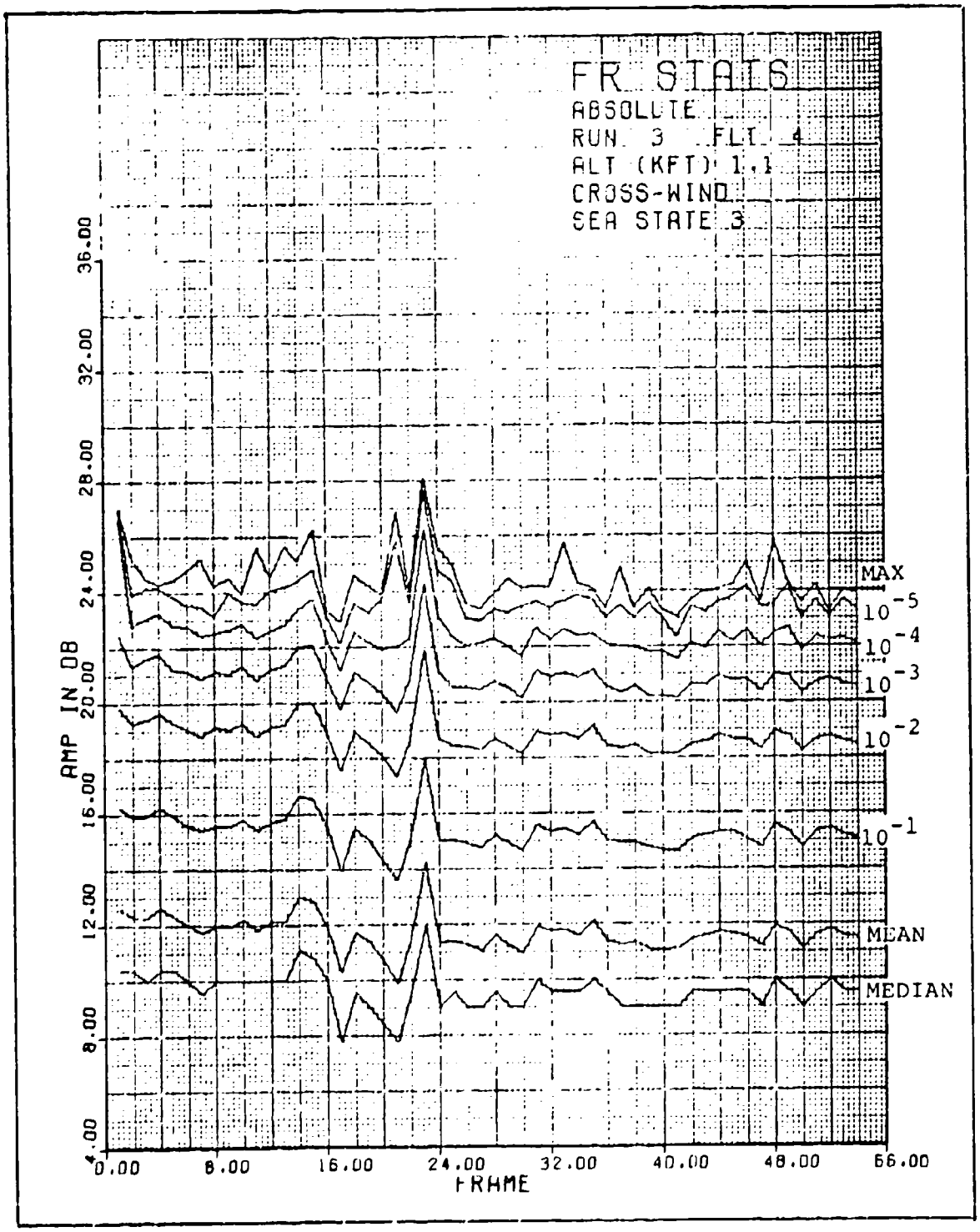

Figure 4-14 Distributions vs. Time (Range Gates Combined)

Thus the suggestion of the varying mean appears to be reasonable.

4.4.3 Normalization of Distribution Functions

Presuming then that the mean does vary with time (frame) it is instructive to explore the effect of normalization further. Figure 4-15 repeats the distribution vs. time of Figure 4-14 except that it has been normalized to the mean for every frame of 5.4 seconds which is equal to 600 FFT's. The smoothing effect is immediately apparent. Comparing the 10^{-5} level of this figure with that of the distribution of Figure 4-11 which was normalized by range gate only, it is seen that the frame normalized curve has a value of about 12dB above the mean while the range gate normalized level is $13\frac{1}{2}$dB. Thus the variation of the mean increased the level of the apparent tail by over 1dB.

It is of course possible to combine the two types of normalization and this was done. The result is a distribution which is normalized both with respect to range gate and mean variation. A distribution plot is shown in Figure 4-16 where it is noted that the 10^{-5} point occurs at the 11dB point. This suggests that frame normalization is more important than range gate normalization in determining the location of the tail of the distribution. Such a conclusion however presupposes . use for the distribution which inherently determines the mean every 5 seconds or less. This is not always the case.

In the work that follows both types of normalization have been carried forth. Those distributions which are only range gate normalized are referred to as A-type and those which are frame normalized in addition are referred to as N-type.

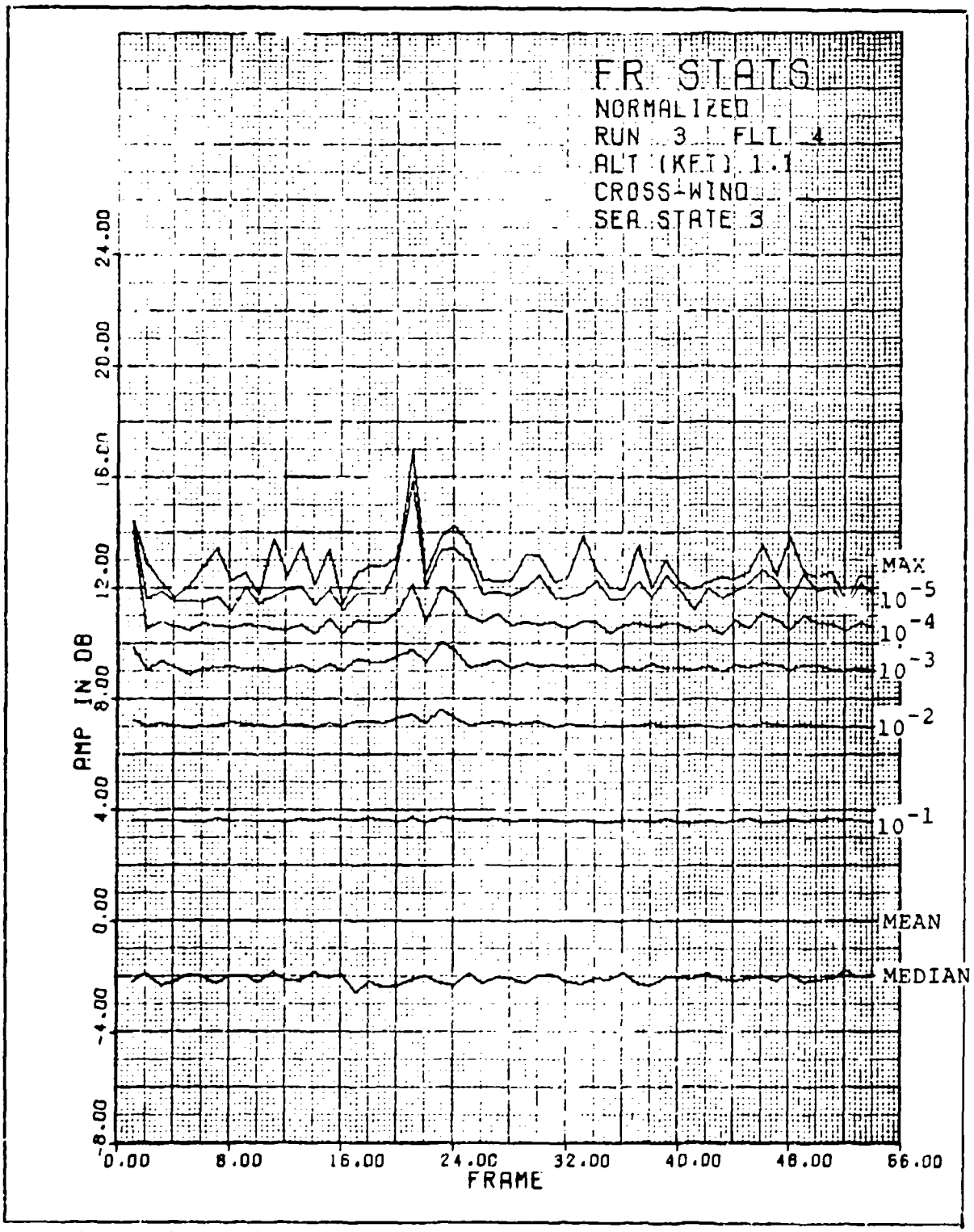

Figure 4-15 Distribution vs. Time (Range Gates Combined) Normalized to Frame Mean

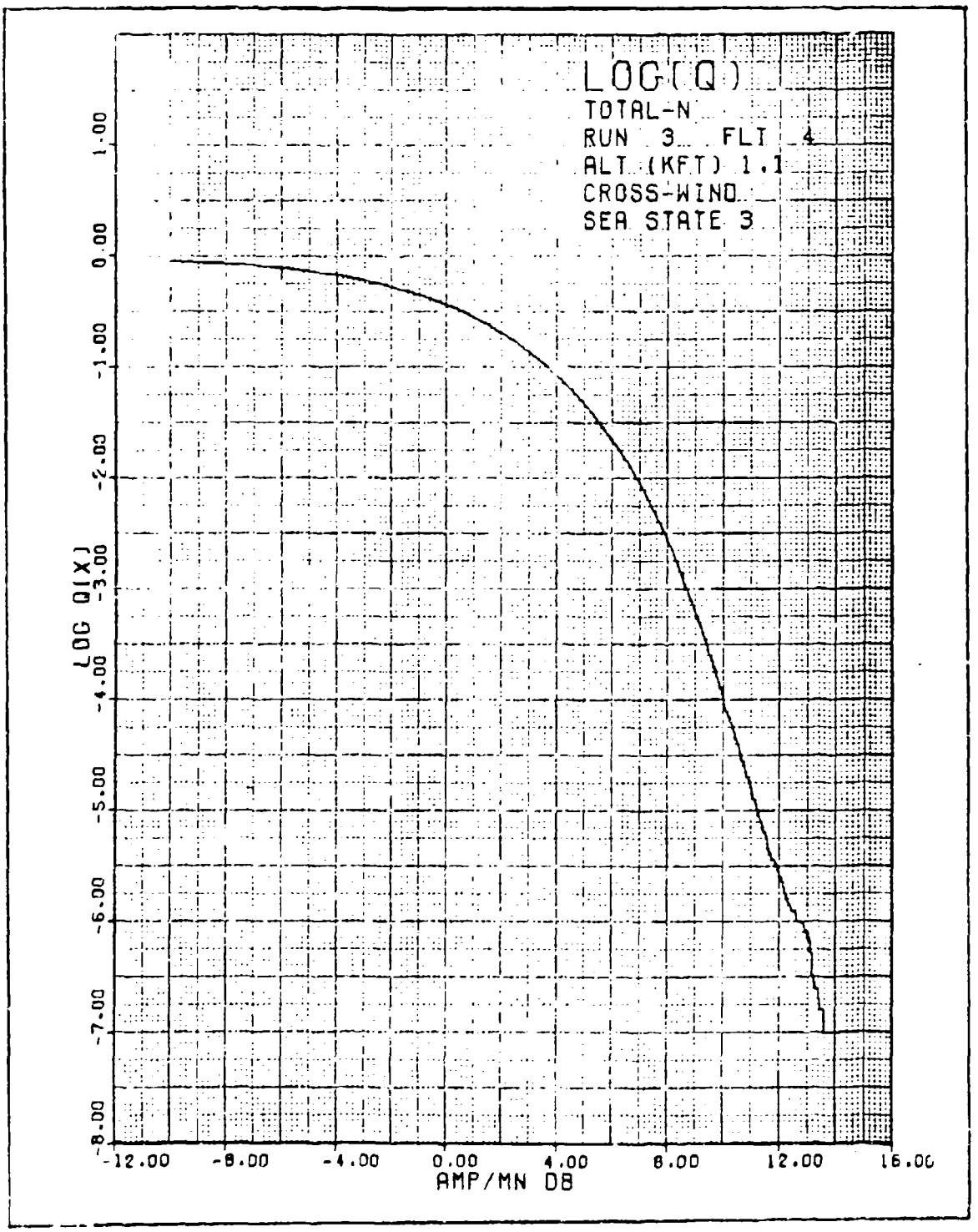

Figure 4-16 Distribution, Normalization by Range Gate and 600 FFT Frame

4.4.4 Shape of the Distribution

The ranges of distribution for horizontal and vertical polarization are shown in Figure 4-17. These were based on the A-type normalization which combined the distributions about the 300 second mean in each range gate and are for the extremes of the valid runs which were analyzed. We see that vertical polarization gives a smaller tail-to-mean ratio than horizontal polarization. Since these were normalized about long-term means, the tails were subject to increases by local variations. The effect of this variation was explored by processing the extreme runs with a 5.4 second normalization time (N-type normalization). The extreme distributions for horizontal polarization stayed within 1/2dB of the previous normalization. However, for vertical polarization, the longer tailed distribution for run 403 moved in appreciably to the dotted curve marked 403N. Curve 803 remained essentially the same.

For distribution 403N, below $P_f = 10^{-5}$, there is a break in the curve. This indicates that there is possibly a second process causing high amplitude echoes.

In examining the distribution curves, it was discovered that polarization affected the dependence of distribution tails on grazing angle. Figure 4-18 shows the general trends. These plots are for the local distribution. That is, they apply to N-type normalization. The 10^{-6} point appears to be relatively constant for vertical polarization, but in the case of horizontal polarization, the 10^{-6} point falls 3dB as grazing angle increased from 10° to 40°. The 10^{-5} point tracked these trends very well but of course with an offset.

4.4.5 Spatial/Temporal Autocorrelation Functions and Power Spectral Densities

Further characterization of the clutter returns were made in terms of their autocorrelation and spectral density. These were uniformly uninteresting in terms of defining clutter

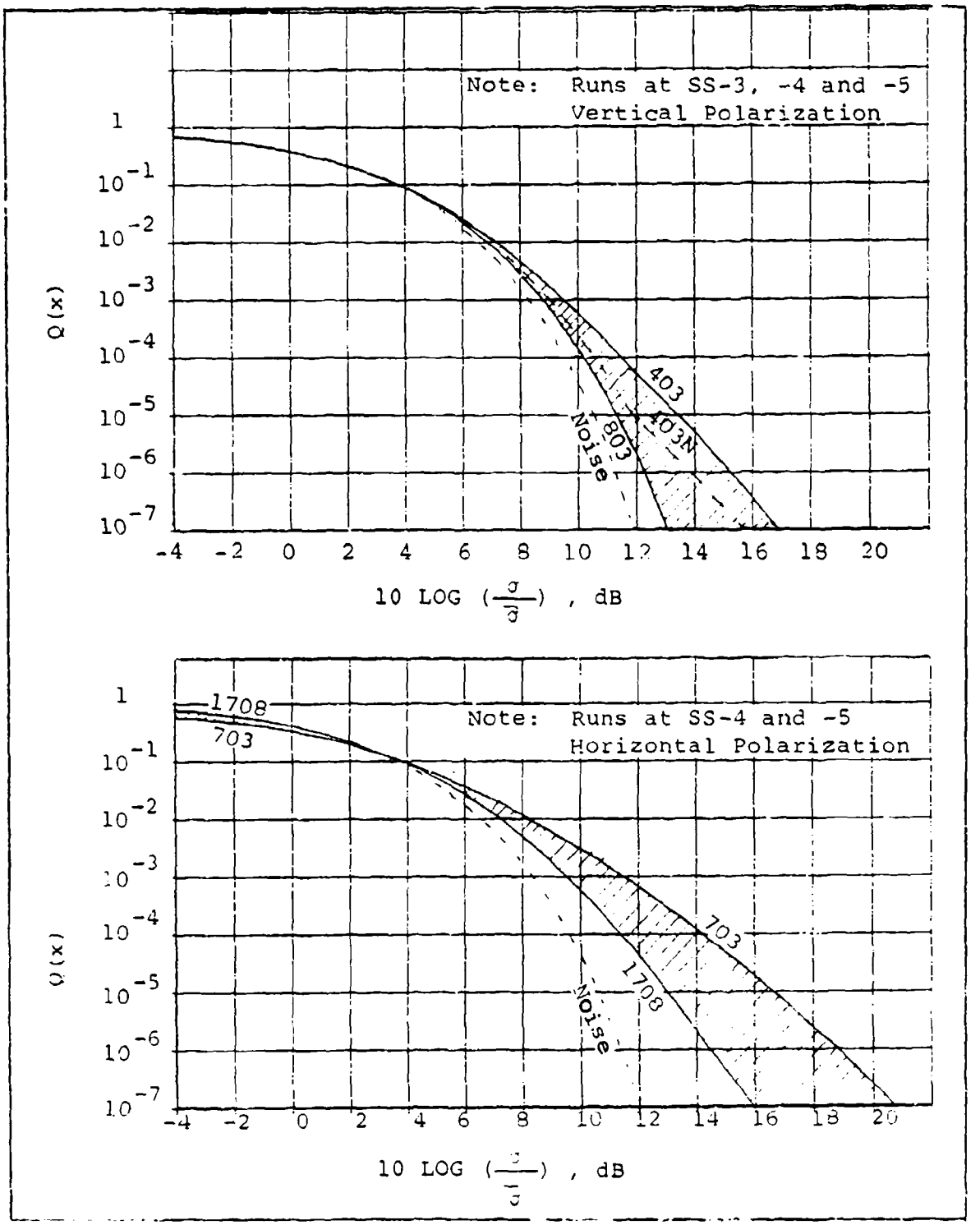

Figure 4-17 Range of Distributions Encountered

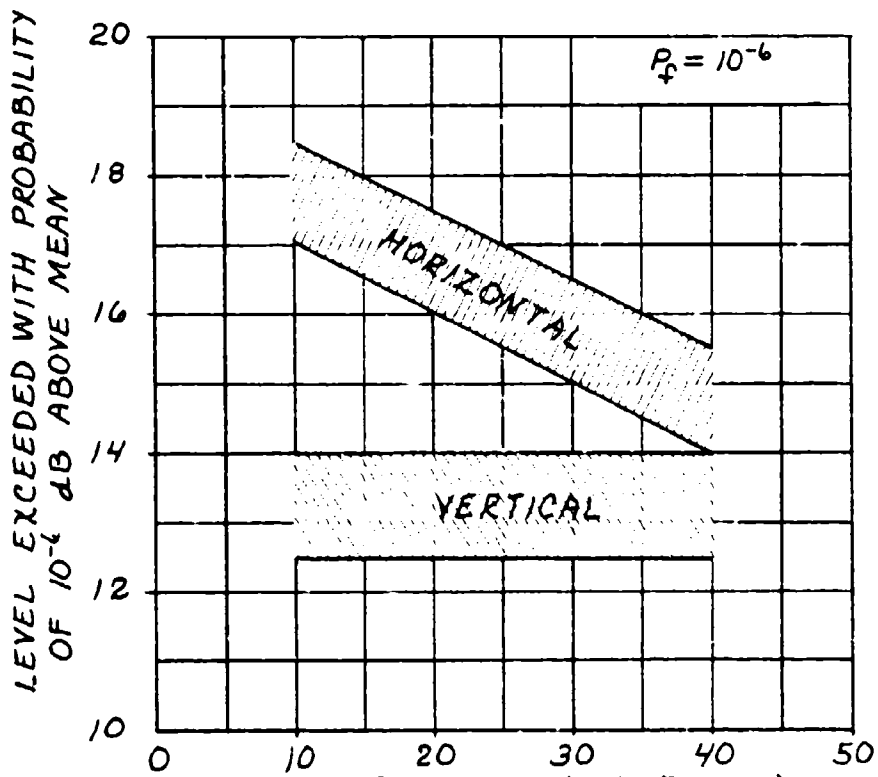

Figure 4-18 Effect of Polarization on Tails of Local Distribution

since they showed that the clutter returns are virtually uncorrelated. This statement does not however apply to the variation of the means of the distributions which will be discussed presently.

Very small correlations which do exist are best brought out by examining the variation of the mean where these effects are averaged over much longer times, which makes them more measureable.

Both the spatial and temporal autocorrelation functions and power spectral densities are similar in that the autocorrelation function is approximately an impulse function at the origin and the corresponding power spectral density is relatively flat. Figures 4-19 through 4-22 are typical examples. It should be noted that a perfectly flat spectrum would result in an impulse at the origin of the autocorrelation function.

Although it cannot be seen on many of the autocorrelation plots the autocorrelation function does indeed reach 1.0 at the origin. Also, the power spectra are zero at the origin since the mean of the data was removed before processing

The apparent increase in the autocorrelation function in the higher cell numbers of both the spatial and temporal varieties is due to an increase in the variance. This increased variance is the result of less and less data being summed into the autocorrelation function at these high "lag" values (cell numbers).

4.4.6 Comparison of Distribution Curves with Previous Data

Comparison data on distribution curves is rather sparse at this time and usually extends only to $P_f = 10^{-4}$ (which is, coincidently, the minimum probability encountered on most probability paper). TAGSEA data on the other hand allows determination of the distribution function to the 10^{-6} point and, with less accuracy, almost to the 10^{-7} point. In Figure 4-23

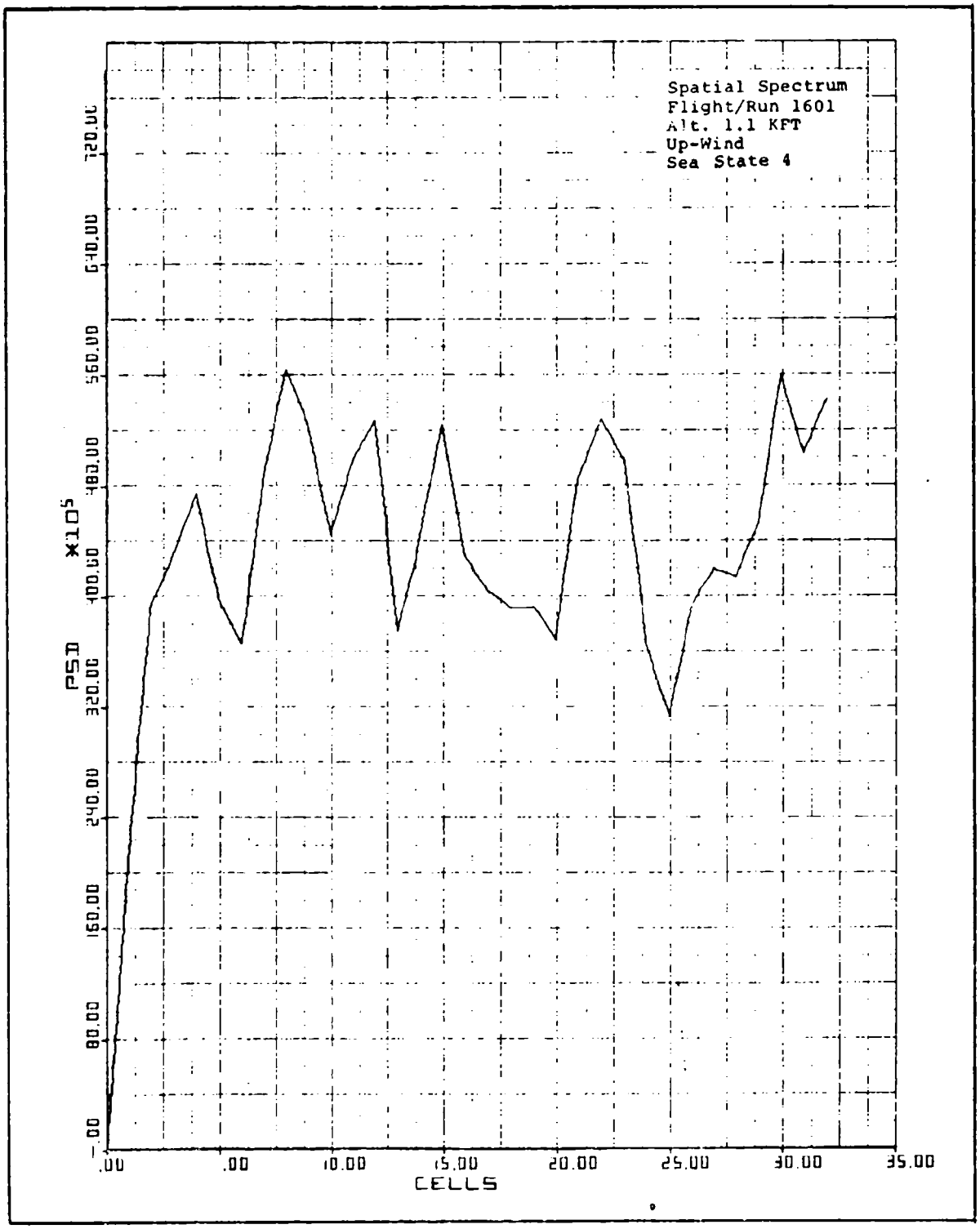

Figure 4-19 Spatial Spectrum

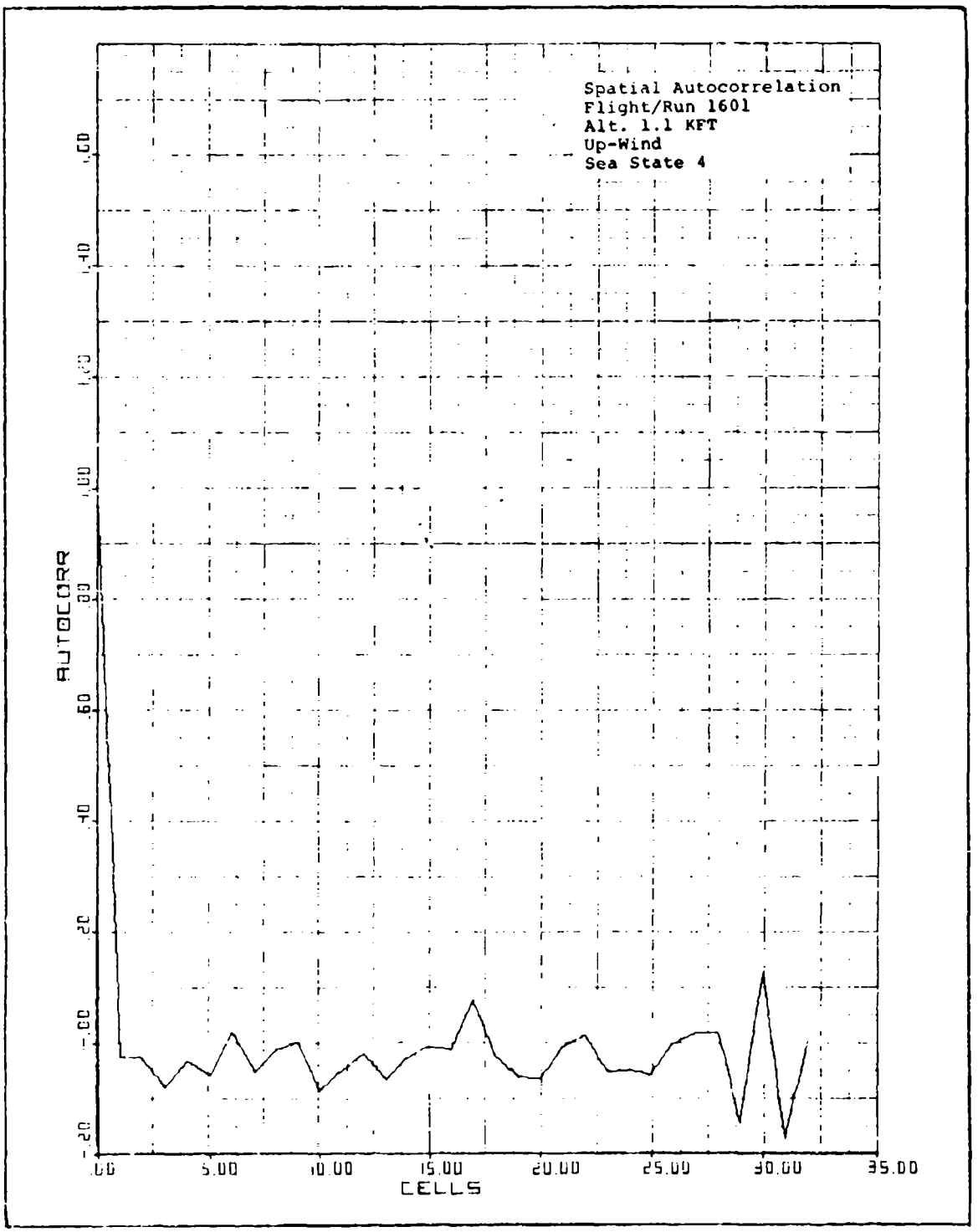

Figure 4-20 Spatial Autocorrelation Function

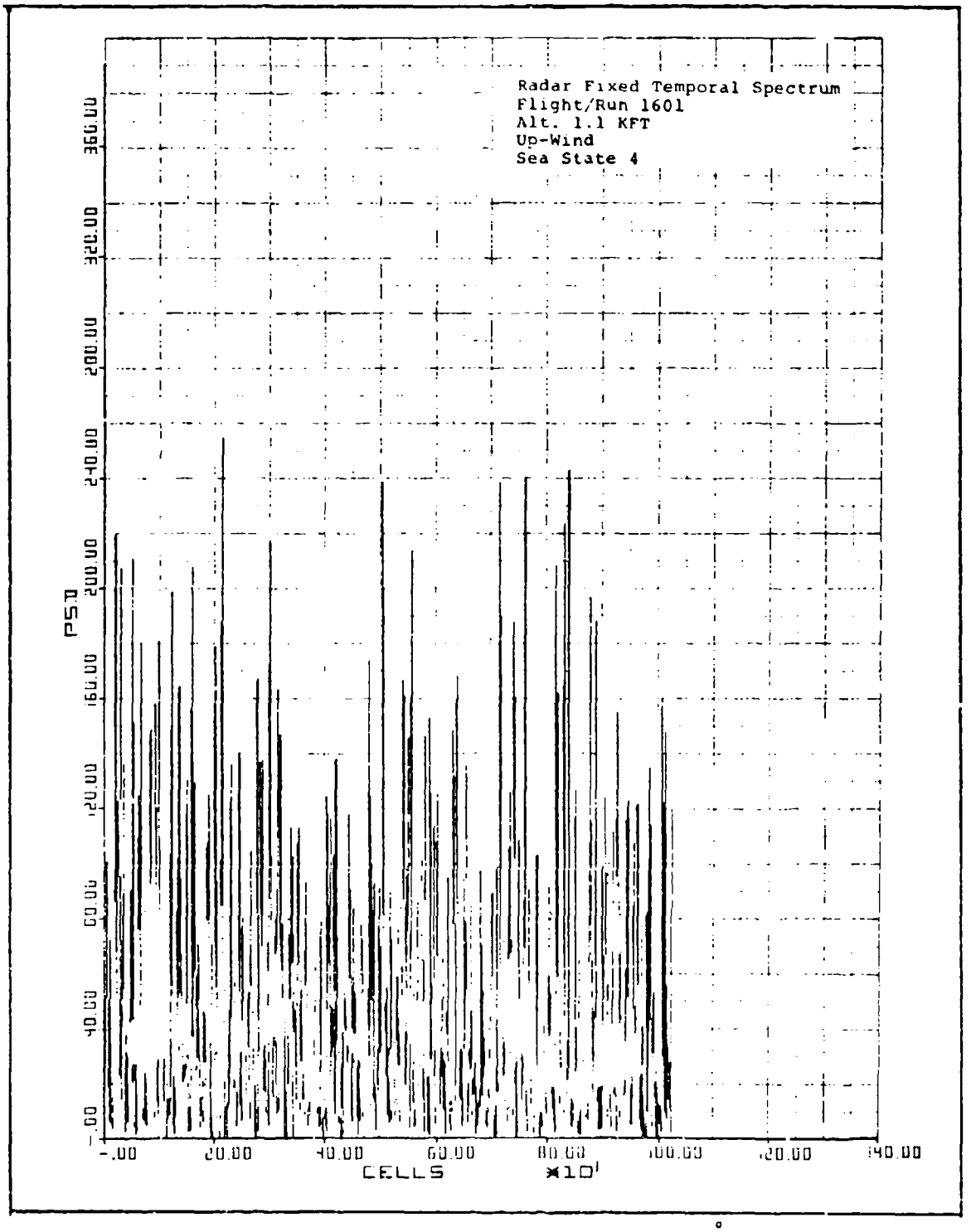

Figure 4-21 Temporal Spectrum

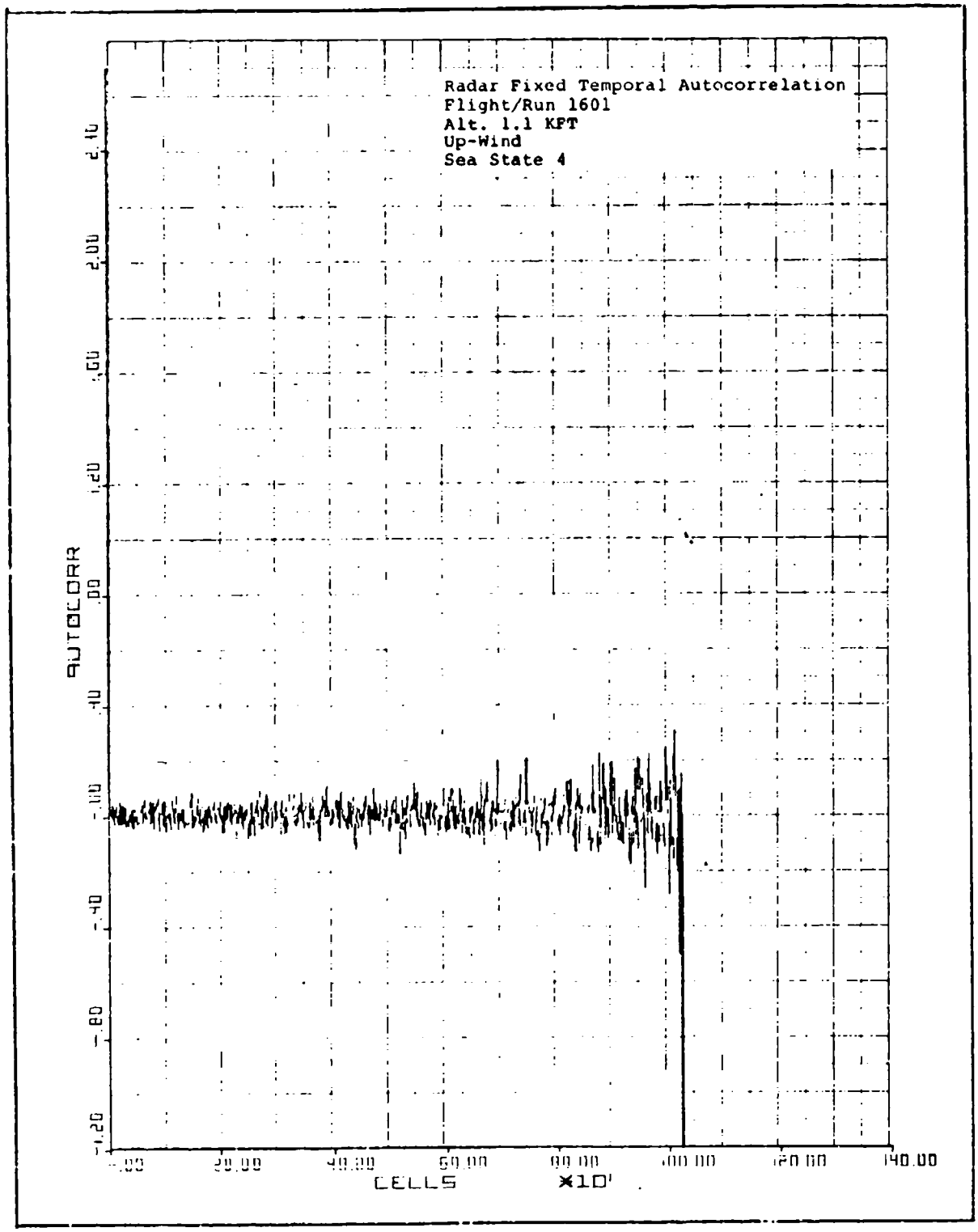

Figure 4-22 Temporal Autocorrelation Function

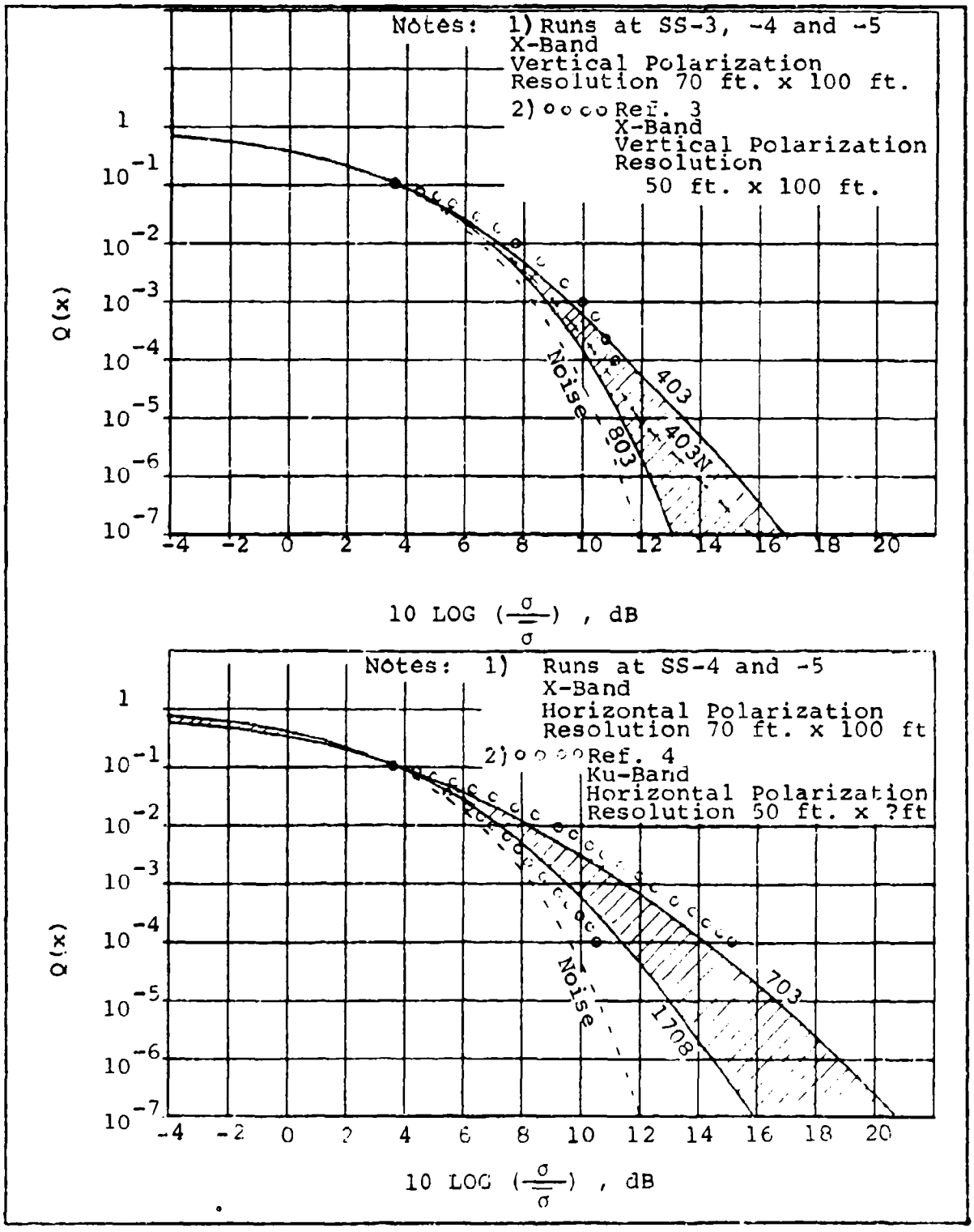

Figure 4-23 Distribution Comparison

distribution obtained from TAGSEA data are compared with data from two comparison sources. A noise (Rayleigh) curve is plotted for reference and extremes of the TAGSEA curves are shown with run number annotation. For vertical polarization, a curve from Trunk's simulation[3] is plotted. This curve is for X-band upwind aspect and for a long pulse case. The mean was not stated in the reference, however, a study of TAGSEA data shows that distributions seem to pass through the $P_f = 0.1$ point at a cross-section of about 3.6dB above the mean. Hence we match Trunk's curve at this point also. In the case of horizontal polarization, data from a memo supplied from APL[4] was used. The curves are interpolated in the memo from measured data points and show an excellent agreement with the shape of the TAGSEA data. Here the APL data was normalized to the mean so that it was not necessary to make any adjustment.

Based on these direct comparisons and on the general acknowledgement in the technical community that the tails of clutter extend further than noise (Rayleigh), the TAGSEA distribution curves are judged to be representative of sea clutter.

In summary, to the whole complex subject of distribution functions it may simply be stated that those developed during this program supply a good base for the clutter model and provide a range of distribution functions which are available and verified for use as either typical or extreme cases and for horizontal or vertical polarization.

---

(3) Trunk, G.V., "Modification of Radar Properties of Non-Rayleigh Sea Clutter", IEEE Trans. on Aerospace and Electronic Systems, p. 110, January, 1973.

(4) Sodergren, P.R., "A Revised Ku-Band Sea Clutter Model", JHU/APL memo MPD72U-033, dated July 19, 1972.

4.5 Analysis of Large Returns

Even though the distribution functions of the last subsection implictly contain information on large returns (in 10^{-3} through 10^{-6} points), a special analysis was made of this characteristic of sea clutter. This was done to gain a better understanding of the nature, occurence and interdependence of those large returns which are of foremost concern in setting the false alarm performance of missile seekers operating over the sea. The name, Hit Analysis, was given to this study.

Hit Analysis Outputs characterize sea clutter radar echoes exceeding an amplitude threshold. The threshold is set such that one hit in one thousand (10^{-3} nominal) will exceed the threshold on a statistical basis.

Clutter echoes exceeding the threshold, known as "hits", were recorded on magnetic tape and processed by digital computer. Cal Comp plots were generated for presentation of outputs from each run conducted during the flight test. Three forms of output known as Hit Counts vs. Time, Hit Maps, and Conditional Probability Maps were used for graphical presentation of Hit data.

Hit Counts vs. Time plots may be viewed as temporal displays of mean (average) hit levels in each range gate. The process is comparable to a moving window integrator used in some CFAR processors.

Hit Maps are spatial cross-range vs. down-range displays of numbers of hits in cross-range/down-range resolution cells. Synthetic aperture mapping techniques were used to map the range-doppler-time coordinates of each hit into sea space. Hit Maps are typically 16 range gates in cross-range by 126,000 feet down-range distance.

Conditional Probability Maps characterize the immediate range-doppler-time vicinity of rare events that have amplitudes exceeding a 10^{-5} probability threshold (T1). Hits exceeding another threshold (T2) set at 10^{-3} hit probability are accumulated in each cell of a 15 X 15 X 15 "conditional probability cube" centered on each rare event encountered during a run. An ensemble of all such rare events is used to estimate conditional probability by computing a ratio of number of hits exceeding T2 to total trials (normalizations) within each cell in the conditional probability cube.

Flight 17, run 7 (1707) was chosen as an example of the Hit Analysis outputs. Horizontal polarization was used during the data gathering flight test.

a) Hit Counts vs. Time

Hit counts vs. time for 1707 are plotted in Figure 4-24. Mean number of hits exceeding threshold in each range gate (0 through 15) are plotted against time in seconds. Data points in the plot are computed by summing hits exceeding a nominal 10^{-3} threshold over a block of 100 FFT time frames and dividing the result by 100 to compute the mean. The resultant "Mean Hits per block" as indicated on the ordinate of the graph is plotted versus "Time in Seconds" -- a number computed as the product of FFT Frame Time (128/12,000 = 0.0091428571 second) and block size. Therefore, mean hits per block data points are plotted every 0.914 second. The ordinate scale factor is 0.2 hits per major division. The smallest quantum step (i.e., one hit within a block) is 1/100 = 0.01 for coarse plots. The mean hit level within each range gate (RG) is roughly the product of hit probability (10^{-3}) and the number of doppler filters (32), or 0.032. The mean hit level for the range gate sum is normally increased by the total number of range gates making the mean hit level 16 X 0.032 = 0.512. Because range gates 3 and 15 were deleted from the hit tape in 1707, the mean hit level is 14 X 0.032 = 0.448. Mean hits for the RG sum are scaled down by a factor

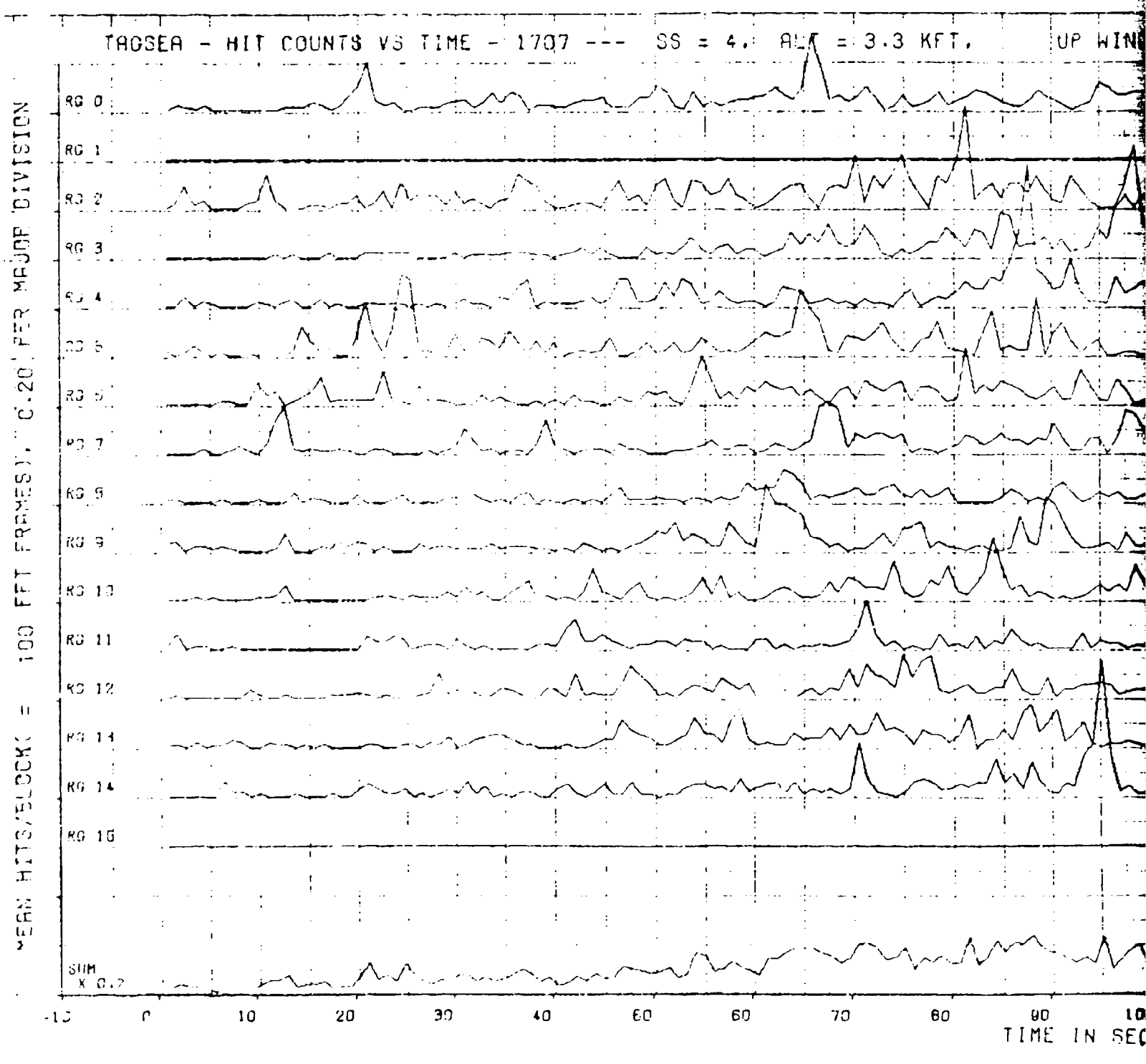
TAOSEA - HIT COUNTS VS TIME - 1707 --- SS = 4. ALT = 3.3 KFT. UP WIN
RG 0
RG 1
RG 2
RG 3
RG 4
RG 5
RG 6
RG 7
RG 8
RG 9
RG 10
RG 11
RG 12
RG 13
RG 14
RG 15
SUM X 0.2
MEAN HITS/BLOCK = 100 FFT FRAMES, 0.20 PER MAJOR DIVISION
-10
0
10
20
30
40
50
60
70
80
90
TIME IN SEC

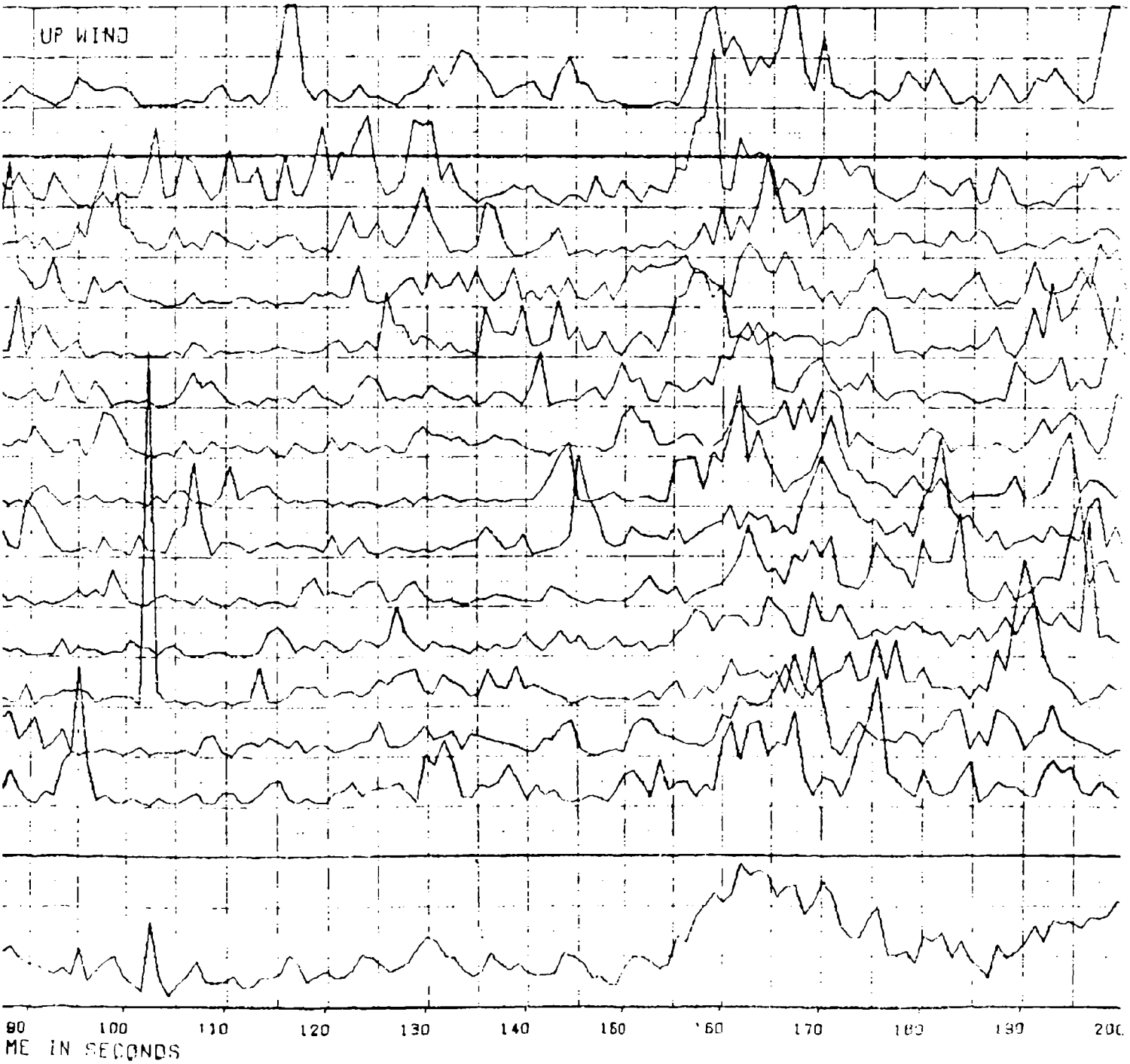

Figure 4-24 Hit Counts vs. Time for Run 1707

of 0.2 resulting in a scale factor of one hit per major division (0.1 for the smallest division).

Hit Counts vs. Time plots show considerable variation from expected mean value for horizontal polarization. The texture and spikes observed in the plots appear to be more prominent than results for vertical polarization runs contained in the appendices (see,for example, 0604 or 0605). A spike observed at 102 seconds into the run is thought to be due to anomolous behavior in the system. The spike (5.2 peak value in the range gate sum) occurs at a time when the mean is low. The spike is clearly visible in Figure 4-24, RG 12, but is nearly obscured in the RG sum plot.

This illustrates a major use of the Hit Counts vs. Time plots. Extensive use was made of the ability to identify anomalies in the data. Two types of editing of data was done based on the hit levels observed. First, obvious data dropouts were identified and deleted from the data base as were very large hits indicating either data reduction artifacts or surface targets. The second use was to identify the time position of the large returns for detailed investigation of either typical wave structure or surface target structure.

b) Hit Map

The Hit Map display format is similar to the Hit Counts vs. Time plots, however, the information presented is spatial rather than temporal. Hit maps display spatial information in the form of hits in each range gate (cross-range) and down-range resolution cell with a resolution approximating 100 feet in each dimension. A synthetic aperture process is used to transform hits from time to down-range distance. Aircraft velocity is compensated in the mapping process.

Radar echoes received from a target of "specular clutter patch" will result in large numbers of hits at the cross-range and down-range position of the reflector. Hits in Figure 4-25 are scaled ten per major division in each RG (the smallest division is one hit) and are plotted as a function of down-range distance in 100 ft. increments. There are 20 such increments per major division. The smallest division is two 100 ft. increments. Down-range distance is computed from velocity (420 ft/sec for 1707) and time in seconds.

Large spikes observed in the Hit Map are characteristic of returns received from clutter when horizontal polarization is used. Spikes were noted in Hit Counts vs. Time plots as well. In some instances, spikes in space (time) can be correlated with events in time (space). For example, a target bounded within one resolution cell will appear as a spike on the Hit Map but can be extended over several seconds in the Hit Counts vs. Time plot. A stationary target is observed for about five seconds by the radar assuming aircraft velocity is 420 ft/sec. Spikes observed on Hit Counts vs. Time may be smeared in the Hit Map. A good example is the spike in RG 12 at 102 seconds in Figure 4-24. It should correspond to 420 X 102 = 42,840 ft. down-range on the Hit Map. The Hit Map shows hits are smeared from 41,800 ft. to 44,200 ft. down-range. Clutter can differ from stationary targets in that a "nearly specular patch" may exist for a short time, on the order of hundreds of milliseconds. For such occurances, spikes may appear on both the Hit Map and Hit Counts vs. Time plot. Examples in RG 0 occur at time/range positions (in seconds, feet) given by (20.5, 8610), (65, 27300), and (116, 48720). Other examples may be clearly identified on these temporal/spatial plots.

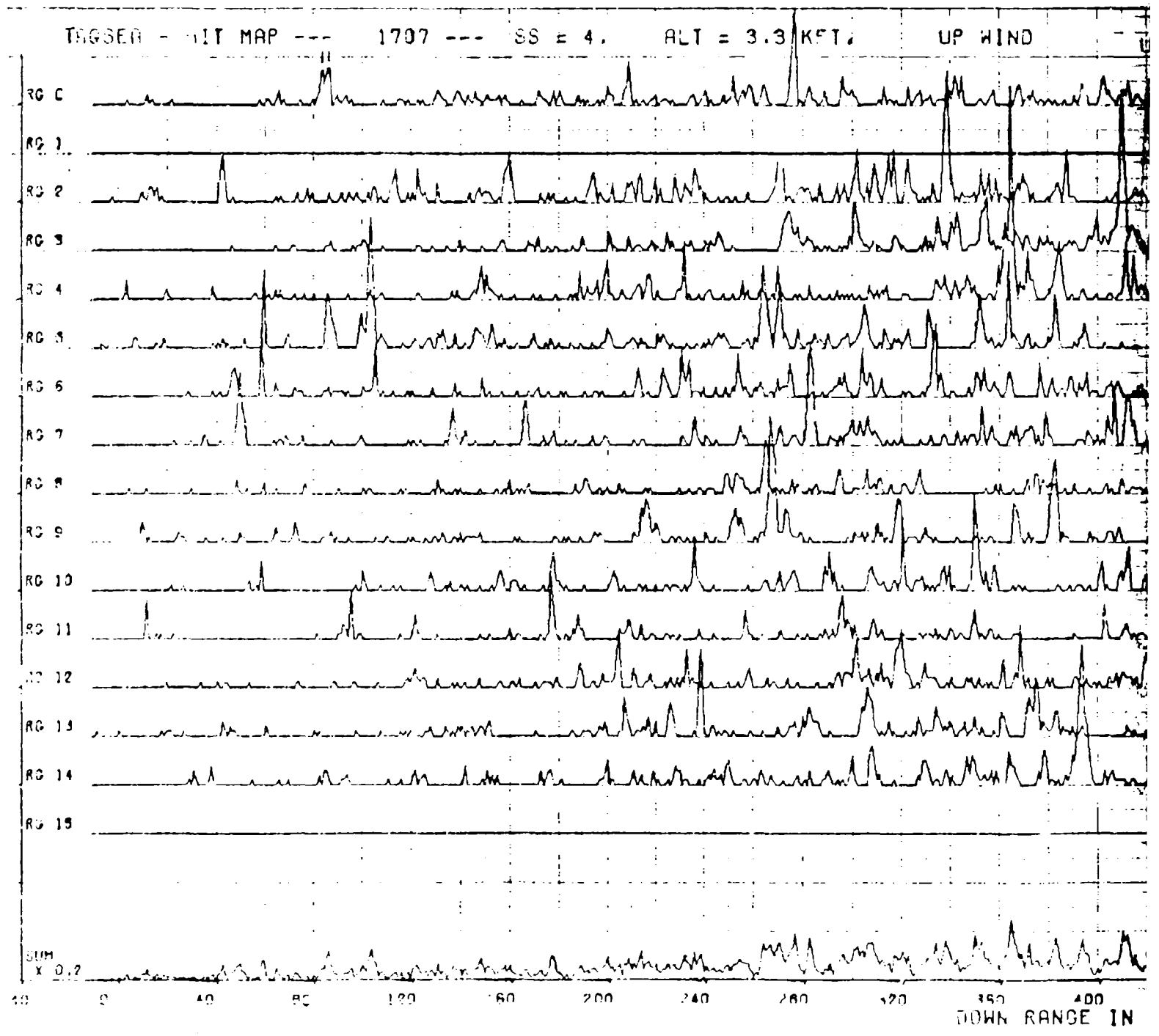
TRGSER - HIT MAP --- 1707 --- SS = 4. ALT = 3.3 KFT. UP WIND
RG 0
RG 1
RG 2
RG 3
RG 4
RG 5
RG 6
RG 7
RG 8
RG 9
RG 10
RG 11
RG 12
RG 13
RG 14
RG 15
SUM X 0.2
10.00 PER RANGE DIVISION
DOWN RANGE IN

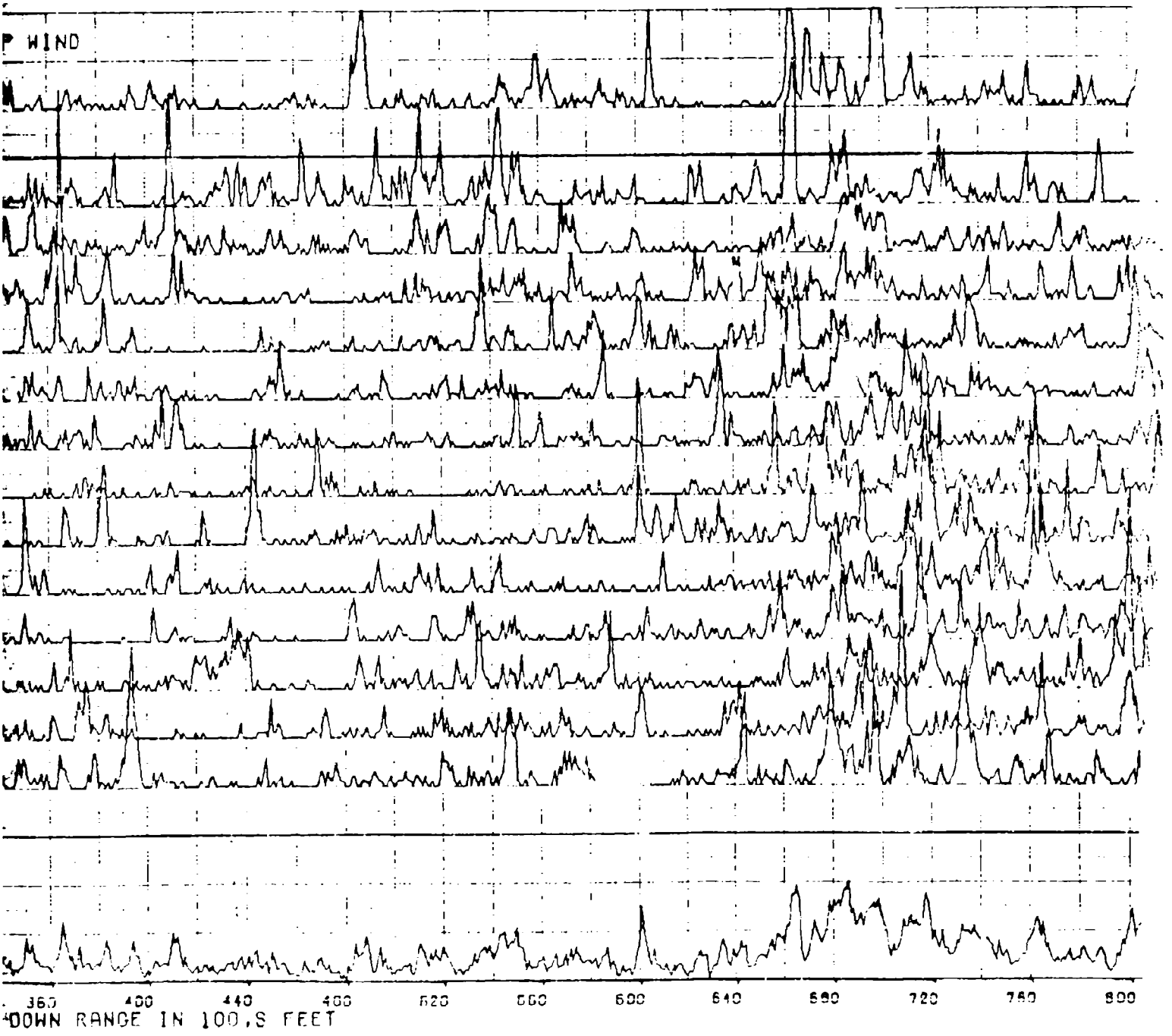

Figure 4-25 Hit Map for Run 170

Hit analysis, then, has served to focus attention on the large returns and supplement and confirm the distribution function analyses. The conclusions drawn are the same as for the distribution function: large returns are more likely with horizontal polarization than for vertical. In addition the hit analysis has defined the behavior in the vicinity of a hit and provided valuable verification of the adequacy of the distribution model. This verification was one result of simulation validation where the distribution function which was simulated was accurate enough to produce hit maps which correspond to those obtained from actual data.

4.6 Characterization of the Mean

In the course of developing the distribution functions of Subsection 4.4 variation of the mean was discussed and it was shown that the variability was eliminated as a factor in the distribution function by frame (time) normalization. For this subsection, it is exactly this variation of the mean which will be characterized.

4.6.1 Behavior of the Mean

An examination of the plots of mean cross-section versus time shows that in most cases, the mean varies about 1/2dB rms. However, in some low sea state runs, large sudden variations were observed. This suggests that at the lower sea states, local effects due to causes other than wind could predominate and suggest that a localized CFAR system should be used for thresholding.

The spatial and temporal correlation functions of the mean were measured for flight 6 and are plotted in Figures 4-26 and 4-27. These plots must be distinguished from the temporal-spatial analysis outputs in Subsection 4.4.5 which characterize correlation between individual FFT outputs,

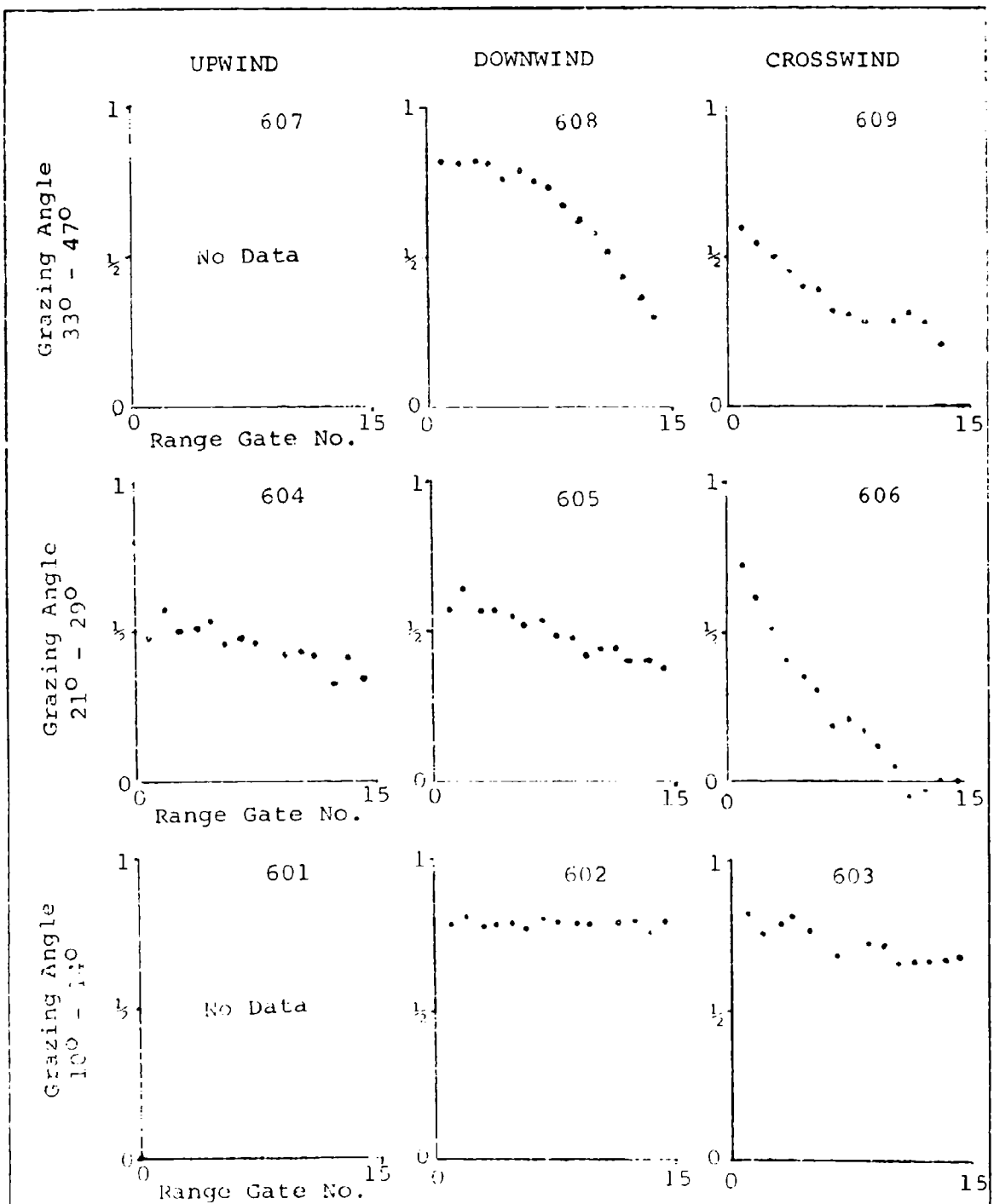

Figure 4-26 Spatial Correlation Coefficient of Mean

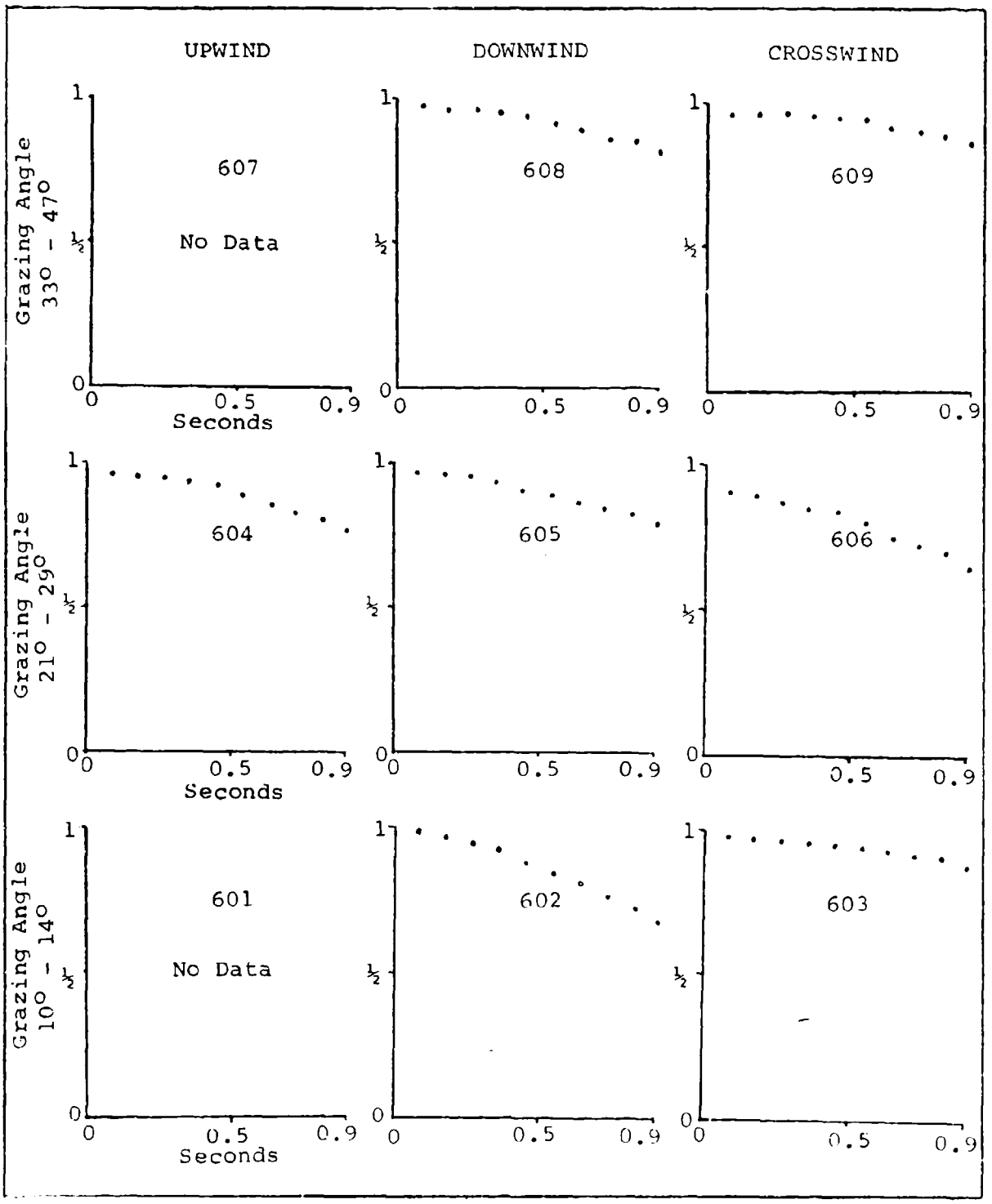

Figure 4-27 Temporal Autocorrelation Function of Mean

rather than the mean of several FFT outputs. In the correlation analysis of the mean presented here, the averaging has the effect of reducing the fast variation effect (a delta function at the origin) and emphasizes the slow variations. An example of the mean autocorrelation is shown in Figure 4-28. Here the full correlation over 40 seconds is shown as against the 0.9 second for Figure 4-27. Figure 4-29 shows examples of spatial and temporal correlation with local sampling effects removed. The residence of the delta function at the origin is caused by the sampling variance about the local mean. The implication of these functions is that reasonably consistent estimates of the mean may be obtained over a distance of a few hundred feet and over several hundred milliseconds. The samples shown represent the extreme cases in flight 6 which used vertical polarization and the sea condition was sea state 5.

4.6.2 Characterization of Variation of the Mean

Because of the slowly varying nature of the local mean large numbers of independent samples were not available for analysis. A partial characterization was extractable, however.

In the time domain the correlation time constant was between 3 and 15 seconds. A time constant of 5 seconds was typical.

In the spatial domain the correlation intervals were different for vertical and horizontal polarization. The decorrelation interval (spatial time constant) for vertical polarization exceeded 1000 ft. For horizontal polarization spatial decorrelation as small as approximately 300 feet were found.

The standard deviation of the mean varied between 6 and 20% of its value (i.e., before 0.06 and 0.2) a typical value was about 0.1.

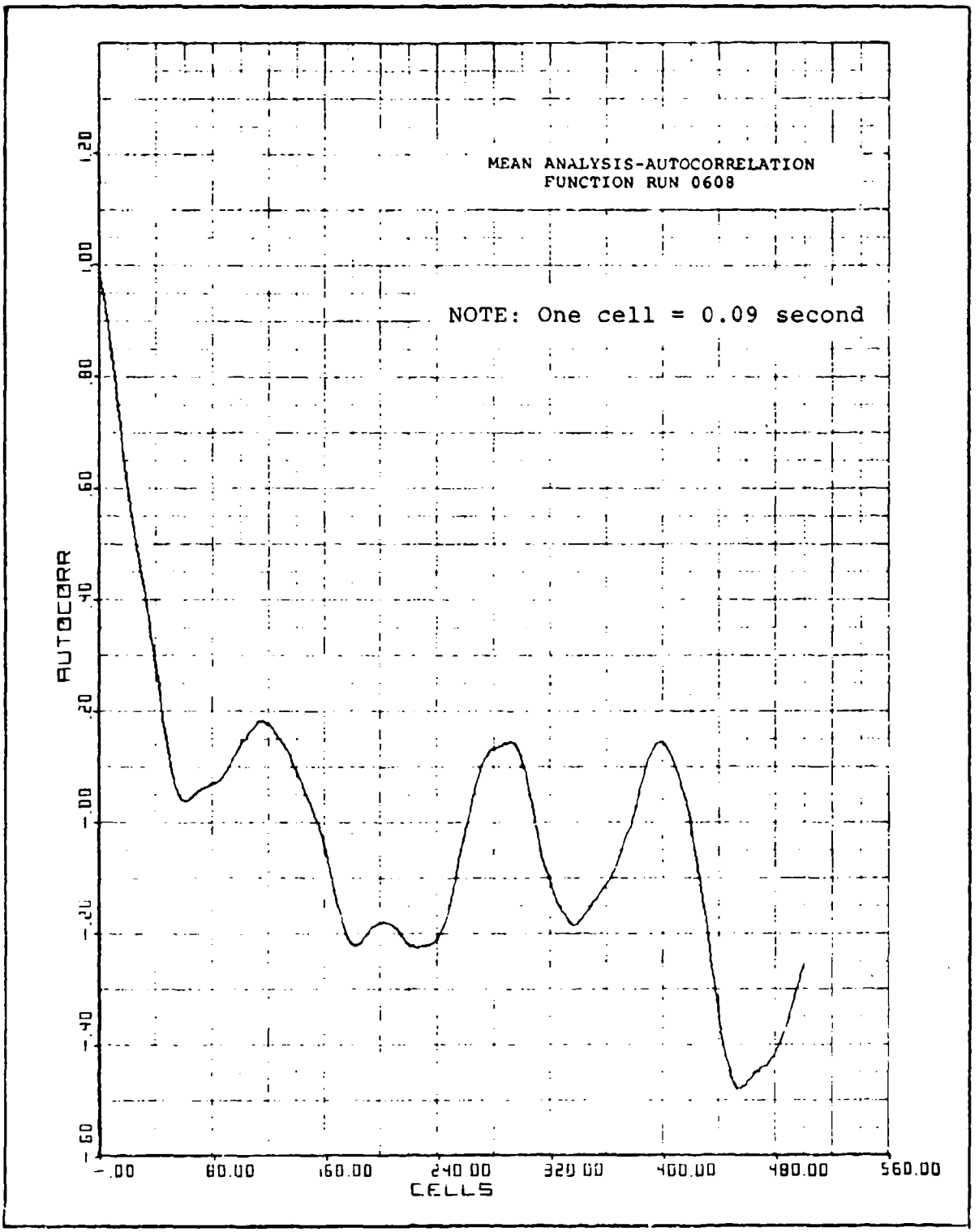

Figure 4-28 Mean Analysis-Autocorrelation Function Run 0608

In conclusion on characterization of the mean it may be said that while it is not as extensive as that for the distribution function it is adequate for use in the clutter model. This is because the variations are not as critical a parameter since a large variability of the mean can be tolerated by any reasonable system.

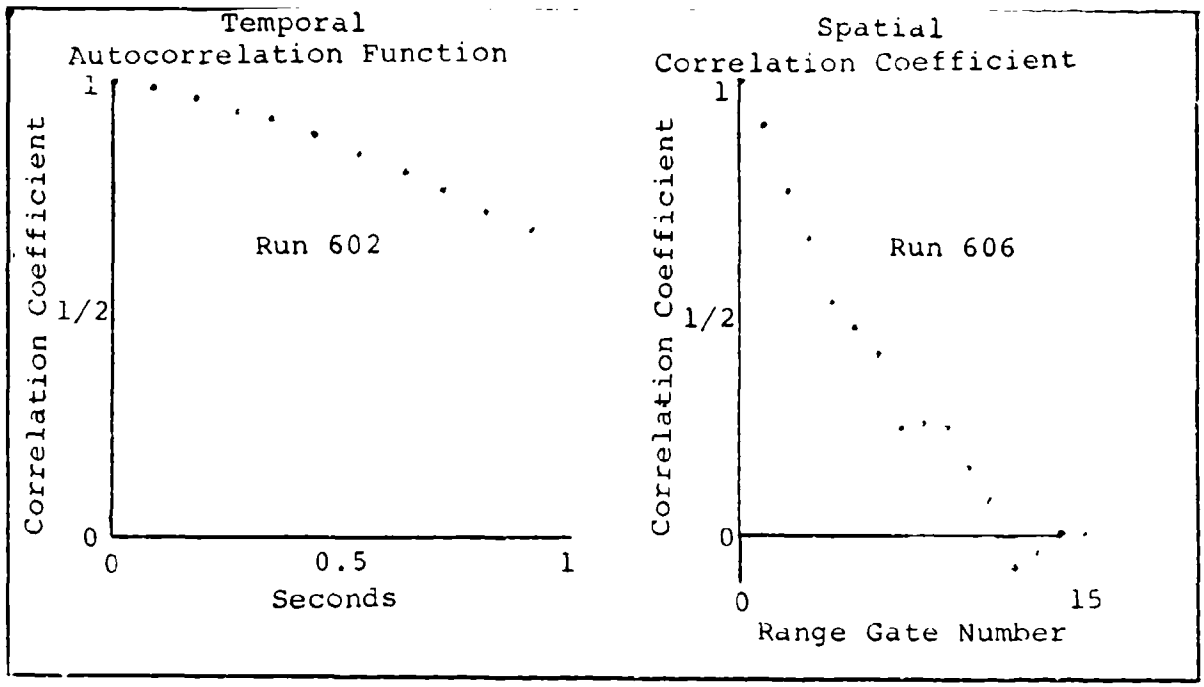

Figure 4-29 Correlations With Sampling Effects Removed

5. CLUTTER MODELS

It is a specific objective of the TARGET clutter task to develop models of sea clutter which would be most useful in the specification, design and performance evaluation for missile seekers operating against targets in a sea clutter background. This section develops a set of models in analytic, graphic and tabular form to accomplish the clutter model objective.

Models are developed for several levels of sophistication ranging from the simplest where only the non-varying mean backscatter ratio, σ_o, is used to the most complex (and most representative of actual clutter). Wherever the information developed during this program allowed a supportable position to be taken, models were characterized as to various parameters such as sea-state, polarization, and other variables. Every attempt has been made to present in this one section all the model information available in the forms most useful for conceptual studies, through more detailed design to extensive performance evaluation by computer simulation.

To provide continuity and to stress the commonality of the models presented, whether simple or complex, one generalized equation is used;

$$\frac{C}{A} = \sigma_o \cdot F \cdot S$$

This equation is the subject of the following subsections.

5.1 Generalized Form of the Models

All models to be presented are of the form;

$$\frac{C}{A} = \sigma_o \cdot F \cdot S . \qquad 5\text{-}1$$

C/A is the backscatter ratio of apparent reflected area to physical area and is in general a random variable. As such it has dimensions of area per area and is dimensionless. It, of course, represents the clutter model no matter what its sophistication or ultimate use and will be presented in many different forms.

All of the forms presented, however, will be constrained by the right hand side of equation 5-1. The most simple models will consider only σ_o by setting the other two factors equal to 1. However, σ_o itself will have a hierarchy of complexity ranging from its often encountered statement as a single number expressed in dB to σ_o as a function of grazing angle, sea state, polarization and wind direction.

The second factor, F, is a random process with distribution $P_F(F)$. (Not to be confused with the false alarm probability, P_f.) The process F is uncorrelated in time and space. Consequently, the autocorrelation function (ACF) is practically a single unity level spike at the origin. This factor will be called the fast component.

Finally, there is the slowly varying random process, S, which is characterized by the distribution function $P_S(S)$ with the ACF, $\phi_s . \phi_S$ is sometimes referred to as the local or variable mean. (The ACF is factorable into spatial and temporal components.)

Three terms are then used to express the clutter model as a random process. The form was chosen since it best represents the models from the simplest to the most complex and is itself a simple multiplicative function.

Each of the three terms will be modeled in detail in the following three subsections. In the material that follows, we shall develop both typical and extreme case models where appropriate. Extreme case models are useful in system and concept testing for the limits of performance. Typical models are useful in assessing expected average performance of system candidates. First-order, second-order and third-order models in increasing levels of sophistication will be considered.

5.2 Mean Backscatter Coefficient, σ_0 and First-Order Model

Mean backscatter is a measure of the reflectivity of the sea. The usual presentation of σ_0 is a set of curves (for various sea states) plotting σ_0 versus grazing angle. The TAGSEA results further separate the σ_0 plots by polarization and wind aspect as upwind, downwind and crosswind.

The TAGSEA data generally shows somewhat larger σ_0 results than previous data (see Section 4). We shall use the curves of Reference (2) in Section 4 for a typical case and the higher results from TAGSEA to construct an extreme case model.

Typical models average all aspects with respect to the wind. The extreme models are for upwind and downwind based on TAGSEA data. If crosswind is the only aspect to be modeled, the extreme levels may be reduced by 3dB.

These models follow in graphic form as Figures 5-1 and 5-2 and in tabular form as Table 5-1.

The same σ_0 models can be expressed in analytic form to a close approximation by noting that the curves of σ_0 in dB versus log of the grazing angle are almost straight lines over the

(2) Nathanson, F. E. and Brooks, P. R., "Data Points for X-Band Sea Reflectivity", Technology Service Corporation memo TSC-WO-251/br, B50711, dated 29 June 1976.

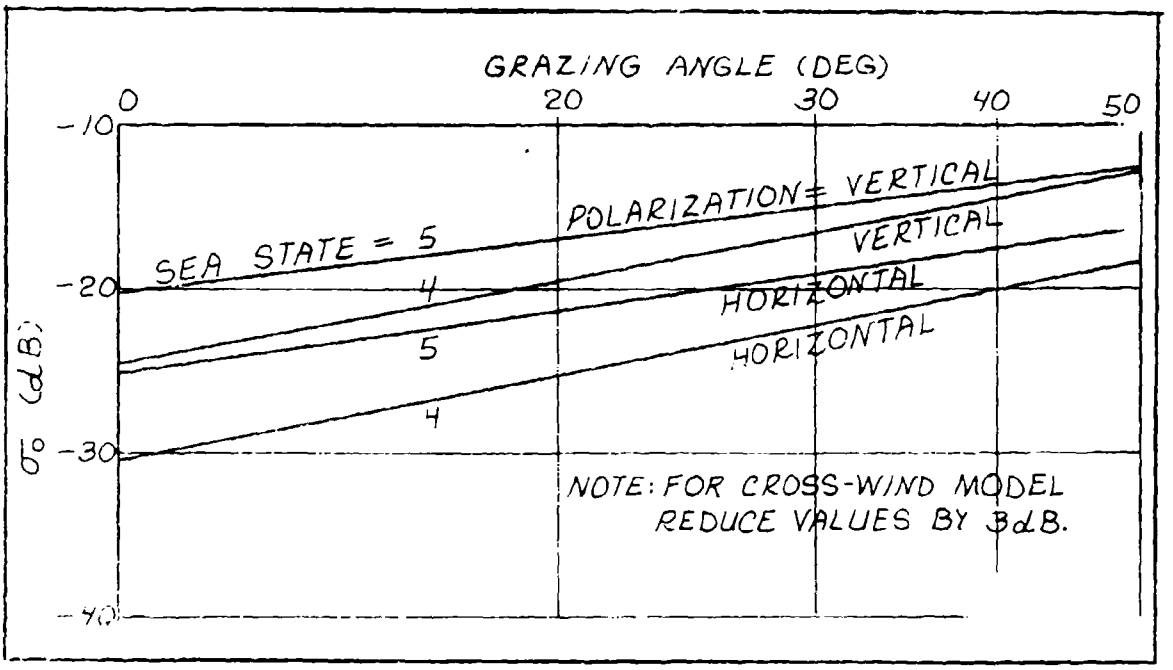

Figure 5-1 σ_o Model - Extreme Case

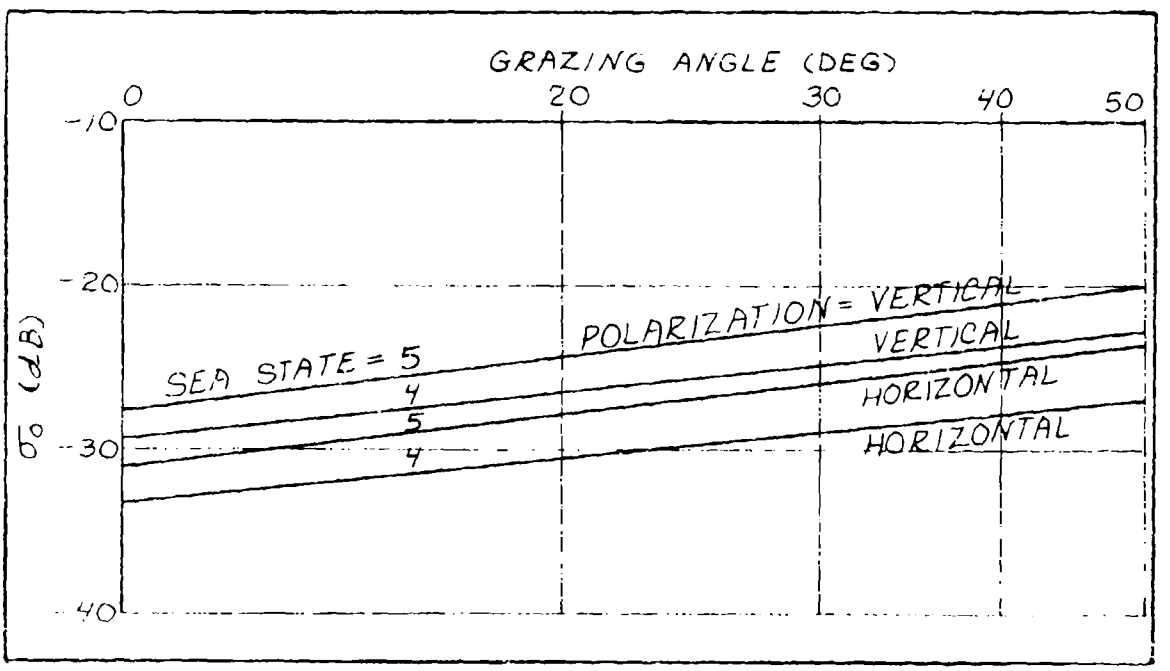

Figure 5-2 σ_o Model - Typical Case

TABLE 5-1

σ_o FOR CLUTTER MODEL

(σ_o IN dB)

GRAZING ANGLE	10°		15°		20°		30°		40°		50°	
WIND ASPECT	U&D	C	U&D	C	U&D	C	U&D	C	U&D	C	U&D	C
EXTREME MODEL												
SS-5												
VERTICAL	-20	-23	-18	-15	-17	-20	-15	-18	-14	-17	-12.5	-15.5
HORIZONTAL	-25	-28	-23	-26	-21	-24	-19	-22	-17.5	-20.5	-16.5	-19.5
SS-4												
VERTICAL	-14.5	-17.5	-21.5	-24.5	-19.5	-22.5	-16.5	-19.5	-14.5	-17.5	-13	-16
HORIZONTAL	-30	-33	-27	-30	-25	-28	-22	-25	-20	-23	-18	-21
TYPICAL MODEL												
SS-5												
VERTICAL	-27.5	-30.5	-26	-29	-24.5	-27.5	-22.5	-25.5	-21	-24	-20	-23
HORIZONTAL	-31	-34	-29	-32	-28	-31	-26	-29	-25	-28	-24	-27
SS-4												
VERTICAL	-29	-32	-28	-31	-27	-30	-25	-28	-24	-27	-23	-26
HORIZONTAL	-33	-36	-31.5	-34.5	-31	-34	-29	-32	-28	-31	-27	-30

UNCLASSIFIED

region covered by the TAGSEA data. The expressions for the typical case are then:

for horizontal polarization and sea state 4,

$$\sigma_o = 8.6 \log A - 41.6 \qquad 5\text{-}2$$

where σ_o is in dB, and A is the grazing angle in degrees;

for horizontal polarization and sea state 5,

$$\sigma_o = 10.1 \log A - 41.1; \qquad 5\text{-}3$$

for vertical polarization and sea state 4,

$$\sigma_o = 9.3 \log A - 38.6 \qquad 5\text{-}4$$

and for vertical polarization and sea state 5,

$$\sigma_o = 12.5 \log A - 41.3 \qquad 5\text{-}5$$

For the special case of crosswind only, the above σ_o values may be decreased by 3dB.

For the extreme case model, the corresponding equations are:

$$\sigma_o = 17.2 \log A - 47.2 \text{ (Horiz., SS-4)} \qquad 5\text{-}6$$

$$\sigma_o = 12.9 \log A - 37.9 \text{ (Horiz., SS-5)} \qquad 5\text{-}7$$

$$\sigma_o = 16.5 \log A - 31.0 \text{ (Vert., SS-4)} \qquad 5\text{-}8$$

and,
$$\sigma_o = 10.7 \log A - 30.7 \text{ (Vert., SS-5)} \qquad 5\text{-}9$$

Which σ_o model is to be used for any one application of the clutter model obviously depends on the parameters of the system being considered and on the extent of the analysis to be done. No error was assigned to any σ_o value given since it is apparent from the way in which they were derived that several dB variabilities exist in the determination of sea state alone. The proper place for determination of which specific σ_o model is

to be used, and indeed whether the first-order model is sufficient, is in system requirements specifications.

This completes the simplest clutter model by replacing the two random variables F and S by their mean values of 1. In this case,

$$\frac{C}{A} = \sigma_o .$$

This first-order model is similar to that used in many simple guidance simulations where distribution effects are not dominant.

5.3 The Fast Component, F and Second-Order Model

The fast random process, F, characterizes the statistical behavior of the clutter model with respect to the mean. The process is characterized by a probability function, $P_F(F)$ and an autocorrelation function Φ_F. This is, in fact, the function discussed in Subsection 4.4. The fast component, when used as part of the clutter model, adds a step in sophistication to the overall model which is now written $C/A = \sigma_o F$. This model uses the σ_o models from the previous subsection and sets the random variable S equal to 1. When S is considered in the next subsection, it will be necessary to modify the F component of the model developed in this subsection.

The fast component is then characterized by $P_F(F)$ and Φ_F which will now be considered.

a. Correlation Properties of F, $\Phi(F)$

In Subsection 4.4, the spatial and temporal correlation functions were shown to have very little correlation from process interval to interval and from spatial resolution cell to cell. In fact, the clutter returns with the mean removed is virtually uncorrelated. This property will be used for the model and Φ_F drops out of consideration in the overall clutter model.

b. Distribution of F, $P_F(F)$

Two different cases for the distribution function need to be considered, one for the second-order model and one for the third-order. For the second model, the effect of the mean variation must be included in the distribution. The effect is to extend the tails and produce the A-type distribution discussed previously. (In contrast, the N-type distribution is normalized to a varying mean and it will be used for the third-order model.)

For the second-order model, A-type distributions were examined to determine typical and extreme cases to be used in conjunction with like σ_o values. Rather than fabricate such distributions, runs typifying each desired distribution function were selected and these were modeled directly. The results are presented here in tabular, graphic and analytic forms. Table 5-2 lists the level in dB above the mean for probability of occurrence from 10^{-1} through 10^{-6} as well as the median value. These are shown for the four cases, vertical and horizontal polarization, and typical and extreme. Plots of these cases were generated by the cubic spline method and are shown in Figures 5-3 through 5-6. Probability of exceeding a given power is plotted. The ordinate is the probability written as the power of 10, viz., $p = 10^{-6}$ is written as -6. The abscissa is simply the amplitude ratio relative to the mean in dB. The analytic form for the cubic splines used to generate the curves, and which are themselves a model which can be used in place of the table or plots, is shown in Table 5-3. The equation shown on the Table is related to the axes of the curves by:

$$S(t) = \log Q, \text{ and } t = \text{Amp/Mean in dB}$$

TABLE 5-2

dB ABOVE THE MEAN FOR VARIOUS STATISTICAL Q TAILS

(Second-order model, A-type)

POLARIZATION	VERTICAL		HORIZONTAL	
MODEL RUN	TYPICAL 605-A	EXTREME 403-A	TYPICAL 704-A	EXTREME 702-A
LEVEL				
MEDIAN	-2.2	-2.2	-2.3	-2.6
10^{-1}	3.6	3.6	3.5	3.4
10^{-2}	7.1	7.0	7.6	8.1
10^{-3}	9.3	9.4	10.4	11.6
10^{-4}	10.9	11.5	12.6	14.5
10^{-5}	12.2	13.4	14.6	17.1
10^{-6}	13.3	15.2	16.4	18.5

TABLE 5-3

CUBIC SPLINE TO GENERATE DISTRIBUTION FUNCTION F(

This chart is based upon the following equation for the cubic spline S(t),

$S(t) = A_{i,1}\,t^3 + A_{i,2}\,t^2 + A_{i,3}\,t + A_{i,4}$ for XK_i to XK_{i+1}

CASE	INDEX i	INTERVAL XK_i $(dB)^i$	INTERVAL XK_{i+1} (dB)	CUBIC $A_{i,1}$
VERTICAL TYPICAL (605-A)	1	-.1301030E+02	.1507753E+01	-.322
	2	.1507753E+01	.1295825E+02	-.1318
	3	.1295825E+02	.1424070E+02	-.283
VERTICAL EXTREME (403-A)	1	-.1301030E+02	-.1112296E+01	-.216(
	2	-.1112296E+01	.379434E+01	-.119
	3	.3794347E+01	.1718100E+02	.548
HORIZONTAL TYPICAL (704-A)	1	-.1301030E+02	.7002952E+01	-.343
	2	.7002952E+01	.1603431E+02	.102(
	3	.1603431E+02	.1781400E+02	-.106]
HORIZONTAL EXTREME (702-A)	1	-.1301030E+02	-.1121429E+01	-.338
	2	-.1121429E+01	.1662384E+02	.550
	3	.1662384E+02	.1905600E+02	-.511

ABLE 5-3

ON FUNCTION FOR SECOND ORDER MODEL (A-TYPE)

ıbic spline S(t),

o XK_{i+1} $\quad i = 1, 2, 3$

	COEFFICIENTS OF CUBIC			
	CUBIC $A_{i,1}$	QUAD $A_{i,2}$	LINEAR $A_{i,3}$	CONSTANT $A_{i,4}$
+01	-.3221903E-03	-.9547749E-02	-.1033355E+00	-.4835364E+00
+02	-.1318826E-02	-.5039706E-02	-.1101325E+00	-.4801203E+00
+02	-.2835235E+00	.1096560E+02	-.1422705E+03	.6135697E+03
+01	-.2166604E-03	-.7359461E-02	-.9162191E-01	-.4696657E+00
01	-.1197694E-02	-.1063306E-01	-.9526313E-01	-.4710158E+00
02	.5480925E-03	-.3050542E-01	-.1986048E-01	-.5663837E+00
+01	-.3435470E-03	-.9858388E-02	-.1045131E+00	-.4941947E+00
+02	.1026808E-03	-.1923312E-01	-.3886230E-01	-.6474446E+00
+02	-.1061421E+00	.5091449E+01	-.8198511E+02	.4373363E+03
+01	-.3386381E-03	-.1010919E-01	-.1105727E+00	-.5254787E+00
+02	.5501449E-06	-.8968062E-02	-.1092930E+00	-.5250003E+00
+02	-.5119683E-01	.2544323E+01	-.4255480E+02	.2346774E+03

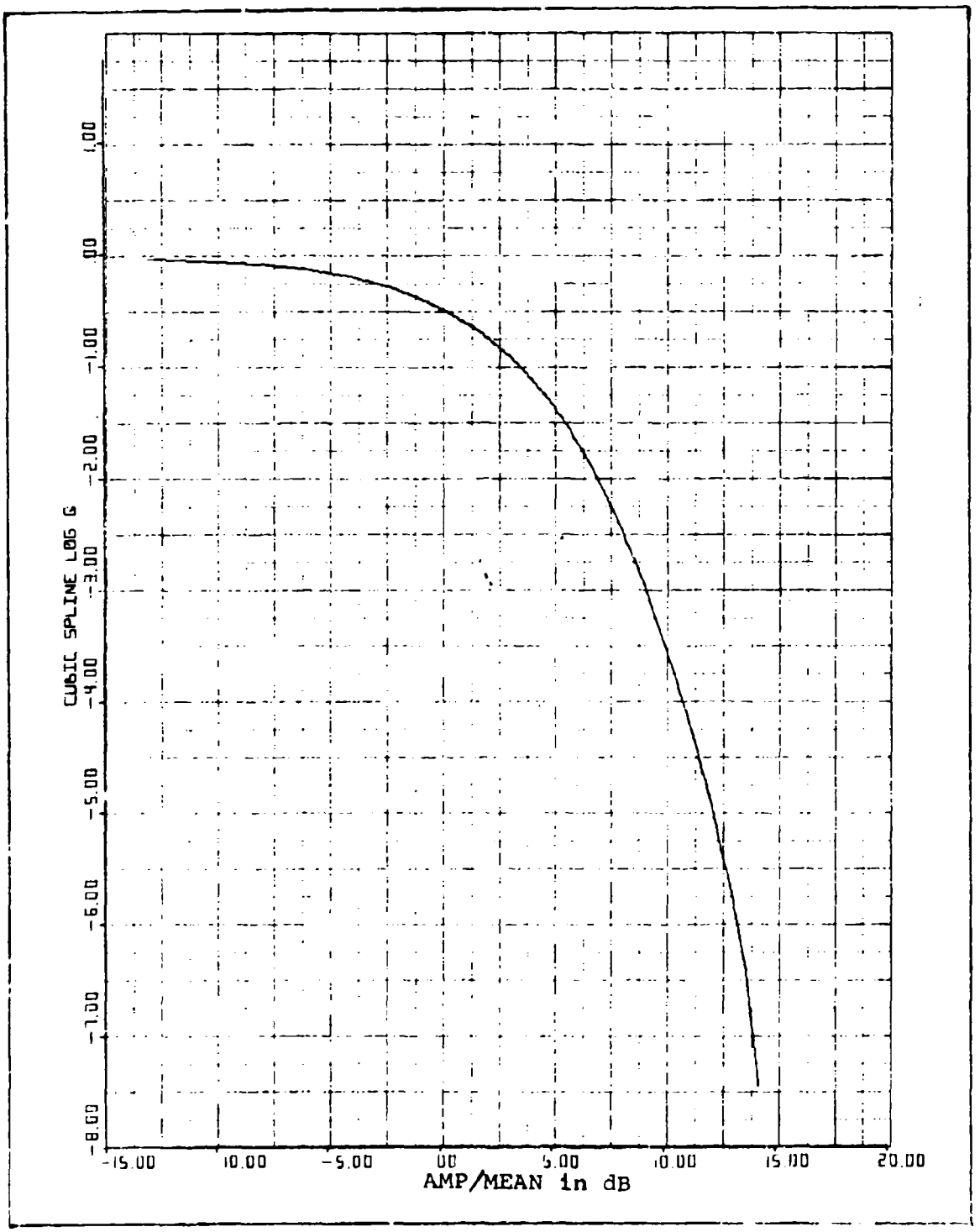

Figure 5-3 Typical Vertical Polarization Second-Order Fast Distribution Model

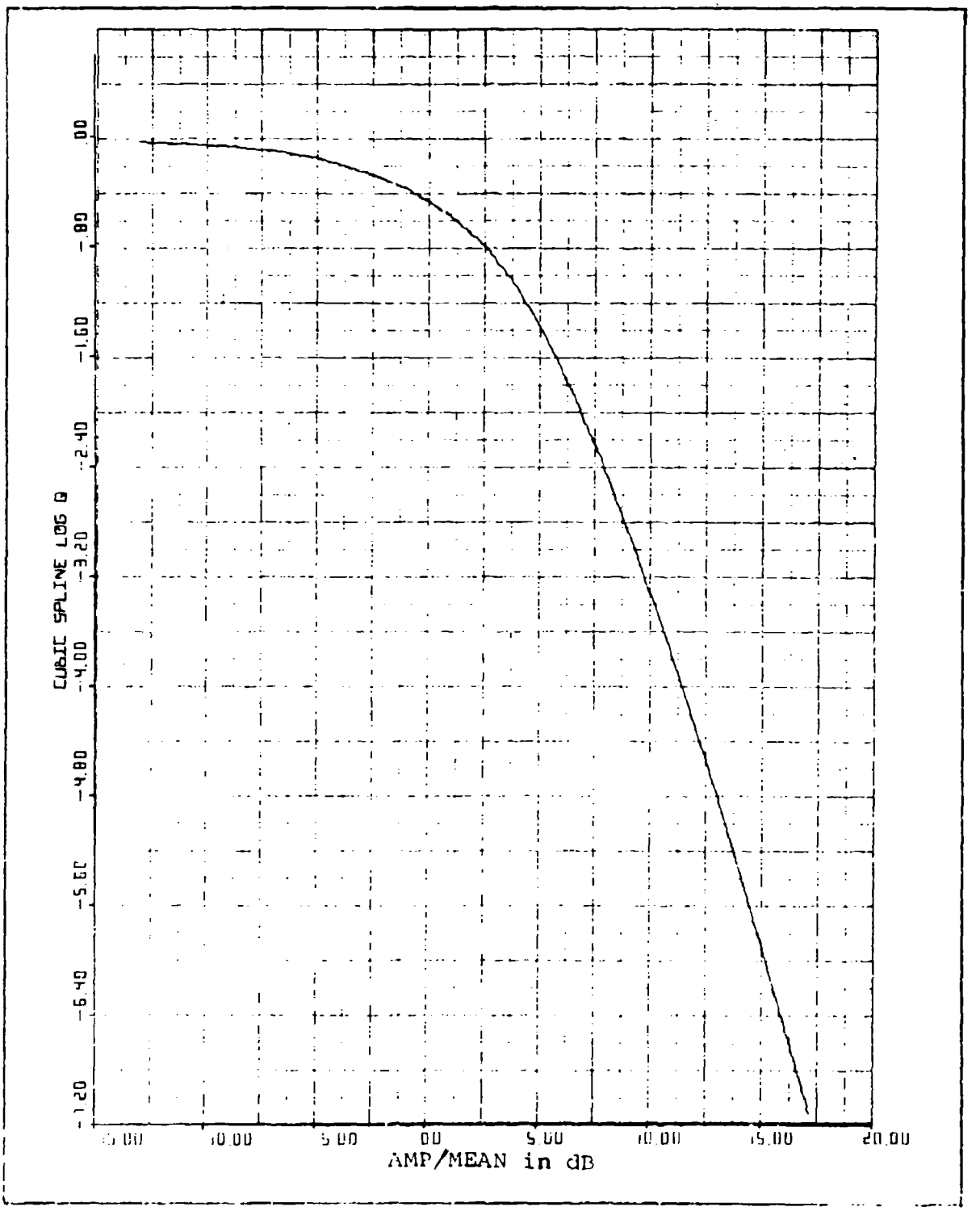

Figure 5-4 Extreme Vertical Polarization Second-Order Fast Distribution Model

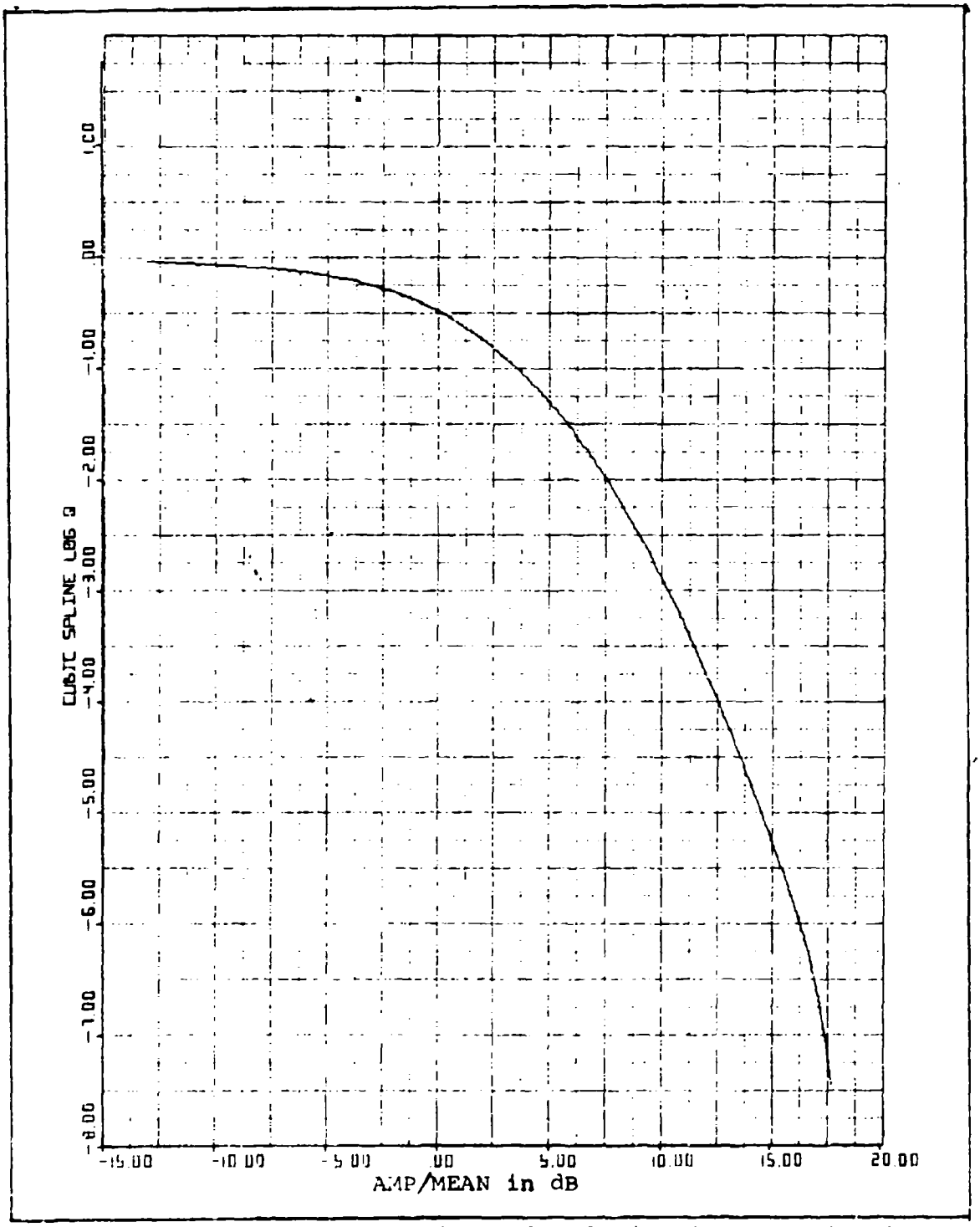

Figure 5-5 Typical Horizontal Polarization Second-Order Fast Distribution Model

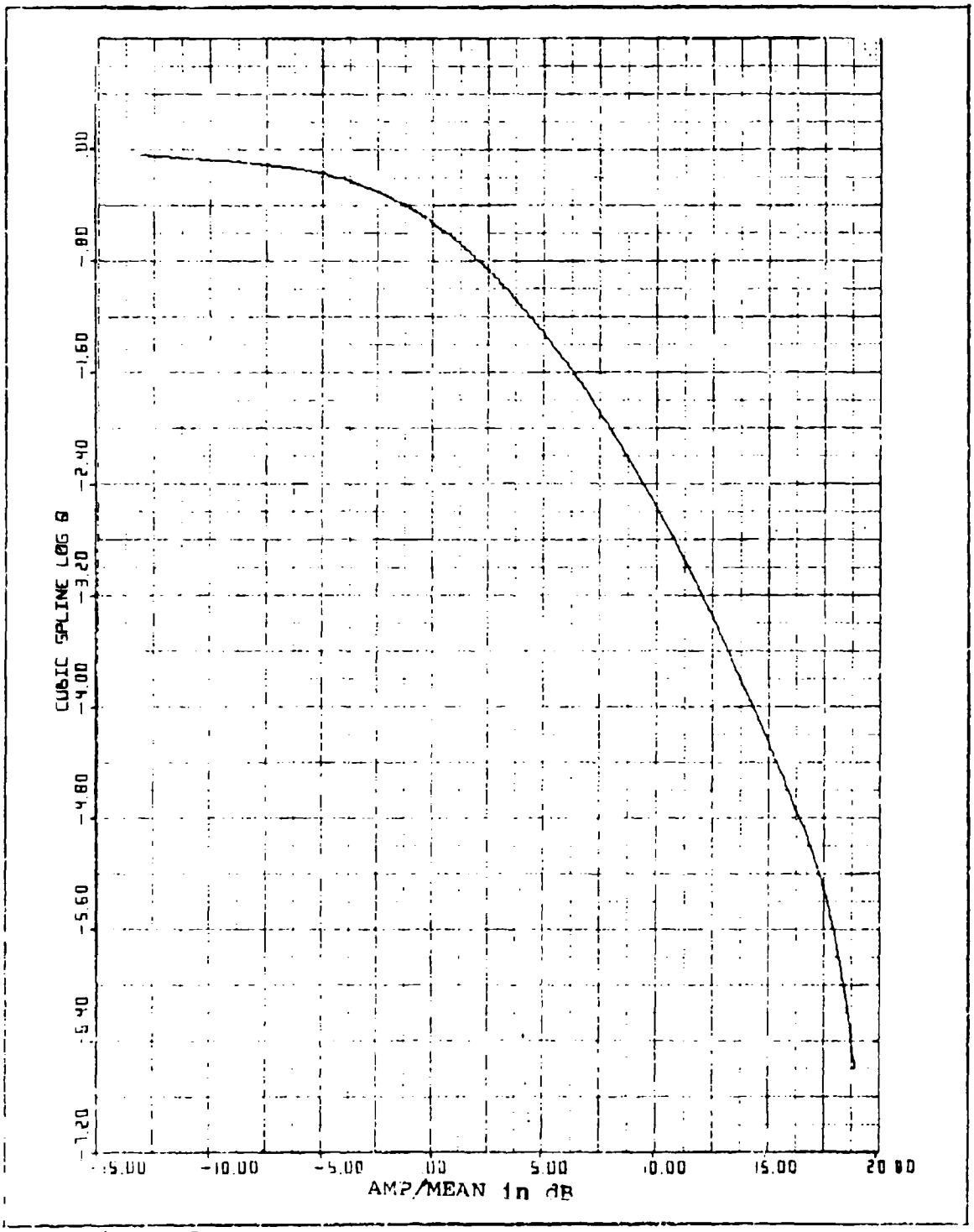

Figure 5-6 Extreme Horizontal Polarization Second-Order Fast Distribution Model

5.4 The Slow Component, S, and the Third-Order Model

The slow random process, S, characterizes the variability of the mean in statistical terms. As with the fast component, two parameters, $P_S(S)$ and Φ_S describe the random process. When the slow component is used in the model, the fast component must be modified. This modification consists of using a locally normalized (N-type) distribution function in place of the long-term averaged A-type.

The third-order model is then the result and it is written as $C/A = \sigma_o.F.S.$ The first term, σ_o, is the same as that for the other two models.

For the fast component, the N-type distribution is used as this type is normalized with respect to the local mean rather than to the long-term mean. The result is a lowering of the tails of the distribution with respect to the mean. In physical terms this can be thought of as the fast distribution being superimposed on the variable mean. As before, the fast process is uncorrelated.

Table 5-4 lists selected points on the distributions for vertical and horizontal polarization for typical and extreme cases. It is immediately apparent that for vertical polarization the tails do not extend as far as those for the A-type. The typical case for horizontal polarization is taken for median grazing angles (24°) while the extreme case corresponds to the lower grazing angles (12°). Also, for vertical polarization, the typical and extreme cases are almost identical. Both of these results are effects of the local normalization. We are now reduced to a single vertical distribution and have two with lower tails for horizontal polarization. Figures 5-7 through 5-10 are the cubic spline generated curves for the four cases. Table 5-5 lists the cubic spline constants from which the curves were generated.

TABLE 5-4

dB ABOVE THE MEAN FOR VARIOUS STATISTICAL Q TAILS

(Third-order model, N-type)

POLARIZATION	VERTICAL		HORIZONTAL	
MODEL RUN	TYPICAL 605-N dB Above Mean	EXTREME 403-N dB Above Mean	TYPICAL 704-N dB Above Mean	EXTREME 702-N dB Above Mean
Level				
Median	-2.2	-2.1	-2.4	-2.5
10^{-1}	3.6	3.6	3.5	3.5
10^{-2}	7.0	6.9	7.5	7.8
10^{-3}	9.2	9.0	10.2	11.3
10^{-4}	10.8	10.5	12.3	14.2
10^{-5}	12.1	12.0	14.2	16.3
10^{-6}	13.2	13.7	15.8	17.9

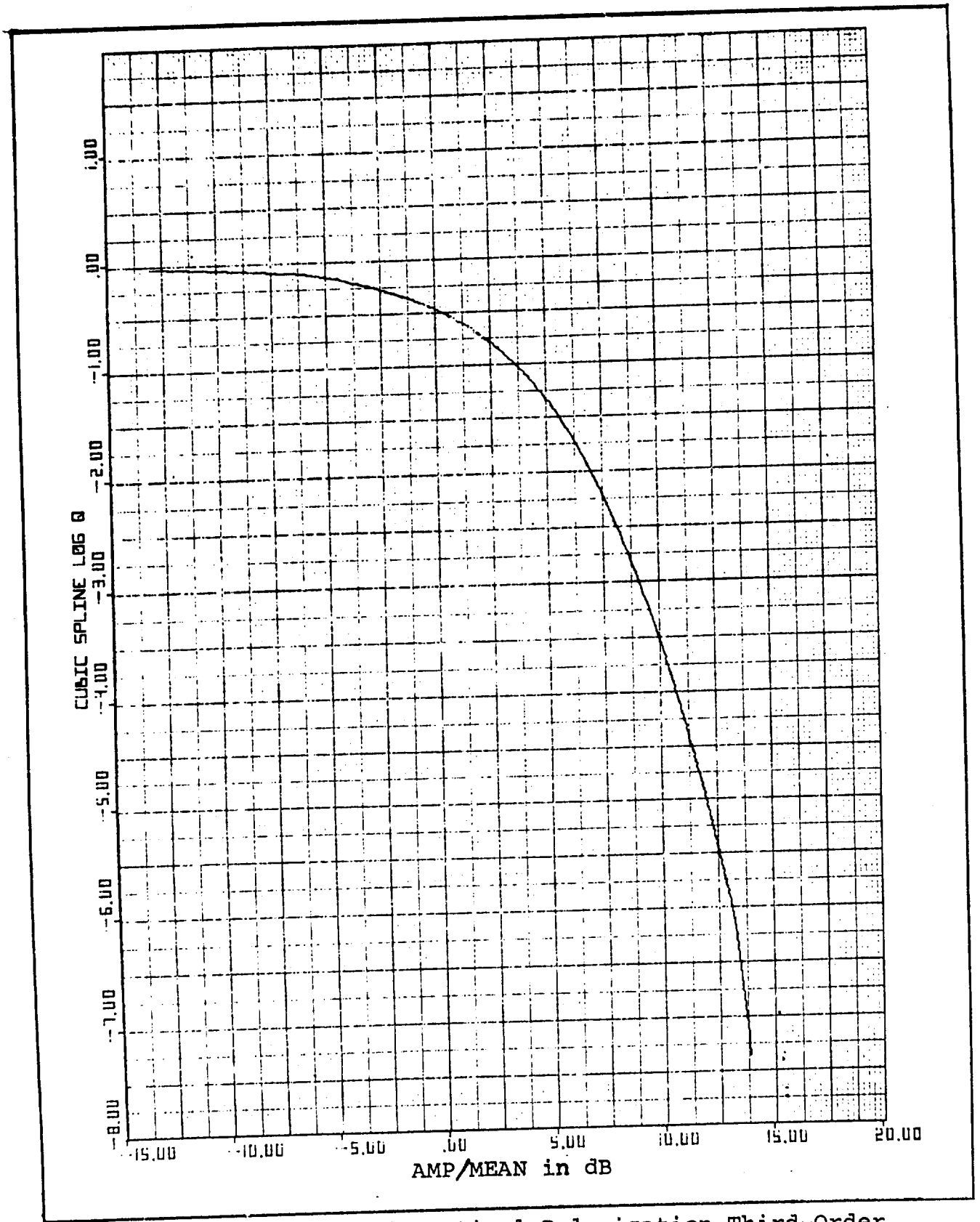

Figure 5-7 Typical Vertical Polarization Third-Order Fast Distribution Model

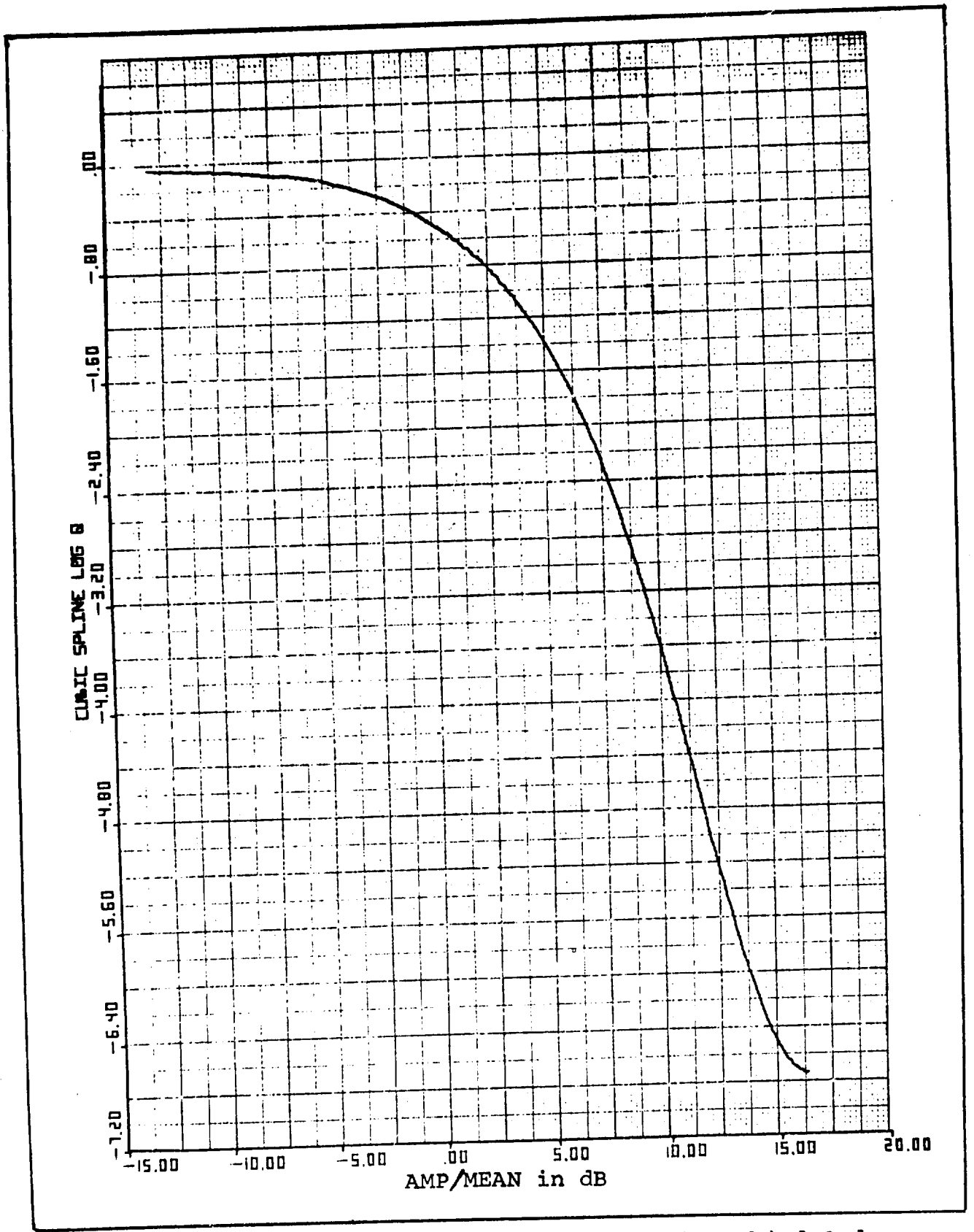

Figure 5-8 Extreme Vertical Polarization Third-Order Fast Distribution Model

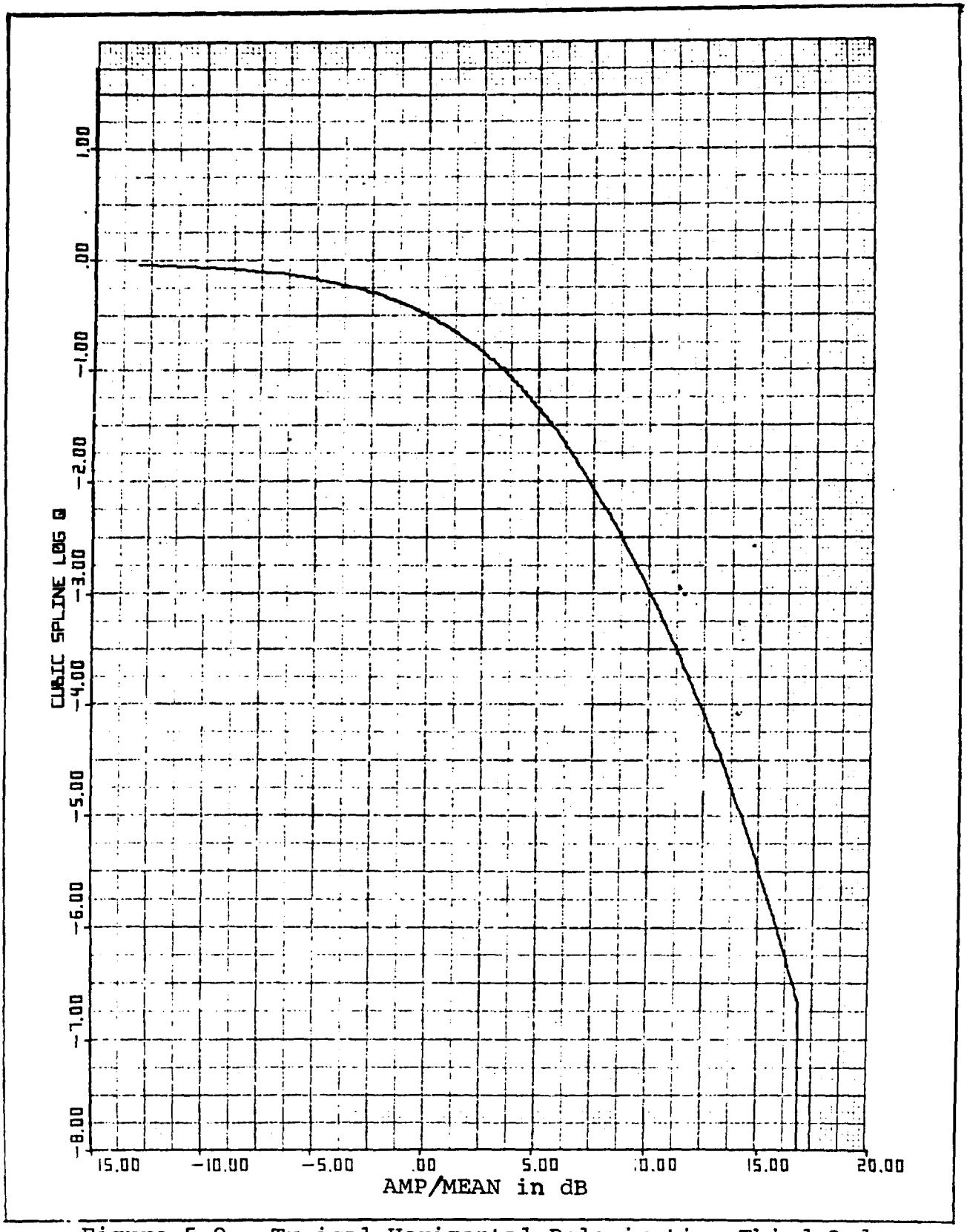

Figure 5-9 Typical Horizontal Polarization Third-Order Fast Distribution Model

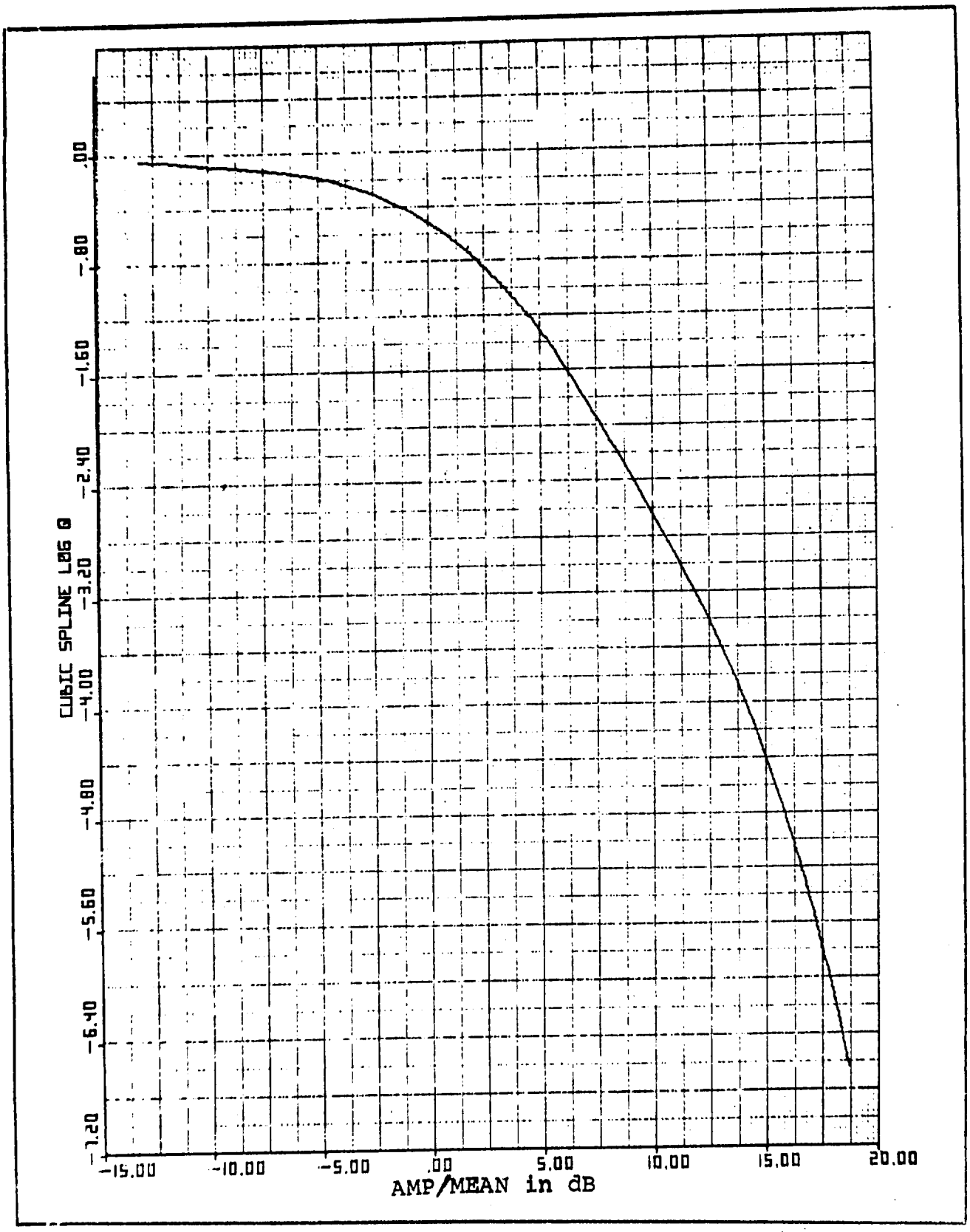

Figure 5-10 Extreme Horizontal Polarization Third-Order Fast Distribution Model

TABLE 5-5

CUBIC SPLINE TO GENERATE DISTRIBUTION FUNCTION FOR THI

This chart is based upon the following equation for the cubic spline, S(t),

$S(t) = A_{i,1}\, t^3 + A_{i,2}\, t^2 + A_{i,3}\, t + A_{i,4}$ for XK_i to XK_{i+1} i

CASE	INDEX i	INTERVAL XK_i (dB)	INTERVAL XK_{i+1} (dB)	CUBIC $A_{i,1}$
VERTICAL TYPICAL (605-N)	1	-.1301030E+02	.5555926E+00	-.2933874E-
	2	.5555926E+00	.1275863E+02	-.1252265E-
	3	.1275863E+02	.1424700E+02	-.3401926E+
VERTICAL EXTREME (403-N)	1	-.1301030E+02	.3049653E+00	-.2964140E-
	2	.3049653E+00	.9294723E+01	-.1348492E-
	3	.9294723E+01	.1625900E+02	.8457972E-
HORIZONTAL TYPICAL (704-N)	1	-.1301030E+02	-.2572675E+01	-.2331089E-
	2	-.2572675E+01	.3026311E+01	-.5385090E-
	3	.3026311E+01	.1680000E+02	-.1965077E-
HORIZONTAL EXTREMES (702-N)	1	-.1301030E+02	.5133380E+01	-.3006142E-
	2	.5133380E+01	.9477663E+01	.10911506E-
	3	.9477663E+01	.1871300E+02	-.2036501E-

BLE 5-5

ON FUNCTION FOR THIRD ORDER MODEL (N-TYPE)

cubic spline, S(t),

to XK_{i+1} $i = 1, 2, 3$

	COEFFICIENTS OF CUBIC			
	CUBIC $A_{i,1}$	QUAD $A_{i,2}$	LINEAR $A_{i,3}$	CONSTANT $A_{i,4}$
+00	-.2933874E-03	-.8995863E-02	-.1008090E+00	-.4806193E+00
-02	-.1252265E-02	-.7397627E-02	-.1016970E+00	-.4804519E+00
-02	-.3401926E+00	.1296584E+02	-.1656224E+03	.7034586E+03
+00	-.2964140E-03	-.9057870E-02	-.1007537E+00	-.4748077E+00
+01	-.1348492E-02	-.8095329E-02	-.1010473E+00	-.4747779E+00
-02	.8457972E-02	-.2815404E+00	.244059E+01	-.8349255E+01
E+01	-.2331089E-03	-.7730527E-02	-.9472498E-01	-.4862581E+00
E+01	-.5385090E-03	-.1008761E-01	-.1007890E+00	-.4914583E+00
C+02	-.1965077E-03	-.1319262E-01	-.9139228E-01	-.5009374E+00
C+01	-.3006142E-03	-.9212000E-02	-.1043591E+00	-.5101228E+00
E+01	.10911506E-02	-.3065084E-01	.569481E-02	.6984387E+00
+02	-.2026501E-02	.5828773E-01	-.8372352E+00	.1964563E+01

To complete the third-order models, $C/A = \sigma_o \cdot F \cdot S$, a model must be generated for the factor S. This factor is itself a random process which characterizes the variation of the mean. It is well known that the mean level of the sea clutter does vary and TAGSEA data, of course, shows such variations. Characterizing the variation in terms of a distribution function and autocorrelation function is, however, not as simple as for the fast factor. This is true primarily for two reasons; first, the slow factor by its very nature varies with a time constant which is not very short compared with the time of the data base. Where the fast component could be sampled hundreds of times during each run, the slow component could only be sampled at most tens of times., This means that the shape of the distribution function is difficult to define. Where the fast distribution function could be defined to the 10^{-6} point, the slow might not even be definable to the 10^{-1} point. The second reason is that correlation for the slow process should be done over both space and time which adds another dimension to the process.

It is felt, however, that the slow process must be characterized for a complete model. To fully evaluate a radar seeker, for example, it should be tested in simulation against a model which varies as sea clutter varies. With these factors in mind, the slow process was defined based on the best available information.

TAGSEA data is compatible with modeling S as a Gaussian process exponentially correlated in both space and time. This was in fact chosen as the form of the model as it has the outstanding attribute of ease of expression and analysis. Furthermore it is the commonly used process when a more appropriate one is not known. Finally, it was the model used during the simulation validation of TAGSEA data and a reasonable check was obtained.

The model, as an exponentially correlated Gaussian process, is specified by the mean and standard deviation of the distribution and the exponential time and space constants. Only one set of time and space constants was chosen for each polarization in deference to the lack of definition noted above. The mean is, by definition, 1 since the average value is in the σ_o term of the model. The standard deviation, σ_s, is 0.1 for the typical case and 0.2 for the extreme case. The analytic expressions for these two cases are:

$$P_S(S) = \frac{10}{2} \exp\left(\frac{-(x-1)^2}{0.02}\right), \text{ typical, and}$$

$$P_S(S) = \frac{5}{2} \exp\left(\frac{-(x-1)^2}{0.08}\right), \text{ extreme.}$$

After removal of the mean, both models of the process S are exponentially correlated with time constants of 3 seconds for vertical polarization and 10 seconds for horizontal. The corresponding space constants are 1000 feet for the vertical and 300 feet for horizontal. The analytic expressions are:

$$\Phi_s(\tau) = \exp\left(-\frac{|\tau|}{3}\right) \text{ vertical time,}$$

$$\Phi_s(\tau) = \exp\left(-\frac{|\tau|}{10}\right) \text{ horizontal time,}$$

$$\Phi_s(x) = \exp\left(-\frac{|x|}{1000}\right) \text{ vertical space, and}$$

$$\Phi_s(x) = \exp\left(-\frac{|x|}{300}\right) \text{ horizontal space.}$$

5.5 Use of the Models

The preceeding sections define the clutter models. This section will indicate in general terms how the models may be useful. Obviously, the first-order model is the backbone of the following two. Certainly in system requirements specifications some such model must be used. There is an advantage in specifying typical and extreme as perhaps a requirement and a goal. Horizontal and vertical σ_o values, as a function of grazing angle, also have value separately in perhaps guiding design in a favorable direction. Wind aspect could only be useful in very limited cases, such as this TAGSEA measurement effort where the wind aspect could be deliberately chosen.

Distribution functions are commonly used in radar system design and should appear more often in specifications. The not unusual practice of using noise distribution for clutter should be discontinued. The models given here lend a more realistic view of the problem of specification and should also encourage better design. Knowing what to design for is half of the battle. As with the σ_o model, the particular distribution function to be used should be part of the system specifications.

Whether or not to use the third-order model in system specifications is a more complex and subjective problem. Certainly in design the way the clutter mean can be expected to vary is helpful. Specifications of the third-order, on the other hand, may appear to be excessive intrusions on the design perrogative. The crucial test of what to use is, however, in the system performance evaluation method. Presuming that computer simulation will be used, it can be stated catagorically that only the use of the third-order model does not penalize the optimum radar when compared to sub-optimum units. Table 5-6 shows in matrix form four possible CFAR designs and what effect the use of the second-order or third-order model has on design and performance evaluation of the system. The conclusion is that only evaluation using the third-order system properly shows that the optimum system is

TABLE 5-6

SECOND- AND THIRD-ORDER MODEL USE

	DESIGN	SYSTEM PERFORMANCE EVALUATION
FIXED THRESHOLD	Second-order adequate Third-order adequate but not fully used and wrong if only fast component is used	Second-order } Same performance indicated Third order }
WIDE CFAR (Much greater than the space-time decorrelation)	Second-order adequate Third-order as above	Second-order } Same performance indicated Third-order }
NARROW CFAR (Much smaller than the space-time decorrelation)	Second-order adequate Third-order adequate	Second-order } Same performance indicated Third-order }
OPTIMUM CFAR	Second-order lacks design guidance Third-order needed	Second-order does not properly checkout CFAR; penalizes radar compared to other designs Third-order properly tests CFAR and shows optimum performance

UNCLASSIFIED

better than the others. In other words, the third-order model evaluates a system during simulation much as it would be against real clutter and shows the advantages and disadvantages of various designs. The second-order model, while simpler, would give no indication that the optimum CFAR was better than the other two CFAR types. It would, however, show that they were all superior to a fixed threshold.

6. SHORT PROGRAM HISTORY

The TAGSEA history, as it pertains to the effort presented in this report, covers the period from June 1975 through August 1976. During this time, efforts directed towards the end result of clutter modeling included determination of an overall method of characterizing sea clutter based on gathered data. To this end, conceptual work was done to define in detail a combined flight test and analysis program. Specifically, the requirements for the data to be gathered were defined and substantiated by analysis, the hardware necessary was specified, ways of reducing and analyzing a vast amount of data were formalized and the types and uses of the resultant clutter models were determined in concept.

While much of this work proceeded in parallel, it is convenient to describe the various activities individually. Initially, the necessity to determine what data would be required and to specify the amount of data to be gathered revolved about four main points; it was desired to have data gathered 1) under various sea state conditions, 2) in three directions with respect to the wind, 3) on both the East and West coasts, and 4) for two polarizations.

Since the objective of this portion of the program was to characterize sea clutter in a manner meaningful for future work on generalized missile seekers, it was necessary to be able to address those parameters which influence seeker design. Prime among these considerations was the requirement to determine the probability of false alarms resulting from sea clutter occur with a probability of about 1 in 10^6 and how this level relates to the mean sea clutter return. The work leading to this

determination is presented in Appendix A, Volume III. Having set this specific point, the quantity of data for each condition was defined amounting to roughly 17 X 10^6 samples for each condition. Test set parameters necessary to gather the data were then derived; these are also presented in Volume III.

It was given that the available hardware (specifically the CMDR seeker) would be used to the maximum extent possible. From this starting point, it was determined that the prf would have to be raised to the maximum that the hardware could support. The resultant selection of about 19 KHz also fit nicely with the speed/doppler regime for the proposed flight test. A reasonable flight time then determined that multiple range gates would be required and that a special (new design) Data Conditioning Unit would be needed to prepare the radar output for recording. The Active Radar Test Set, or ARTS mounted in an existing pod was the result (see Volume II). This effort was essentially complete by the end of 1975.

Other equipment in the flight test pod and also in the A-3 carry aircraft was needed to control ARTS and to record the data. GD/P was directly responsible for this portion of the effort with Raytheon support through the use of existing equipment, modifications of other test instruments and during integration and checkout both in the pod and in the test aircraft.

Flight testing proper was also a GD/P effort with Raytheon supplying a technical flight crew for flights on both coasts. The total flight program ran from February through mid-March 1976.

As was mentioned above a vast amount of raw data was necessary to adequately define the 10^{-6} probability point. Further, since it was desired to gather and reduce this data so as to be representative of about a 100 foot by 100 foot patch of sea, doppler processing was necessary which, together with the 100 foot range gates, gave the desired area. Doppler processing was done in non-real time both for the sake of simplicity and so that the specific characteristics of the test equipment would have minimum impact on the data. Data reduction then consisted of converting the analog recorded data to digital form, doppler processing, and recording the results for further analysis. All of the data reduction was completed by mid-July 1976.

Finally, the analysis of the reduced data was divided into two parts; computer analysis and conceptual analysis. Computer analysis was used to do straightforward but lengthy computations and curve plotting which are included in Volumes II and III of this report as appendices. Conceptual analysis, on the other hand, covered all the cerebral work necessary to determine how the computer analyses should be performed and how the results should be translated into the sea clutter models which are the essence of this work.

Throughout the portion of the TAGSEA program concerned with clutter in all its aspects, Raytheon has had the support and guidance of a specially appointed validation team consisting of representatives from GD/P, APL and Technology Service Corporation with NAVSEA as an ex officio member. This group was specifically tasked with overseeing and validating the Raytheon efforts. Many helpful suggestions ranging from the general methodology to specific points, such as precise ways of presenting distribution functions, were received and incorporated in the fabric of Raytheon's work. This effort extended from January through August 1976 with a series of six meetings held approximately at one month intervals. These were in addition to the more

formal Program Review Meetings.

The final effort by Raytheon on the TAGSEA program has been the preparation of this report. The structure and outline of Volume I was covered in the introduction to this volume. A brief outline of the remaining three volumes follows.

Volume II, Procedures and Output Forms provides information on what hardware and data reduction and analysis processes were used to gather and interpret the data. A detailed explanation is given of the forms and meaning of the outputs; then, the simulation and validation procedures provides information on how the results of the work were verified. This volume provides the background necessary to substantiate the quality of the work which was done. Given this, those interested in using the detailed outputs as well as the models in further analyses can satisfy themselves of the validity of the work and the applicability to their purposes.

Volume III, Supportive Analyses and Outputs, consists first of technical analyses and simulation descriptions to support the procedures and results of Volumes II and I respectively. Also contained are outputs which were useful in a specialized way during this work and which may provide unique insight to others who may wish to use the results in related work. These specialized outputs include: histograms, spectra and autocorrelation functions of the mean; tables of variation of the statistical points; a special analysis and view of a ship and how it appears in the various plots; locally normalized histograms; and an illustrative section on the behavior of a large return.

Volume IV, Standard Clutter Analysis Outputs, contains plots and tables of much of the data reduced and analyzed for individual runs. This large volume has four appendices on Histograms, Hit, Average, and Spatial and Temporal outputs.

The main intent of including this material, other than to comply with the "deliverables" requirements of the Objectives (see Section 2), is to provide a data base for any who may want to conduct further investigations or to verify the results presented in this final report.

REFERENCES

(1) Nathanson, F.E., "Radar Design Principles", McGraw-Hill, 1969.

(2) Nathanson, F.E., and Brooks, P.R., "Data Points for X-Band Sea Reflectivity", Technology Service Corporation memo TSC-WO-251/br B 50711, dated 29 June 1976.

(3) Trunk, G.V., "Modification of Radar Properties of Non-Rayleigh Sea Clutter", IEEE Trans. on Aerospace and Electronic Systems, p. 110, January 1973.

(4) Sodergren, P.R., "A Revised Ku-Band Sea Clutter Model", JHU/APL memo MPD-72-U-033, dated July 19, 1972.

(5) General Dynamics, Flight Test Operation Final Report, 1 May 1976, Data Item A001 CDRL Contract N00017-73-C-2244, Document Confidential.